AN ECONOMICS STUDY OF CONTAINER PORTS IN THE GLOBAL NETWORK OF CONTAINER SHIPPING

A Thesis
Presented to
The Academic Faculty

by

Pisit Jarumaneeroj

In Partial Fulfillment
of the Requirements for the Degree
Doctor of Philosophy in the
School of Industrial and Systems Engineering

Georgia Institute of Technology
December 2014

AN ECONOMICS STUDY OF CONTAINER PORTS IN THE GLOBAL NETWORK OF CONTAINER SHIPPING

Approved by:

Professor John J. Bartholdi, III, Advisor
School of Industrial and Systems Engineering
Georgia Institute of Technology

Professor Chelsea C. White, III
School of Industrial and Systems Engineering
Georgia Institute of Technology

Professor Alan Erera
School of Industrial and Systems Engineering
Georgia Institute of Technology

Professor Alejandro Toriello
School of Industrial and Systems Engineering
Georgia Institute of Technology

Professor Amar Ramudhin
The Logistics Institute
University of Hull

Date Approved: 27 October 2014

To my parents, who raised me with greatest love, care, and inspiration.

To my educators, who taught me how to live a better life to the fullest.

And finally, to my beloved friends, who always supported me without fail.

ACKNOWLEDGEMENTS

First and foremost, I would like to express my sincere gratitude to my dissertation committee, Professor John J. Bartholdi III, Professor Chelsea C. White III, Professor Alan Erera, Professor Alejandro Toriello, and Professor Amar Ramudhin, for their time, valuable comments and suggestions.

Particularly, I would like to thank my advisor, Professor John J. Bartholdi III, for his valuable guidance on this dissertation, his continuous financial support during the hard time of economic downturn, and his generous sharing of thoughts and experiences regarding academia. Without his dedication and encouragement, I would not have been able to complete this dissertation to this standard.

I am also grateful to the faculty of both the School of Industrial and Systems Engineering, Georgia Institute of Technology, and the Department of Industrial Engineering, Chulalongkorn University, for what they have taught me, especially Professor Sirichan Thongprasert, my late mentor.

During my seven-and-a-half-year Ph.D journey at Georgia Tech, there were both good and bad times, happy and sad moments. Without all the help and support from my beloved friends, the names of which may not appear here, I would not have been able to reach the finish line, safe and sound.

Thank you, Katawut Namdee for organizing several wonderful and memorable trips since New York Road Trip in 2007, Kittipong Rattanaporn for his mental support, Soravit Vitoontus who taught me how to use MATLAB, the tool which was instrumental to my work, up to the day of my graduation, Pakkapol Kanchanalai for his tremendous help and effort in debugging my GAMS codes, all of my ex- and current roommates who patiently lived with me this whole time, last but not least, the cashier at the Student Center's Canteen who gave me kind reassurance before I knew that I had passed the comprehensive exam.

Finally, I would like to express my deepest gratitude to my parents, Supornchai and Suvimon Jarumaneeroj, who gave me constant love, support, and encouragement. I can still recall those moments when we were on a call. They usually asked me the same questions — have I been sleeping well, eating well, and studying well. Simple though the conversation was, it surprisingly washed away my worry and strengthened me with resolve to take another step forward. Unfortunately, my dad passed away before he could witness the day of my success; however, I truly believe that he would have been very proud of me and probably is still cheering me on from the heavens. From the bottom of my heart, thank you, Mom and Dad, for everything you have done and for being there for me.

TABLE OF CONTENTS

LIST OF TABLES

LIST OF FIGURES

SUMMARY

This dissertation focuses on three topics. The first is the construction of a new network model based on the *Liner Shipping Connectivity Index* (LSCI), which is a measure reflecting trade intensity between ports. We then use such a model to better understand the patterns of world trade.

We also propose a new measure, called the *Container Port Connectivity Index* (CPCI), to more accurately reflect the relative importance of container ports within the global network of container shipping. Unlike any of the existing measures, this index is based on both economics and network topology, where the strength of a port is based on the strength of its connection to neighbors, and neighbors of those neighbors, and so on — not just on local information such as the number of TEUs handled or direct links to other ports. As measured by the CPCI, the most important ports are not necessarily those with the most links, or those handling the most TEUs, but the ones with good connections to other well-connected ports. This is a reflection of fact that the CPCI does not depend only on the number of links but also on link quality and the connectivity of the ports to which they connect.

This thesis also proposes a framework for evaluating market stability of a logistics hub in a competitive environment. In particular, we build a model to predict how the community of liners calling at a hub might develop as the result of actions by competitors. We can use such a model to study the behavior of shipping lines, as well as the resulting trade-flow changes, as the system gradually moves toward equilibrium. Our model predicts that bigger lines are expected to be the first to move transshipment operations to a cheaper port, thereby inducing the smaller ones to follow. Though our model is only preliminary and not yet populated with actual data, it seems consistent with the observation of shipping line's relocation at the port of Singapore, where Maersk, the biggest operating line, was the first to move to the port of Tanjung Pelapas, followed subsequently by Evergreen.

CHAPTER I

INTRODUCTION

1.1 Port Attractiveness and Measures of Port Importance

What makes a container port attractive as a logistics hub? From an operational point of view, a port derives importance from three main factors. The first is the infrastructure required to move containers, such as cranes, quays, hinterland transportation, and so on. Another important factor is location, which includes geography, and, in particular, distance from other ports. Finally, there is connectivity within the network of container shipping: *to what degree do shipping liners call at the port?*

Practically, the annual number of TEUs handled is widely used as a traditional port importance indicator. However, it is merely a local statistic that reflects handling and not patterns of trade flow. To include more information about location and connectivity, others have proposed more systematic measures of port importance that reflect something about the position of the port in the global network of container shipping. Examples include *degree centrality*, *closeness centrality*, *betweenness centrality*, or the number of origin-destination pairs that the port serves — the *Network Connectivity Index* [85] and the *Port Cooperative Index* [54]. Emphasizing on connectivity, nevertheless, all of these measures do not directly reflect economics — and none exists, to the best of our knowledge.

On the other hand, from the economist's point of view, the *United Nations Conference on Trade and Development* (UNCTAD) has established another measure for comparing countries' trade competitiveness with respect to maritime logistics and transportation called the *Liner Shipping Connectivity Index* (LSCI), which is an aggregation of the following five statistics: number of liner services calling, number of liner companies, number of ships, combined container capacity of the ships (in TEUs), and capacity of the largest ship calling [71][1]. By construction, the LSCI implicitly treats each country as if it were a single location

[1]Despite the narrowness of focus and somewhat arbitrary method of aggregating component statistics, the LSCI is based on hard numbers and is felt to accurately reflect trade competitiveness. Indeed, the LSCI

and the entire rest of the world is its counterpart trading partner. Following the same idea, we may establish an economics-based measure reflecting trade intensity between ports by using the same calculation like that of the LSCI, except for ports rather than the countries. Though the LSCI is meaningful to some extent, it still lacks ability to reflect port importance from the network's perspective.

Accordingly, in this dissertation, we propose to establish a new measure, called the *Container Port Connectivity Index* (CPCI), to more accurately reflect the relative importance of container ports taking both network structure and economic information into account. In doing so, we first establish a new network model of container shipping called the *Global Container-Shipping Network* (GCSN), which is constructed in such a way that there is a link from port i to j, if there is direct service from port i to j. Furthermore, that link is assigned a weight that is computed as the LSCI, reflecting direct connectivity and trade intensity between ports. We then compute the CPCI by applying the *Hyperlink-Induced Topic Search* (HITS) algorithm [46] to such a network.

In particular, the CPCI takes the proposed LSCI-like measure as link weights, reflecting rate of container capacity moving between container ports, and assigns two types of importance scores to each port, that is, the *inbound* and *outbound scores*. Conceptually, a port with a high inbound score has greater power to aggregate goods, and a port with a high outbound score has greater power to distribute goods.

This measure has several advantages over the existing ones. Firstly, while the aforementioned measures are based on either network topology or economic information, the CPCI more directly reflects both. In addition, it provides separate scores for inbound and outbound, which could consequently be used to analyze and explain the strategic position that terminal ports serve independently. Finally, the CPCI supports what-if analysis in such a way that survey-based indices, like the LSCI or the LPI, cannot.

---

has been observed to be strongly correlated with the *Logistics Performance Index* (LPI), a comprehensive survey of perceptions that is reported annually by the World Bank [6].

1.2 Market Stability of a Logistics Hub in a Competitive Environment

From a port's perspective, in order to become a logistics hub, a port must possess at least two important characteristics. The first is the infrastructure that allows customers, or shipping lines, to operate at lower cost but with higher speed. The latter is its geographical location, or *centrality*. A strategically located port with advanced and efficient infrastructure may attract more liners, container flow, and so achieves the connectivity for freight consolidation or transshipment — which, in turn, allows its customers to open new markets by calling at such a port. Yet there are several threats that might affect the stability of such a hub.

It is worth noting that it is the customers of a port, not the port itself, that provide port connectivity. Losing a customer inevitably reduces connectivity and so the attractiveness of the port. This may, in turn, trigger a series of defections by others whose transshipment opportunities have been reduced. A hub, especially the transshipment one, is more vulnerable to this threat than the others due to its smaller demand and supply, which might not otherwise justify port calls made by the liners.

One prominent example demonstrating this circumstance is the competition between the ports of Singapore and Tanjung Pelepas, Malaysia [10]. While Tanjung Pelepas and Singapore are located on the opposite side of the *Johor Strait*, next to each other, labor cost at the port of Tanjung Pelepas is much lower. In order to secure lower operational costs, in 2000, Maersk Sealand, the largest operating line at the port of Singapore, decided to move its operating hub from the port of Singapore to the port of Tanjung Pelepas. Afterward, in 2002, Evergreen, the second biggest line, also moved to the port of Tanjung Pelepas. Under economic pressure on small lines, some have to establish connection services to the port of Tanjung Pelepas in order to transship their containers with those who moved, while the others have decided to follow them to the port of Tanjung Pelepas. By these succession moves, the port of Singapore has lost millions of container flow to its competitor. Ironically, the most important customer is also the greatest threat to the hub itself since it could abandon the current hub and easily move to the competing ones, which increases economic pressure on the rest to follow.

Inspired by such an event, we establish an analytical framework to investigate and explain market stability of a logistics hub in a competition with other ports within its vicinity, taking both ports' and shipping lines' decisions into consideration, where, at the state of stability, no liner-shipping company is better off moving his business away to competing ports. Conceptually, in our proposed scheme, port operators decide on the configurations of their infrastructure and fees charged. And, once observed, liner-shipping companies then decide on their operational plans that minimize their total operating costs via a model called the *Liner Shipping Cooperative Model*.

Our proposed methodology differs from the existing research in three ways. Firstly, while most of the existing models, such as [25], [26], and [27], may incorporate both explicit and implicit costs into consideration, an implicit cost, such as waiting or congestion, is improperly captured by a *piecewise-linear function*, where the containers are assessed with different cost rates rather than one, as it should be in the steady state. In our proposed cooperative model, we have addressed this issue by using an alternative modeling approach assigning a single cost rate to all containers, called the *piecewise-affine cost function* [89].

Secondly, to the best of our knowledge, we are the first to tackle this problem by means of an optimization-based cooperative game theoretic approach. More precisely, instead of defining relationship between interested quantities, we take advantage of the optimization model to explain the mechanism among them.

Lastly, the structure of our proposed methodology allows us opportunity not only to investigate the behavior of shipping lines taking port information into account but also to provide insights into changes of container-flow patterns as the system gradually moves toward equilibrium. This information, in turn, allows a logistics hub to comprehend and quantify the threats posed by its competitors, which might consequently be used to devise counter strategies or policies to safeguard its business.

1.3 Dissertation Outline

The remainder of this dissertation is organized as follows. In Chapters 2 and 3, we provide comprehensive reviews of *Centrality Measures* and *Community Structure*, which would

be used as foundation for the construction of the the *Global Container-Shipping Network* (GCSN) and the *Container Port Connectivity Index* (CPCI) in Chapter 4. An interesting extension of the CPCI is provided in Chapter 5, where the overall port importance score is decomposed into components to help us better understand why a particular port has become important — and by which factors.

The discussion of market stability of a logistics hub in a competitive environment is provided in Chapter 6, while the detailed construction as well as the results of our proposed framework is provided in Chapter 8. Since our model is constructed based on the concept of cooperative game theory, where the Shapley value has played a prominent role in defining the condition sustaining the stable community of customers at ports, readers might find Chapter 7 to be useful as it provides a detailed discussion of the Shapley value, including its interpretation and some interesting applications.

Finally, Chapter 9 concludes our works, limitations, and future research directions — particularly, the effects of the *Panama Canal Expansion* and the construction of a canal on *Kra Isthmus*, the narrowest part of the *Malay Peninsula* separating the *Gulf of Thailand* from the *Indian Ocean*, on the patterns of freight-flow diversion.

CHAPTER II

CENTRALITY MEASURES

In social networks, *Centrality Measures* are frequently used as tools to measure the potential involvement of nodes in the networks. Although there are a great number of centrality measures that have been established lately, they all could be arranged and grouped into three categories, based on their dimensions of measurement, namely, (i) *degree centrality*, (ii) *closeness centrality*, and (iii) *betweenness centrality* [17, 34, 35]. Some authors, such as [17] and [45], classified *eigenvector centrality* as another class of centrality measures. Yet it could be considered as a variant of degree centrality. Since eigenvector centrality and its variants, such as the *Google's PageRank* algorithm and the *Hyperlink-Induced Topic Search (HITS)* algorithm, possess several important properties and play a prominent role in our proposed ranking scheme, we will treat them separately from degree centrality. Based on the foundations of these basic measures, many contemporary measures have been constructed, including *multidimension centrality*, where the relationship among nodes are allowed to interact with three or more entities. In order to show the viability of such tools, we also provide several interesting applications of the centrality measures at the end of this chapter.

2.1 Terminology

Let $G = (V, E)$ be a graph, or network, where V represents a set of nodes of size N, and E represents a set of links or edges, which sometimes might be referred to as *ties* or *lines* in the literature. In general, we frequently represent a network and its components by either (i) an adjacency matrix or (ii) an incidence matrix.

- The adjacency matrix is a matrix where both of its rows and columns represent nodes. The entry of such a matrix is one, if there exists an edge connecting nodes of the underlying row and column, and zero otherwise.

- The incidence matrix is a matrix where each row and column represent a particular

node and edge, respectively. In addition, its entry is one for pairs of nodes incident to an edge, and zero otherwise.

Another set of notations associated with connections between nodes is provided as follows.

- A walk is a sequence of nodes and adjacent edges.
- A trail is a walk with no repeated edges.
- A path is a trail with no repeated nodes.

2.2 Classical Centrality Measures

In this section, we explore the three classical centrality measures in Social Science, namely, (i) *degree centrality*, (ii) *closeness centrality*, and (iii) *betweenness centrality*, which are the foundations of the sophisticated centrality measures discussed in the following sections. These three measures are different in terms of their control level. More specifically, degree centrality is considered as a measure of immediate effect, since it counts only the number of direct links connecting to its immediate neighbors, while betweenness centrality is regarded as a measure of global control, since the centralities of other nodes depend on the position of the interested one.

2.2.1 Degree Centrality

Degree centrality, the simplest centrality measure, measures an importance of a node based on the number of direct links to its immediate neighbors. Mathematically, for any node i, degree centrality, denoted as $C(i)$, could be calculated by Equation (1).

$$C(i) = \sum_{j \in V} a_{ij}, \tag{1}$$

where

$$a_{ij} = \begin{cases} 1 & \text{, if there exists an edge connecting nodes } i \text{ and } j, \\ 0 & \text{, otherwise.} \end{cases}$$

When the direction is of interest, *in-degree centrality* and *out-degree centrality* could be defined using in-coming and out-going links instead of the adjacent ones.

In the literature, the comparison of nodes' degree centrality across networks could be done by scaling such a measure into the range between 0 and 1 with the maximum theoretical value [34]. In such a case, the theoretical maximum degree for any nodes in the network is $N-1$, hence, the scaled version of degree centrality could be defined as Equation (2).

$$C(i) = \frac{\sum_{j \in V} a_{ij}}{N-1} \tag{2}$$

Since degree centrality of any node is independent of the others, it is usually referred to as a measure of intermediate effect. Many variants of degree centrality are also studied in the field of social science, such as (i) *edge-weighted degree centrality*, where the frequency of connection between nodes is also included in the calculation, (ii) *k-path centrality*, where all paths of length k or less emanating from a node are counted instead of immediate connecting edges, (iii) *geodesic k-path centrality*, which is similar to k-path centrality; but, we count only the shortest paths up to length k, starting from a node of interest, (iv) *edge-disjoint k-path centrality*, which counts all paths of lengths up to k between two nodes with no shared edges, and (v) *vertex-disjoint k-path centrality*, which is quite similar to edge-disjoint k-path centrality; but, in this case, repeated nodes are prohibited.

2.2.2 Closeness Centrality

An alternative concept of centrality may be based on total shortest distance from a node to the rest of the network, which is known as *closeness centrality*. Mathematically, closeness centrality, denoted as $C_C(i)$, is defined as Equation (3).

$$C_C(i) = \sum_{j \in V} d(i,j), \tag{3}$$

where $d(i,j)$ is the shortest path length from node i to j.

Notice that the measure defined in Equation (3) is indeed a farness measure, i.e. the larger the value of $C_C(i)$, the less centrality a node possesses. In order to make a better interpretable measure, we may redefine closeness centrality by using Equation (4) instead of (3) — where the inverse of farness properly defines closeness.

$$C_C(i) = \frac{1}{\sum_{j \in V} d(i,j)} \tag{4}$$

Similar to that of degree centrality, for comparison purpose, the standardized closeness centrality could be defined as Equation (5).

$$C_C(i) = \frac{N-1}{\sum_{j \in V} d(i,j)} \tag{5}$$

It is worth mentioning that, when a network is not strongly connected, closeness centrality is not well defined, i.e. there would be some nodes $j \in V$ with $d(i,j) = \infty$. In order to avoid such a circumstance, one can consider only the reachable nodes from node i, denoted as J_i, and redefine closeness centrality as Equation (6).

$$C_C(i) = \frac{|J_i|/(N-1)}{\sum_{j \in J_i} d(i,j)/|J_i|} \tag{6}$$

Information centrality is one interesting variant of closeness centrality, where the centrality of a node is defined as the difference of node's closeness when node deactivation is allowed [51].

2.2.3 Betweenness Centrality

The concept of *betweenness centrality* is based on the observation that the communication between any pairs of nodes usually depends on a set of nodes that lies between them. Based on this idea, a node that lies on many shortest paths might be considered as the most central one. More formally, betweenness centrality, denoted as $C_B(i)$, is defined as Equation (7).

$$C_B(i) = \frac{\sum_{i \neq j \neq k} g_{jk}(i)}{g_{jk}}, \tag{7}$$

where g_{jk} denotes the number of shortest paths connecting nodes j and k, and $g_{jk}(i)$ denotes the number of shortest paths connecting nodes j and k passing intermediate node i. In the literature, betweenness centrality is sometimes referred to as a measure of information control, since the most central node could be viewed as the most important information gateway [17].

Many interesting variants of betweenness centrality include (i) *group betweenness centrality* [47], where the influence of a set of nodes are of interest rather than that of an individual node, (ii) *co-betweenness cetrality* [47], where the shortest paths counted must pass a pair of interested nodes, (iii) *flow betweenness centrality*, whose calculation is based

on the concept of maximum flow, where all information is treated like fluid continuously pumped through the network, (iv) *random-walk betweenness centrality* [64], where information is assumed to flow freely from node to node, and (v) *communicability betweenness centrality* [22], which is quite similar to random-walk betweenness centrality; but, in this case, only self-avoiding paths are considered and counted.

Although betweenness centrality provides us better insight into node importance, its computational time is much greater than those of the previous measures, especially in large and complex networks.

2.3 Eigenvector Centrality

The main feature that differentiates *eigenvector centrality* from the others is the way it defines node centrality. In many classes of networks, centrality might be a function of the interaction among nodes rather than the intrinsic properties of a node itself. For example, in social network, if we are chosen by someone popular, our status should be higher than that if being chosen by the least popular ones. Based on this idea, if we let x_i be the centrality of node i and a_{ij} be the weighted contribution that node i gives to node j, we have $x_i = a_{1i}x_1 + a_{2i}x_2 + \ldots + a_{ni}x_n$. When we write this relationship in matrix form, we have,

$$A^T x = x, \tag{8}$$

where matrix A represents weighted contribution of all adjacent nodes.

Interestingly, solving such a set of linear equations for x is equivalent to finding the eigenvector associated with the eigenvalue of one. However, this might be infeasible if one is not a member of the eigenvalues of A^T. In order to make such a system of equations solvable [13], eigenvector centrality, denoted as C_E, is defined as Equation (9).

$$\lambda C_E = A^T C_E, \tag{9}$$

where λ and C_E are the principal eigenvalue and eigenvector corresponding to matrix A^T, respectively.

Note that, when negative relationships exist, our popularity might decrease if we are associated with someone being disliked by the others. In such a case, eigenvector centrality

defined in Equation (9) is still applicable, with a slight modification (see [14] for more details).

Similar to all centrality measures, eigenvector centrality has some properties that might be considered as its weaknesses. First of all, in directed networks, nodes with zero in-degree possess zero centrality and any nodes being pointed by them would gain no contribution. For example, all nodes shown in Figure 1 have zero eigenvector centrality, since nodes 1 and 2 have no in-degree and the rest are pointed from these two nodes.

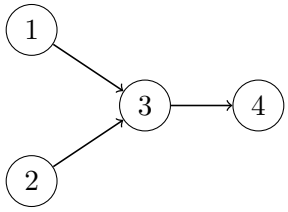

Figure 1: A network with all zero eigenvector centrality [13].

As a remedy, we might add initial status, denoted as ε, which is independent of interaction among nodes to all nodes [13]. This modified version of eigenvector centrality is called *alpha-centrality*, which is defined as Equation (10).

$$\alpha A^T x + \varepsilon = \lambda x, \tag{10}$$

where x is the alpha-centrality and α is the relative importance of peers' contribution.

It is also known that, in regular graphs, i.e. networks where all nodes have the same degree, eigenvector centrality yields the same result as degree centrality [11, 23], which, consequently, provides no meaningful information. However, this might be viewed as a property rather than its drawback in the networks that degree of nodes drives their importance [11].

In the literature, broader class of centrality measures based on the eigen analysis is called *spectral centrality measures* [75], which include the *Google's PageRank algorithm* and the *Hypertext Induced Topic Search (HITS) algorithm*.

2.4 Google's PageRank Algorithm

The *PageRank algorithm* is an algorithm used by *Google Search Engine*, where a page is assigned an importance score, or centrality value, based on the number of its backlinks and their importance. For example, consider an example of a network with four pages shown in Figure 2, let x_k be the importance score of page k, where $x_i > x_j$ implies that page i is more important than page j. By using the number of page's backlinks as a measure of page importance, pages 3 and 1 will be the most and the least important ones, respectively. However, from the practical standpoint, the links from important pages should be much more valuable than those of the trivial ones. Therefore, we may redefine the importance score of page k using the scaled version as shown in Equation (11).

$$x_k = \sum_{j \in L_k} \frac{x_j}{n_j}, \tag{11}$$

where L_k is the set of page k's backlinks and n_j is the number of emanating links from page j used to scale the importance score of each page $j \in L_k$.

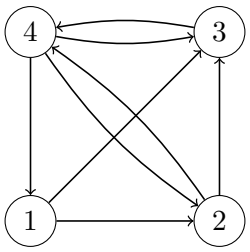

Figure 2: An example network with four pages [19].

If we rewrite Equation (11) in matrix form, we then have a linear system $Ax = x$, where the entry a_{ij} of matrix A is the weighted contribution that page i obtains from its backlink page j.

In our example, by scaling the solution of $Ax = x$ with an additional equality $\sum_j x_j = 1$, the importance score vector of these four pages is $[0.129\ 0.194\ 0.290\ 0.387]^T$. With this ranking scheme, it has been revealed that, indeed, page 4, not page 3, is the most important page, while page 1 remains the least important one, which could be explained as follows: since the importance score of a particular page i is transmitted from several source pages to

such a page, a link from a page with higher importance score contributes more than those of the trivial ones. In this case, page 4 could be accessed only by page 3 and page 3 could be accessed by any pages; thus, the importance of page 4 has been increased by its backlink page, namely, page 3.

In practice, web surfers might end up with pages with no outgoing links, such as *pdf* documents or pages containing only picture files. From network perspective, this type of page is called the *dangling node*. For example, in Figure 3, page 3 has no outgoing links; thus, it is a dangling node where the column associated with page 3 in matrix A has all zero entries.

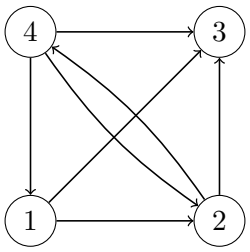

Figure 3: Page 3, which is a dangling node, has no outgoing link.

With the existence of dangling nodes, importance scores of all nodes other than the dangling ones will be zero. In order to address this issue, we may fictitiously create outgoing links from the dangling nodes to all nodes, including themselves, with some specific probability vector, called the *personalization vector* V. For example, if $V = \frac{1}{n}e$, where e is a column vector of all unity entries, we assume that once a web surfer reaches a dangling node, the probability that she will move to any pages is $\frac{1}{n}$. In the literature, we refer to this assumption as the *idealized random web surfer assumption* [98].

It was shown in [19] that, when the network consists of several unconnected subnetworks, there was no unique importance score. But this could be fixed by maintaining network connectedness. In doing so, matrix A is modified to matrix M as shown by Equation (12).

$$M = m\overline{A} + (1 - m)S, \tag{12}$$

where $\overline{A}$ is a modified matrix A after adding fictitious links to all dangling nodes, S is

an $n \times n$ square matrix, where all elements are $\frac{1}{n}$, and m, known as a damping factor (see [50] for more details), is a real number within the range of 0 to 1. In general, m is set at 0.85. Observe that such a matrix is maximally irreducible and column stochastic, i.e. each column is added up to one, which guarantees having only one eigenvalue on its spectral circle [49]. Interestingly, this problem is equivalent to the problem of finding limiting probability of an *ergodic markov chain*.

Example 2.4.1 *Consider a network of seven pages shown in Figure 4, where matrix A is shown by Equation* (13)*. Since page 7 is a dangling node, or an absorbing state in the context of markov chain,* $[0\ 0\ 0\ 0\ 0\ 0\ 1]^T$ *is the solution of the system of equations* $Ax = x$*.*

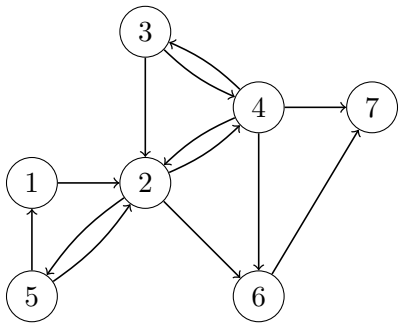

Figure 4: A network of seven pages used for the calculation of Google's PageRank algorithm [50].

$$A = \begin{bmatrix} 0 & 0 & 0 & 0 & \frac{1}{2} & 0 & 0 \\ 1 & 0 & \frac{1}{2} & \frac{1}{4} & \frac{1}{2} & 0 & 0 \\ 0 & 0 & 0 & \frac{1}{4} & 0 & 0 & 0 \\ 0 & \frac{1}{3} & \frac{1}{2} & 0 & 0 & 0 & 0 \\ 0 & \frac{1}{3} & 0 & 0 & 0 & 0 & 0 \\ 0 & \frac{1}{3} & 0 & \frac{1}{4} & 0 & 0 & 0 \\ 0 & 0 & 0 & \frac{1}{4} & 0 & 1 & 0 \end{bmatrix} \tag{13}$$

By adding fictitious links connecting page 7 to all pages, including page 7 itself, the modified matrix A could be constructed and shown by Equation (14)*, where the resulting importance score vector of all pages is* $[0.085\ 0.239\ 0.066\ 0.143\ 0.11\ 0.146\ 0.212]^T$*. Based on this modification, pages 2 and 3 are the most and the least important ones, respectively.*

$$\overline{A} = \begin{bmatrix} 0 & 0 & 0 & 0 & \frac{1}{2} & 0 & \frac{1}{7} \\ 1 & 0 & \frac{1}{2} & \frac{1}{4} & \frac{1}{2} & 0 & \frac{1}{7} \\ 0 & 0 & 0 & \frac{1}{4} & 0 & 0 & \frac{1}{7} \\ 0 & \frac{1}{3} & \frac{1}{2} & 0 & 0 & 0 & \frac{1}{7} \\ 0 & \frac{1}{3} & 0 & 0 & 0 & 0 & \frac{1}{7} \\ 0 & \frac{1}{3} & 0 & \frac{1}{4} & 0 & 0 & \frac{1}{7} \\ 0 & 0 & 0 & \frac{1}{4} & 0 & 1 & \frac{1}{7} \end{bmatrix} \tag{14}$$

If we replace matrix $\overline{A}$ with matrix M using expression (12) *with an equiprobable personalization vector, i.e. $V = \frac{1}{7}e$, and set m as 0.85, the resulting importance score vector of all pages would be* $[0.135\ 0.170\ 0.130\ 0.143\ 0.133\ 0.139\ 0.151]^T$. *Still, pages 2 and 3 remain the most and the least important ones in the network.*

It is worth noting that, based on random surfer assumption, the personalization vector is equiprobable and it might not properly reflect the interest of web surfers' inquiry. For better quality of search engine, the *Biased PageRank* algorithm has been developed by using the customized personalization vector for each web surfer instead [50].

2.5 The HITS Algorithm

While the *Hyperlink-Induced Topic Search (HITS)* algorithm [46] and the Google's PageRank algorithm fall into the same class of centrality measure, where node importance is derived from the principal eigenvector, the HITS algorithm provides two different scores based on two different functions of the web pages, namely, the *authority* and the *hub scores*, as output.

In this context, a good authority page is a page with many in-coming links, while a good hub page is a page with many out-going links (see Figure 5). The main idea of the HITS algorithm is that any authority pages being pointed from important hub pages should be considered as important authority pages, and vice versa.

Mathematically, we can say that the hub score of a page is a function of authority pages, and, similarly, the authority score of a page is a function of hub pages. If we let x_i and y_i

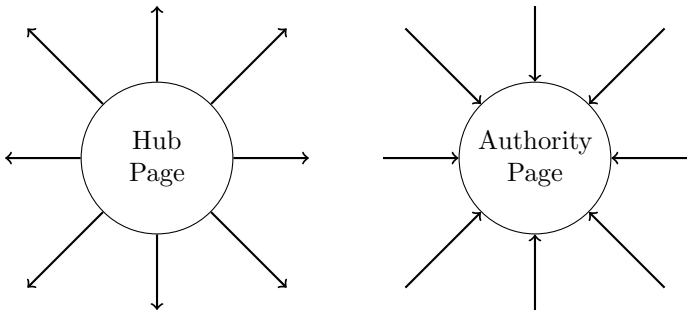

Figure 5: An illustration of hub and authority pages.

be the authority and the hub scores of page i, we have the following.

$$\lambda x_i = \sum_{j:e_{ji} \in E} y_j, \tag{15}$$

$$\lambda y_i = \sum_{j:e_{ij} \in E} x_j, \tag{16}$$

where E is the set of links and λ is the weighted constant of such functions. If we replace (i) all y_i in Equation (15) with that of Equation (16), (ii) all x_i in Equation (16) with that of Equation (15), and rewrite them in matrix form, we can calculate these two scores by Equations (17) and (18).

$$\lambda x = A^T y \Rightarrow \lambda^2 x = A^T A x, \tag{17}$$

$$\lambda y = A x \Rightarrow \lambda^2 y = A A^T y, \tag{18}$$

where A is an adjacency matrix. In the literature, $A^T A$ and AA^T are referred to as the authority and the hub matrices. Since $A^T A$ and AA^T are both symmetric, all eigenvalues are positive. Both the authority and the hub scores are properly defined by the principal eigenvectors corresponding to each matrix.

2.6 Multidimension Centrality Measure

Interestingly, most of the centrality measures discussed so far emphasize only the relationship between two entities; however, in practice, additional entities might be required to completely explain the interaction among them. For example, in a buyer-seller-broker transaction, we need three interactions to be recognized all at once, see Figure 6[1].

[1]Other than objects, additional dimensions may include (i) time, (ii) location, and (iii) group [12].

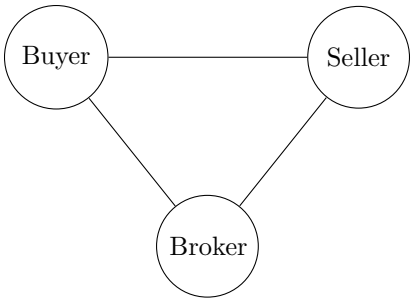

Figure 6: A network representing a buyer-seller-broker transaction.

We may represent multidimensional relationship among entities by *hyperedge* and *hypergraph*, where a hyperedge is an edge connecting more than two nodes at a time and a graph containing hyperedges is called a hypergraph. For example, the network shown in Figure 7 is a hypergraph containing three buyer-seller-broker transactions.

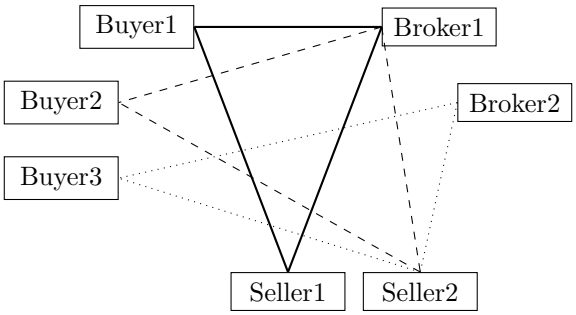

Figure 7: A hypergraph containing three buyer-seller-broker transactions [12].

In this setting, a hypergraph can be described by means of an incidence matrix, where rows and columns of such a matrix represent hyperedges and nodes, respectively. For example, the incidence matrix of the network shown in Figure 7 could be written as follows.

$$A = \begin{bmatrix} 1 & 0 & 0 & 1 & 0 & 1 & 0 \\ 0 & 1 & 0 & 0 & 1 & 1 & 0 \\ 0 & 0 & 1 & 0 & 1 & 0 & 1 \end{bmatrix}$$

Based on the construction of the hypergraph, each node might be involved in more than one transaction, whose importance differs by its involving members. In this circumstance, node importance does not depend only on the entities it is connected with but also on the transactions it involves. Based on this fact and the concept of eigenvector centrality, we may

apply Expressions (17) and (18) on matrix A to obtain two different importance measures; one for node, denoted as x, and another for hyperedge, denoted as y.

With this approach, it has been revealed that the most centrality nodes of the network shown in Figure 7 are Seller2 and Broker1, as expected, since they are involved in two out of three transactions, and the most important transaction is the one involving Buyer2, Seller2, and Broker1.

It is worth noting that the measurement hyperedges, i.e. fictitious hyperedges measuring group centrality, must be treated differently — using small values to represent those edges in the matrix — when they are added to the incidence matrix since they might reduce the importance of data hyperedges [12].

2.7 Other Contemporary Centrality Measures

Notice that most of the standard centrality measures, like degree, closeness, and betweenness centralities, implicitly make several assumptions about (i) the trajectory of information flow and (ii) the method of information spread [15]. Regarding the trajectory assumption, closeness and betweenness centralities, for example, count only the shortest paths since we assume that the information always flows through such paths. However, in many cases, such an assumption does not hold. For example, consider the spread of news, where the senders have no information about the shortest paths; thus, using them as centrality measures is definitely inappropriate. Regarding method of spread, interested information might be an indivisible object flowing only on one path, such as the pathway of novel in the community, or it might be simultaneously spread out from a node like an infection. Thus, one measure might be preferable to the others, and its appropriateness mostly depends on the critical characteristic of information flowing throughout the network.

By properly altering these assumptions and adding practical constraints based on network perspectives, many contemporary centrality measures have been established. The examples include as (i) *subgraph centrality* [24], which is defined as the sum of weighted closed walk of any length k, (ii) *entropy-based centrality* [90], which is developed based on path-transfer processes, like a chain letter network, where any node has an ability either

to stop or transmit information flow to the others, and (iii) *alternative path centrality* [81], where the contribution of a node in backup paths is also part of its centrality.

Interestingly, while these centrality measures emphasize connectivity, additional information inherited on both nodes and edges is treated equally important, or even worse as it might be neglected. For example, in social networks, all connections are assumed to be equal in terms of influence, which might not be true in practice. Similarly, in logistics networks, where each node and edge has different capacity, throwing away such information and focusing only on connectivity may not reflect centrality of a node properly.

In the literature, there are only few measures incorporating network components' information into consideration. For example, (i) *generalized classical centralities* [72], where the authors have extended the use of weighted edges into the calculation of degree, closeness, and betweenness centralities, (ii) *weighted graph centrality* [63], where weighted edges are used for the calculation of eigenvector centrality, and (iii) *path value and path length measures* [101], where path value is defined as a measure of bottleneck link of a path connecting two nodes, and path length is defined as the summation of weighted links comprising a path between two nodes.

2.8 Applications of Centrality Measures

In this section, we will provide a detailed discussion of several interesting applications of centrality measures in a more realistic setting. We begin with the establishment of two indices for measuring port connectivity in maritime logistics networks, called the *Network Connectivity Index* (NCI) [85] and the *Port Cooperation Index* (PCI) [54]. The next is the implicit use of eigenvector centrality in college football ranking [74]. And finally, we present a contemporary concept of defining key players in social networks [16].

2.8.1 The Network Connectivity Index

In a maritime logistics network, a shipping line must decide where to host its operation, which is usually known as *hub selection problem* in the literature. This decision depends on several factors which dynamically change with regard to both ports' and other lines' decisions.

In the literature, this problem is typically solved by means of empirical methods, such as the *Analytical Hierarchy Process (AHP)* or the *Multinomial Logit Model (MNL)*. Since these traditional methods depend mostly on surveys, subjectivity may not be avoided. In order to reduce subjectivity, [85] proposed a new measure of port attractiveness reflecting port connectivity based on the total number of origin-destination (O-D) pairs that such a port served, called the *Network Connectivity Index* (NCI).

In that setting, given a network of ports G, we have the following.

- A_i is a set of O-D pairs served by an individual port i and $n(A_i)$ is the total number of such pairs which could be calculated by Equation (19).

$$n(A_i) = 2n_i n_{ij} + 2n_{ij} n_{ij}, \tag{19}$$

  where n_i is the number of exclusive ports that could be reached by port i including port i itself, accounting for the transshipment at port i, and n_{ij} is the number of common ports that could be reached by both ports i and j.

- $A_i \cap A_j$ is a set of O-D pairs served by both ports i and j and $n(A_i \cap A_j)$ is the total number of such pairs which could be calculated by Equation (20).

$$n(A_i \cap A_j) = 2n_{ij} n_{ij} \tag{20}$$

- $A_i \cup A_j$ is a set of O-D pairs served by either port i or port j and $n(A_i \cup A_j)$ is the total number of such pairs which could be calculated by Equation (21).

$$n(A_i \cup A_j) = 2n_{ij}(n_i + n_j + n_{ij}) \tag{21}$$

- $A_i \otimes A_j$ is a set of O-D pairs jointly served by both ports i and j and $n(A_i \otimes A_j)$ is the total number of such pairs which could be calculated by Equation (22).

$$n(A_i \otimes A_j) = 2n_i n_j \tag{22}$$

Since $A_i \cup A_j$ and $A_i \otimes A_j$ are mutually independent, we have $n((A_i \cup A_j) \cup (A_i \otimes A_j)) = 2(n_i + n_{ij})(n_j + n_{ij})$ and, by definition, the network connectivity index of node i, denoted

as NC_i, could be expressed by Equation (23).

$$NC_i = \sum_j 2(n_i + n_{ij})(n_j + n_{ij}) \tag{23}$$

Example 2.8.1 *Consider the network shown in Figure 8, where ports i and j have served five and four destination ports, respectively. Among these ports, ports 4 and 5 are considered as common ports served by both ports i and j.*

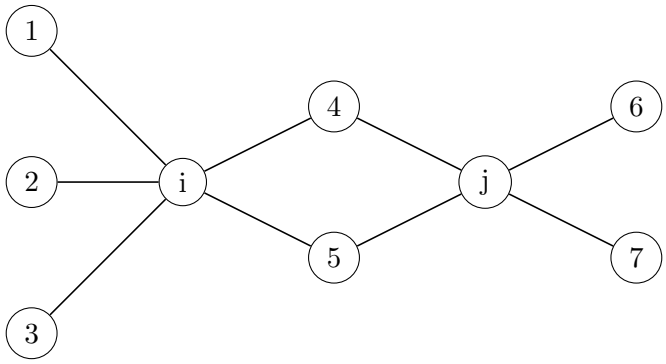

Figure 8: An example of network for the calculation of the NCI [85].

Based on the aforementioned notations, we have $n_i = 5 + 1 - 2 = 4$, $n_j = 4 + 1 - 2 = 3$, and $n_{ij} = 2$. From Equation (23)*, total number of O-D pairs between ports i and j is* $2 \times (4 + 2)(3 + 2) = 60$.

In addition, for comparison purpose, one can scale such an index by the theoretical maximum number of O-D pairs, which leads to Expression (24).

$$NC_i = \frac{\sum_j 2(n_i + n_{ij})(n_j + n_{ij})}{\sum_i \sum_j 2(n_i + n_{ij})(n_j + n_{ij})} \tag{24}$$

Observe that the NCI is indeed a variant of betweenness centrality, where the shortest path assumption is relaxed.

2.8.2 The Port Cooperation Index

To emphasize the sustainability of ports in a competitive environment, [54] developed another index for measuring degree of cooperation between a pair of ports, called the *Port Cooperation Index* (PCI). The PCI is derived from the observation that total number of

O-D pairs served between any pairs of ports are either cooperative or competitive routes. In the first case, a cooperative route is an O-D pair requiring connection from both ports; and, in the latter case, a competitive route is an O-D pair that could be reached by either port.

For clarity, consider two networks shown in Figure 9. While ports i and j have a perfectly cooperative structure in the network on the left, they are perfectly competitive in the one on the right.

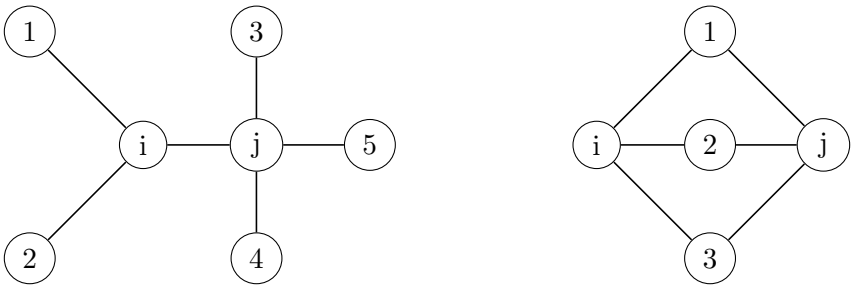

Figure 9: Networks with perfect cooperative and competitive structures [54].

If we let A_i denote a set of O-D pairs served by an individual port i with either cooperation or competition with port j and $n(A_i)$ is the total number of such pairs, we could calculate $n(A_i)$ by Equation (25).

$$n(A_i) = n_i n_j + n_{ij}(n_i + n_j + n_{ij}), \tag{25}$$

where n_i and n_{ij} are defined the same way as those of the NCI.

Notice that the first term of Expression (25) could be viewed as cooperative routes, and the latter one may be regarded as the competitive routes. The degree of cooperation between any pairs of ports could be defined as the ratio between total number of O-D pairs that both ports have jointly served and total number of O-D pairs served either by port i or j. Mathematically, the *Port Cooperation Index* (PCOI) of a pair of ports i and j is defined as Equation (26).

$$PCOI(ij) = \frac{n_i n_j}{(n_i + n_{ij})(n_j + n_{ij})} \tag{26}$$

Similarly, degree of competition between a pair of ports i and j, called the *Port Competitive Index* (PCI), is the ratio between total number of O-D pairs independently achieved

without deploying direct connection between them and total number of O-D pairs served either by port i or port j.

$$PCI(ij) = \frac{n_{ij}(n_i + n_j + n_{ij})}{(n_i + n_{ij})(n_j + n_{ij})} \tag{27}$$

2.8.3 College Football Ranking

In [74], a variant of eigenvector centrality was introduced and used to primarily reduce the subjectivity of the existing college football ranking scheme — which was mostly based on polls and the opinions of experts. Based on the fact that (i) the number of matches played are much fewer than the number of existing teams (indeed, the games are mostly played in conference system where a conference consists of a number of teams in the same region) and (ii) the strength of schedule, i.e. some teams might have to play with some tough teams compulsorily since they are in the same conference, should be considered in the ranking scheme, ranking them all in one list would require a more formal unbiased scheme which could be established through the concept of *direct* and *indirect wins*.

In this context, indirect win is defined based on logical implication. For example, if team A has beaten team B, and team B has beaten team C, this intuitively implies that team A has indirectly beaten team C with the length of two (see Figure 10). As this length keeps increasing, indirect wins might not properly reflect the true strength of a team. And, therefore, indirect win should be weighted with some values, where the longer the length, the less the weight is assigned.

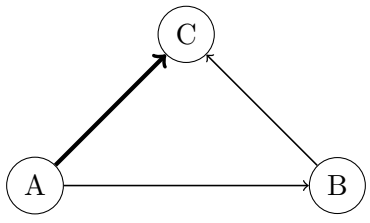

Figure 10: An example of indirect win of length two, which is shown by bold arrow [74].

Based on the aforementioned, given an adjacency matrix A, where a_{ij} denotes the number of times team i has beaten team j, direct and indirect wins of length two of team i

could be calculated by Equations (28) and (29), respectively.

$$\text{direct wins of team } i = \sum_{j \in V} a_{ij} \tag{28}$$

$$\text{indirect wins of team } i \text{ with length of two} = \sum_{j,k \in V} a_{ij} a_{jk} \tag{29}$$

By applying weighting factor α to all lengths of indirect win, *team i's win score*, denoted as w_i, could be calculated by Equation (30).

$$\begin{aligned} w_i &= \sum_j a_{ij} + \alpha \sum_{k,j} a_{ij} a_{jk} + \alpha^2 \sum_{l,k,j} a_{ij} a_{jk} a_{kl} + ... \\ &= \sum_j (1 + \alpha \sum_k a_{jk} + \alpha^2 \sum_{lk} a_{jk} a_{kl} + ...) a_{ij} \\ &= \sum_j (1 + \alpha w_j) a_{ij} \\ &= k_i^{out} + \alpha \sum_j a_{ij} w_j, \end{aligned} \tag{30}$$

where k_i^{out} is the out degree of team i. Similarly, *team i's loss score* could be defined as Equation (31).

$$l_i = k_i^{in} + \alpha \sum_j a_{ji} w_j, \tag{31}$$

where k_i^{in} is the in degree of team i.

In [74], the rank of a team is defined and ordered by the difference between win and loss scores, denoted as s_i, where $s_i = w_i - l_i$. In matrix form, win and loss scores of all teams could be rewritten as Equations (32) and (33).

$$\begin{aligned} w &= k^{out} + \alpha A \cdot w \\ &= (I - \alpha A)^{-1} \cdot k^{out} \end{aligned} \tag{32}$$

$$\begin{aligned} l &= k^{in} + \alpha A^T \cdot w \\ &= (I - \alpha A^T)^{-1} \cdot k^{in} \end{aligned} \tag{33}$$

It has been shown in [74] that this measure is well defined as long as the value of α is smaller than the principal eigenvalue of matrix A.

2.8.4 Key Players in Social Networks

In [16], two new problems associated with key player identification in social networks were introduced, (i) the *Key Player Problem/Negative (KPP-Neg)* and (ii) the *Key Player Problem/Positive (KPP-Pos)*. In the KPP-Neg, key players are the ones whose absence would reduce the cohesiveness of the network. The examples of the KPP-Neg are as follows.

- In public health, we might want to immunize or quarantine a set of people in order to prevent the epidemic.
- In military, we might want to arrest a set of terrorists in order to interrupt its network.

In contrast, key players of the KPP-Pos are the ones whose presence would maximize the connectedness of the network. Some examples of such a problem are provided below.

- In public health, we might need to select a set of people to act as seeds to diffuse the practices that would promote better health in society.
- In military, we might want to select a set of double agents in order to spread misinformation to the terrorist network.

Standard centrality measures might not appropriately identify key players in both problems since (i) the objectives of the problems are different and (ii) centrality of one node depends on the centrality of the others. For clarity, in the KPP-Neg, deleting a node with high centrality might not reduce the cohesiveness comparing to that of the trivial ones (see Figure 11). Similarly, in the KPP-Pos, adding one more highly central node might not increase the connectedness of the network since the added node might have the same neighbors as those of the existing ones (see Figure 12).

In both cases, the redundancy principle might explain the reason of such consequences. More precisely, the redundancy of the KPP-Neg is associated with the bridges linking the same third parties, while the redundancy of the KPP-Pos is associated with adjacency and distance. Realizing both redundancy and the objective of each problem would help us devise a better measure.

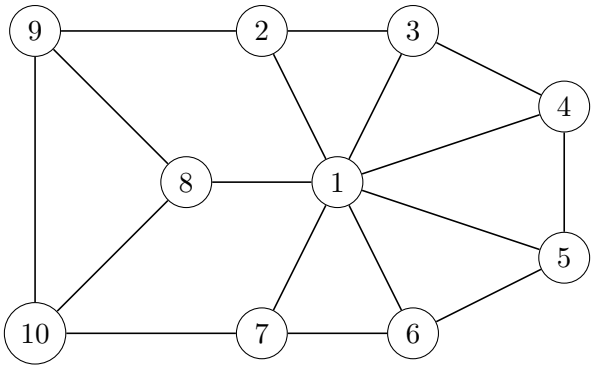

Figure 11: Although node 1 is the most centrality node, deleting such a node does not destroy the connectedness of the network [16].

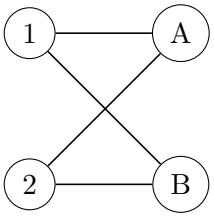

Figure 12: The addition of node B in the network does not provide any benefit in terms of network connectedness [16].

For example, an appropriate measure for the KPP-Neg might be the number of fragments after node deletion; however, this proposed measure does not account for the size of each fragment. In order to incorporate fragmental size into consideration, the number of pairs of nodes that are disconnected from each other might be a better representation reflecting key players in the KPP-Neg. Based on this observation, we may define a fragmental measure as Equation (34)

$$F = 1 - \frac{2\sum_{i=1}^{n-1}\sum_{j=i+1}^{n} r_{ij}}{n(n-1)}, \tag{34}$$

where r_{ij} equals one if we can reach j from node i, and zero otherwise.

Notice that the computation time of Equation (34) is quite expensive, especially in large and complex networks, since all pairs of nodes must be evaluated for connectedness. Fortunately, since a node in one fragment cannot communicate with nodes in other fragments, we might alternatively compute such a measure by using the size of each fragment, denoted by s_k, where k is the fragment index, instead of the number of pairwise reachable nodes.

$$F = 1 - \frac{\sum_k s_k(s_k - 1)}{n(n-1)} \tag{35}$$

In KPP-Pos, the cohesion measure of sets k of nodes, denoted as C_k, could be defined as Equation (36).

$$C_k = \sum_{i \in k, j \in V-k} a_{ij}, \tag{36}$$

where a_{ij} equals one if nodes i and j are adjacent to each other, and zero otherwise. However, the redundancy with respect to the adjacency has not yet been captured by such an expression. To include such information, a more complicated cohesion measure might be defined as Equation (37).

$$C_k = \sum_{j \in V-k} \bigcup_{i \in k} a_{ij}, \tag{37}$$

where $\bigcup$ is a non-specific aggregation function like maximization or minimization. For example, in terms of maximization aspect, C_k measures the maximum nodes outside k that the members of k are adjacent to.

2.9 Conclusions

In this chapter, we provide a comprehensive review of centrality measures beginning with the three classical centrality measures, namely, degree, closeness, and betweenness. While interesting, these measures rely too much on several strict assumptions about information flow, making them less appropriate in practice. To make them more informative, many variants of them are extensively revised by removing those restrictions and/or incorporating relevant network topology as part of the computation.

We complete the discussion of centrality measures by providing several applications of such measures in a more realistic setting, including (i) the establishment of port connectivity indices, (ii) the development of a new ranking scheme for college football teams, and (iii) the formulation of new measures reflecting centrality of nodes in different settings.

Based on the concept of centrality measures, in Chapter 4, we introduce a new measure of port importance, named as the *Container Port Connectivity Index* (CPCI), which is computed by the HITS algorithm, where the resulting scores are referred to as the *inbound* and *outbound scores*.

We also show that (in Chapter 5) the CPCI could be implemented in a disaggregation fashion, where the overall port importance score is decomposed into components. With

this decomposition scheme, we could make a detailed analysis on how a port has become important — and by which factors.

Besides centrality measures, another fundamental characteristic of networks which is extensively studied in social science is *community structure*, where the network is divided into groups of nodes with dense and strong connections among themselves but sparser and weaker connections to the others. For smooth transition, we will next discuss community structure in Chapter 3 before providing intensive results of our study in Chapter 4.

CHAPTER III

COMMUNITY STRUCTURE

Besides centrality measures, *Community Structure* might be regarded as another fundamental characteristic of a network. While there is no well-defined definition for a community, in our study, we choose a generally accepted term, where a community within a network is a group of nodes with dense and strong connections among themselves but sparser and weaker connections to the others. It is well known that community detection problem is $\mathcal{NP}$-complete [18] and there exist many algorithms to solve such a problem. One prominent class of algorithms that we will discuss in this Chapter is the *Spectrum-Based Algorithms*, which use eigenvectors as guidelines for dividing a network into communities such that the *modularity value* is maximized. It is worth noting that this class of algorithms is mainly used in a non-overlapping setting, where each node is a member of only one community. For the overlapping case, where a node might be a member of multiple communities, a community adjusting algorithm is introduced. Conceptually, a hard partition of non-overlapping community structure is transformed into a soft partition of the overlapping one guided by a local measure of improvement, called *community strength* [96]. We also discuss a systematic way of comparing community structures over time, based on the *similarity value* [102].

3.1 Introduction

Community structure has played an important role in network analysis. It helps us understand interaction among nodes; in many cases, it provides us valuable insights into intrinsic characteristics of the underlying network, which consequently allows us to explain the mechanism of the system, as well as expected behavior of its members. For example, by revealing the communities of customers of an online retailer network, we can enhance operational efficiency by directing the right services to the right groups of customers.

In the literature, communities might be referred to as *clusters* and there are numerous methodologies to identify communities within a network. The traditional ones are *Graph*

Partitioning and *Hierarchical Clustering Methods*. In the first method, a network is partitioned into a specific number of groups such that the total number of edges running between groups is minimal. Since the optimal number of groups is usually unknown and it differs from one to another network, finding the best partition may seem computationally prohibitive, especially in large and complex networks. In the latter method, the clusters of nodes are iteratively constructed based on some predefined criteria, using either agglomerative or divisive algorithms. For example, the *Girvan-Newman Algorithm* (GN) [37] used *edge betweenness* as a criterion for constructing a cluster — where edge betweenness of a link was defined as the total number of the shortest paths between all pairs of nodes running through such a link. If there were more than two shortest paths, each path was counted so that the summation was unity. Since links with high edge betweenness are the ones acting like gateways, where the flow of information between communities must pass through, deleting such links would reveal community structure of the network. In [37], they shown that the GN algorithm gave better results compared to those of the standard hierarchical methods on several benchmarking networks.

Unfortunately, in weighted network, where the weight of an edge is defined as the reciprocal of its length, the GN algorithm performs badly, since it tends to remove edges that connect nearby nodes together; i.e. the flow is expected to flow via the shortest paths and nodes that are closely connected usually attract more edge betweenness [63]. In order to improve the performance of the GN algorithm in weighted network, [63] proposed an extension of such an algorithm by replacing weighted edges with multi-edges. With this modification, the shortest paths would remain unchanged, but they would be counted less and less if they possess higher weight.

Another class of community detection methodologies extensively studied in Social Science is the *Modularity Maximization Method*, where the *modularity value* is the mathematical reflection of community's definition.

Definition 3.1.1 *A community within a network is a collection of vertices in which the connections among themselves are dense, but they are sparser across communities.*

More specifically, the *modularity value* is defined as the difference between actual and expected edges within a community. Clearly, the higher the modularity value, the stronger the community structure is, and, the optimal community structure is the one that maximizes such a value.

Mathematically, the modularity function for undirected unweighted networks [65] could be written as Equation (38).

$$Q = \frac{1}{2m} \sum_{ij} \left(A_{ij} - \frac{k_i k_j}{2m} \right) \delta(c_i, c_j), \tag{38}$$

where

- A_{ij} is the actual number of edges connecting nodes i and j, which is either 1 or 0, when A is an adjacency matrix,
- k_i and k_j are degrees of nodes i and j, respectively,
- m is the half of total number of edges within the network, i.e. $2m = \sum_{ij} A_{ij}$,
- $\delta(c_i, c_j) = 1$, if nodes i and j are in the same community, and 0 otherwise.

For directed networks [67], the modularity function could be written as Equation (39).

$$Q = \frac{1}{W} \sum_{ij} \left(A_{ij} - \frac{k_i^{out} k_j^{in}}{W} \right) \delta(c_i, c_j), \tag{39}$$

where

- $k_i^{out} = \sum_j k_{ij}$ and $k_j^{in} = \sum_i k_{ij}$ are out-degrees of node i and in-degrees of node j, respectively,
- $W = 2m = \sum_i \sum_j A_{ij}$.

Lastly, for directed and weighted networks [4], such a function is calculated through Equation (40).

$$Q = \frac{1}{W} \sum_{ij} \left(w_{ij} - \frac{w_i^{out} w_j^{in}}{W} \right) \delta(c_i, c_j), \tag{40}$$

where

- w_{ij} denotes the weight of an edge connecting nodes i and j,
- $w_i^{out} = \sum_j w_{ij}$ and $w_j^{in} = \sum_i w_{ij}$ are output strength of node i and input strength of node j, respectively,
- $W = \sum_i \sum_j w_{ij}$.

Based on the fact that the modularity maximization problem is $\mathcal{NP}$-complete, even in undirected unweighted networks [18], numerous heuristics have been proposed in order to tackle this problem, including *Spectrum-Based Methods*, where eigenvectors are used as guidelines for dividing a network into communities.

3.2 Spectrum-Based Methods

In this section, a detailed discussion of two interesting spectral clustering algorithms, namely, the *Leading Eigenvector Method* and the *Multi-Eigenvector Method*, is provided. In the first method, only the principal eigenvector is used for the partitioning, while, in the latter method, we use as many eigenvectors as possible, up to the number of positive eigenvalues plus one, for the clustering.

3.2.1 The Leading Eigenvector Method

The leading eigenvector method is an iterative method, where a network is partitioned into two subgraphs, or communities, using only the principal eigenvector. For better understanding, we will first discuss the development of this method in a simpler case and then extend its results to the more general cases.

Given an undirected unweighted network of size N and its associated modularity function defined by Equation (38), we redefine $\delta(c_i, c_j)$ by replacing it with two belonging indicators, s_i and s_j.

$$\delta(c_i, c_j) = \frac{1}{2}(s_i s_j + 1), \tag{41}$$

where

$$s_k = \begin{cases} 1 & \text{, if } k \text{ belongs to community 1,} \\ -1 & \text{, if } k \text{ belongs to community 2.} \end{cases}$$

If both nodes i and j are in the same community, $\delta(c_i, c_j) = 1$, and $\delta(c_i, c_j) = 0$ otherwise. Additionally, let $\mathbf{s}$ be a column vector consisting of all $s_i's$, then the modularity function could be rewritten as Equation (42).

$$\begin{aligned} Q &= \frac{1}{4m}\sum_{ij}\left(A_{ij} - \frac{k_i k_j}{2m}\right)(s_i s_j + 1) \\ &= \frac{1}{4m}\sum_{ij}\left(A_{ij} - \frac{k_i k_j}{2m}\right)(s_i s_j) \\ &= \frac{1}{4m}\mathbf{s}^T\mathbf{B}\mathbf{s}, \end{aligned} \tag{42}$$

where $\mathbf{B}$ is a real symmetric matrix, called the *modularity matrix*, whose element B_{ij} is defined as $B_{ij} = A_{ij} - \frac{k_i k_j}{2m}$. Since the row sum of the modularity matrix is always zero, its spectral radii must contain zero. If we let $\mathbf{s} = \sum_i^N a_i \mathbf{u}_i$ and $a_i = \mathbf{u}_i^T\mathbf{s}$, where $\mathbf{u}_i$ is the i^{th} normalized eigenvector of the modularity matrix, we can rewrite Equation (42) as Equation (43).

$$\begin{aligned} Q &= \frac{1}{4m}(\sum_i a_i\mathbf{u}_i)^T\mathbf{B}(\sum_j a_j\mathbf{u}_j) \\ &= \frac{1}{4m}(\sum_i a_i\mathbf{u}_i^T)(\sum_j a_j\mathbf{B}\mathbf{u}_j) \\ &= \frac{1}{4m}(\sum_i a_i\mathbf{u}_i^T)(\sum_j a_j\lambda_j\mathbf{u}_j) \\ &= \frac{1}{4m}\sum_i\sum_j a_i a_j\lambda_j(\mathbf{u}_i^T\mathbf{u}_j) \\ &= \frac{1}{4m}\sum_i \lambda_i a_i^2, \end{aligned} \tag{43}$$

where λ_i is the i^{th} eigenvalue of the modularity matrix. Based on Equation (43), if λ_i is ordered in a non-increasing order, i.e. $\lambda_1 \geq \lambda_2 \geq \ldots \geq \lambda_N$, we can maximize Q by pairing a_i^2 in the same order as that of λ_i.

As we use only the principal eigenvector in this method, the value of Q will depend only on the value of a_1^2. And since $a_i = \mathbf{u}_i^T\mathbf{s}$, where s_i is either 1 or -1, a_1^2 is maximized only when the positive $s_i's$ are matched with the positive elements of the principal eigenvector, and vice versa. More precisely, in order to maximize the modularity value Q, s_i must be assigned a value based on the sign of its associated element of the principle eigenvector as

shown in Equation (44).

$$s_i = \begin{cases} 1 & \text{, if } u_i^{(1)} > 0, \\ -1 & \text{, if } u_i^{(1)} \leq 0, \end{cases} \tag{44}$$

where $u_i^{(1)}$ is the $i^{(th)}$ element of the principal eigenvector.

Algorithm 1 shows the summary of the leading eigenvector method where a network is partitioned into two subgraphs, or communities, based on the sign of the principal eigenvector's elements.

Algorithm 1 The Leading Eigenvector Method: The partition of a network into 2 communities

1: **Input**: A network of size N, where $N > 1$
2: Compute the principal eigenpair $(\lambda_1, \mathbf{u}_1)$ of the modularity matrix $\mathbf{B}$, where $B_{ij} = A_{ij} - \frac{k_i k_j}{2m}$.
3: **if** λ_1 is positive **then**
4: Assign the value of s_i based on the sign of its associated element of the principal eigenvector, that is, $s_i = 1$ if such an element is positive, and $s_i = -1$ otherwise.
5: **if** $\mathbf{s}^T\mathbf{B}\mathbf{s}$ is positive **then**
6: **return** Two communities
7: **else**
8: **return** Original network
9: **end if**
10: **else**
11: **return** Original network
12: **end if**

Observation 3.2.1 *Since zero eigenvalue is always a member of the modularity matrix's spectrum radii, when Algorithm 1 terminates, either the original network or the two partitioned subgraphs must be returned as output.*

For further partitioning, we cannot iteratively apply Algorithm 1 to the resulting subgraphs since we will unintentionally neglect the connecting edges between communities. Instead, we have to modify the algorithm so that connecting edges between subgraphs are part of the modularity value's calculation in further divisions. This could be done by computing the incremental value of Q, denoted as ΔQ, from subgraph partitioning.

Given a subgraph g, the incremental value of Q is defined as Equation (45).

$$\begin{aligned}
\Delta Q &= \frac{1}{2m}\left[\sum_{ij\in g} B_{ij}\left(\frac{s_i s_j + 1}{2}\right) - \sum_{ij\in g} B_{ij}\right] \\
&= \frac{1}{4m}\left[\sum_{ij\in g} B_{ij}(s_i s_j) - \sum_{ij\in g} B_{ij}\right] \\
&= \frac{1}{4m}\left[\sum_{ij\in g} B_{ij}(s_i s_j) - \sum_{ij\in g}\delta_{ij}\sum_{k\in g} B_{ik}\right] \\
&= \frac{1}{4m}\sum_{ij\in g}\left[B_{ij} - \delta_{ij}B_{ij}\right](s_i s_j) \\
&= \frac{1}{4m}\mathbf{s}^T\mathbf{B}^{(g)}\mathbf{s}, \qquad (45)
\end{aligned}$$

where $\delta_{ij} = 1$ if $i = j$, and 0 otherwise, and,

$$B_{ij}^{(g)} = B_{ij} - \delta_{ij}\sum_{k\in g} B_{ik}. \qquad (46)$$

Algorithm 2 provides the summary of subgraph partitioning. Similar to Algorithm 1, Algorithm 2 takes any subgraph g as input, and returns two subcommunities that maximally increase the incremental modularity value, or the original subgraph, if no improvement on Q has been found.

Algorithm 2 The Leading Eigenvector Method: Subgraph Partitioning

1: **Input**: A subgraph of N_g, where $N_g > 1$
2: Establish matrix $\mathbf{B}^{(g)}$ and compute the principal eigenpair $(\lambda_1, \mathbf{u}_1)$ of $\mathbf{B}^{(g)}$.
3: **if** λ_1 is positive **then**
4: Assign the value of s_i based on the sign of its associated element of the principal eigenvector, that is, $s_i = 1$ if such an element is positive, and $s_i = -1$ otherwise.
5: **if** $\mathbf{s}^T\mathbf{B}^{(g)}\mathbf{s}$ is positive **then**
6: **return** Two subcommunities
7: **else**
8: **return** Original subgraph
9: **end if**
10: **else**
11: **return** Original subgraph
12: **end if**

Observation 3.2.2 *Since the row sum of $\boldsymbol{B}^{(g)}$ is zero for all rows, zero eigenvalue is always a member of its spectrum radii. When Algorithm 2 terminates, either the original subgraph*

or the two partitioned subgraphs are returned, and, in the latter case, the modularity value is definitely improved.

Observation 3.2.3 *Since the number of communities is bounded by the size of the network. Eventually, when Algorithm 2 terminates, community structure of a network would be revealed, together with its associated modularity value Q.*

As a heuristic, the leading eigenvector method might err and misplace nodes in wrong community, especially in large and complex networks — since the magnitude of the principal eigenvector is preserved and distributed to all members of the network. In order to alleviate this effect, a simple fine-tuning process (see Algorithm 3) might be implemented at the end of each partitioning. The concept of a fine-tuning process is to swap node's community, one at a time, until no improvement has been found [66].

Algorithm 3 A Fine-Tuning Process (First Search)

1: **Input**: A network of size N, where $N > 1$, and vector $\mathbf{s}$
2: For the first member of the list, swap its community and evaluate new modularity value (or new incremental modularity value).
3: **if** the new modularity value (or the new incremental modularity value) increases **then**
4: Swap node community and back to line 2.
5: **else**
6: Move to the next member of the list and repeat the evaluation of node swapping until no improvement has been found.
7: **end if**
8: **return** An updated list of community members

When the network is directed, matrix $\mathbf{A}$ might be asymmetrical, as well as the modularity matrix $\mathbf{B}$. In such a case, there is no guarantee that $\mathbf{B}$ is diagonalizable; thus, Algorithms 1 and 2 might fail to reveal community structure of the network. In [67], an extension of the leading eigenvector method on directed networks was established. Conceptually, the modularity matrix $\mathbf{B}$, as well as $\mathbf{B}^{(g)}$, is modified so that it has become symmetric. Equations (47) and (48) show such modifications for Q and ΔQ.

$$Q = \frac{1}{4W}\mathbf{s}^T(\mathbf{B} + \mathbf{B}^T)\mathbf{s}, \tag{47}$$

where $W = 2m = \sum_i \sum_j A_{ij}$ and $B_{ij} = A_{ij} - \frac{k_i^{out} k_j^{in}}{W}$.

$$\Delta Q = \frac{1}{4W} \mathbf{s}^T (\mathbf{B}^{(g)} + \mathbf{B}^{(g)T}) \mathbf{s}, \tag{48}$$

where $\delta_{ij} = 1$, if $i = j$, and 0 otherwise, and,

$$B_{ij}^{(g)} = B_{ij} - \frac{1}{2} \delta_{ij} \sum_{k \in g} (B_{ik} + B_{ki}). \tag{49}$$

For directed weighted networks, the modularity value and its incremental value from the partitioning are defined almost the same as Equations (47) and (48), but with $W = \sum_i \sum_j w_{ij}$ and A_{ij}, k_i^{out}, k_j^{in} replaced by w_{ij}, w_i^{out}, and w_j^{in}, respectively.

In sum, Algorithm 4 shows the summary of the leading eigenvector method with fine-tuning process for directed weighted networks.

3.2.2 The Multi-Eigenvector Method

[65] provided an example where the leading eigenvector method might fail to detect the optimal number of communities due to its nature that repeatedly partitions a network or subgraph into a fixed number of communities at a time. The author also argued that, by using only the principal eigenvector, the information inherited by other eigenvectors was underutilized. In order to overcome these shortcomings, the *Multi-Eigenvector Method* was introduced and tested [65].

In that setting, let $\mathbf{S}$ be a matrix, whose dimension is $N \times c$, where c is the total number of communities. In addition, each column of $\mathbf{S}$ contains only 0 or 1, where,

$$S_{ij} = \begin{cases} 1 & \text{, if node } i \text{ belongs to community } j, \\ 0 & \text{, otherwise.} \end{cases}$$

Since each row sum of $\mathbf{S}$ is unity and all columns of $\mathbf{S}$ are mutually orthogonal, we must have $\mathbf{Tr}(\mathbf{S}^T \mathbf{S}) = N$. In addition, we can rewrite $\delta(c_i, c_j)$ in terms of S_{ij} as,

$$\delta(c_i, c_j) = \sum_{k=1}^{c} S_{ik} S_{jk}. \tag{50}$$

With Equation (50), we can rewrite Equation (38) as,

$$Q = \frac{1}{2m} \sum_{i=1}^{N} \sum_{j=1}^{N} \sum_{k=1}^{c} B_{ij} S_{ik} S_{jk} = \frac{1}{2m} \mathbf{Tr}(\mathbf{S}^T \mathbf{B} \mathbf{S}). \tag{51}$$

Algorithm 4 The Leading Eigenvector Method With Fine-Tuning (First Search)

Input: A network of size N, where $N > 1$
Compute the principal eigenpair $(\lambda_1, \mathbf{u}_1)$ of the modified modularity matrix $(\mathbf{B} + \mathbf{B}^T)$, where $B_{ij} = w_{ij} - \frac{w_i^{out} w_j^{in}}{W}$.
if λ_1 is positive **then**
    Assign the value of s_i based on the sign of $\mathbf{u}_1$.
    if $\mathbf{s}^T(\mathbf{B} + \mathbf{B}^T)\mathbf{s}$ is positive **then**
        return Vector $\mathbf{s}$, which provides a guidance for the fine-tuning process

        Call a fine-tuning algorithm.

        return A list of temporary communities and their associated members
    else
        return Original network
    end if
end if
return Original network

while the list of temporary communities is not empty **do**
    Input: A subgraph in the temporary community list of size N_g, where $N_g > 1$.
    Establish matrix $\mathbf{B}^{(g)}$ and compute the principal eigenpair $(\lambda_1, \mathbf{u}_1)$ of $(\mathbf{B}^{(g)} + \mathbf{B}^{(g)T})$, where $B_{ij}^{(g)} = B_{ij} - \frac{1}{2}\delta_{ij} \sum_{k \in g}(B_{ik} + b_{ki})$.
    if λ_1 is positive **then**
        Assign the value of s_i based on the sign of $\mathbf{u}_1$.
        if $\mathbf{s}^T(\mathbf{B}^{(g)} + \mathbf{B}^{(g)T})\mathbf{s}$ is positive **then**
            return Vector $\mathbf{s}$, which provides a guidance for the fine-tuning process

            Call a fine-tuning algorithm.

            return A list of two new temporary communities
            Delete input community from the temporary list.
            Add two new temporary communities to the temporary list.
        else
            Mark input community as permanent and delete input community.
        end if
    else
        Mark input community as permanent and delete input community.
    end if
end while

return A list of permanent communities and their associated members, with the finalized modularity value

Since $\mathbf{B}$ is a real symmetric matrix, we must have $\mathbf{B} = \mathbf{U}\mathbf{D}\mathbf{U}^T$, where $\mathbf{U} = (\mathbf{U}_1|\mathbf{U}_1|\ldots|\mathbf{U}_N)$ is the eigenvector matrix of $\mathbf{B}$ and $\mathbf{D}$ is the diagonal matrix, where $D_{ii} = \lambda_i$. In terms of calculation, $\frac{1}{2m}$ is a constant and it has no effect on the partitioning algorithm, we can remove it and rewrite Equation (51) as Equation (52).

$$Q = \sum_{j=1}^{N}\sum_{k=1}^{c} \lambda_j(\mathbf{u}_j\mathbf{S}_k)^2 \tag{52}$$

Based on Equation (52), if we want to maximize the modularity value, we have to choose eigenvectors associated with the positive eigenvalues such that the contributions to the modularity value are positive. If $\mathbf{S}$ is not constrained by binary constraint, and there are c communities in total, there exist $c-1$ independent and mutually orthogonal columns, since one of them is being fixed for the unity row sum constraint. In other words, the number of communities c is the number of positive eigenvalues plus one.

Observation 3.2.4 *Since the elements of $\boldsymbol{S}$ are binary, finding vectors $\boldsymbol{s}_i$ as many as suggested might not be possible, but we know that the upper bound on the number of communities is the number of positive eigenvalues plus one.*

Even though the multi-eigenvector method exercises multiple eigenvectors to extract all communities at once, we usually have no a priori knowledge about the value of c. In addition, it requires longer computational time compared to that of the leading eigenvector method. Based on these reasons, the leading eigenvector method is usually implemented in the study of community structure.

Other than those two previously discussed methods, interested readers could find a detailed discussion of other spectrum-based methods for clustering in [62]; and, lastly, a comprehensive review of community detection study could be found in [31].

3.3 Overlapping Community Structure

Notice that, in both the leading eigenvector and the multi-eigenvector methods, we do not allow a node to be assigned in more than one community. However, in many applications, a particular node might have closed relationships with members in other communities, which

possibly makes it be a member of them. In such a case, *Overlapping Community Structure* might be a better representation.

3.3.1 Overlapping Community Identification Algorithms

In the literature, overlapping community identification receives quite less attention compared to that of the non-overlapping case; and, most of the algorithms devised for overlapping community identification are based on clique and its variants.

In *Clique Prelocation Method* [73], the total numbers of cliques associated with nodes are counted and used to identify overlapping community structure. However, extracting all cliques, especially in large and complex networks, usually requires costly computational time. Instead of using pure clique-based methods, many researchers have alternatively extended the results of the modularity maximization method, from non-overlapping to the overlapping setting, by defining new modularity functions and devising algorithms that maximize such values.

Since there is no clear definition for the wellness of overlapping community, many forms of the modularity functions have been proposed. In [68], they defined the modularity function for directed networks as Equation (53), and maximized it by means of genetic algorithm.

$$Q_o = \frac{1}{W} \sum_{c \in C} \sum_{i,j \in V} \left(\beta_{l(i,j),c} A_{ij} - \frac{\beta^{out}_{l(i,j),c} k^{out}_i \beta^{in}_{l(i,j),c} k^{in}_j}{W} \right), \tag{53}$$

where

- $\beta_{l(i,j),c}$ is the belonging coefficient of link (i, j) in community c,
- $\beta^{out}_{l(i,j),c}$ is the expected belonging coefficient of any link $l(i, j)$ pointed from nodes in community c,
- $\beta^{in}_{l(i,j),c}$ is the expected belonging coefficient of any link $l(i, j)$ pointing to nodes in community c.

[82] argued that the explanation of the belonging coefficient defined in [68] was not clear and it was quite difficult to apply such a framework on large and complex networks. Instead,

they defined an alternative formulation of the modularity function in a much simpler form, as shown by Equation (54).

$$Q_o = \frac{1}{W} \sum_{c \in C} \sum_{i,j \in V} \delta_{ic} \delta_{jc} \left(A_{ij} - \frac{k_i^{out} k_j^{in}}{W} \right), \tag{54}$$

where δ_{ic} and δ_{jc} are belonging coefficients reflecting the degree that nodes i and j belong to community c defined by Equation (55).

$$\delta_{ij} = \frac{1}{\delta_i} \sum_{j \in V(c)} \frac{O_{ij}^c}{O_{ij}} A_{ij}, \tag{55}$$

where

- $V(c)$ is the set of all nodes belonging to community c,
- O_{ij}^c denotes total number of maximal cliques containing link (i, j) in community c,
- O_{ij} denotes total number of maximal cliques containing link (i, j) in the entire network,
- δ_i is a normalization term of of δ_{ic}, i.e. $\delta_i = \sum_{c \in C} \sum_{j \in V(c)} \frac{O_{ij}^c}{O_{ij}} A_{ij}$.

In addition, these belonging coefficients must satisfy the following normalization properties.

1. $0 \leq \delta_{vc} \leq 1$, for all $v \in V$ and $c \in C$.
2. $\sum_{c \in C} \delta_{vc} = 1$, for all $v \in V$

With the aforementioned definitions, [82] revealed an overlapping community structure by first constructing the maximal clique network associated with the network of interest, and then applying a community detection algorithm on such a network. They shown that the maximization of Q_o on the original network was equivalent to the maximization of the modularity function defined on its associated maximal clique network. This approach is expected to work well in undirected networks, but, unfortunately, not for the directed ones as directed clique is not well defined.

Recently, [32] pointed out that the modularity optimization might fail to detect communities whose sizes were smaller than a specific scale, which is known as the *resolution limit*.

In order to avoid the resolution limit, [83] established a two-step algorithm to identifying overlapping community structure. In the first step, they first marked all leaders in the network, where a leader was defined as a node having more influence on its neighbors. All nodes other than the leaders were assigned membership coefficients associated with each leader in the second step. While this approach is a resolution-limit-free algorithm, we still need some well-defined measures to evaluate its performance, which, unfortunately, do not exist.

3.3.2 Community Adjusting Algorithms

One interesting class of overlapping community detection algorithms that we will discuss next is the *Community Adjusting Algorithm*, where we adjust a hard partition of non-overlapping structure to a soft partition of overlapping one based on some predefined criteria of improvement that still maximizes the modularity value.

Examples include the algorithms proposed by [96] and [99], where the modularity function for undirected unweighted networks is defined as Equation (56),

$$Q_o = \frac{1}{2m} \sum_{c \in C} \sum_{i,j \in C_c} \frac{1}{O_i O_j} \left(A_{ij} - \frac{k_i k_j}{2m} \right), \tag{56}$$

where O_i and O_j are the numbers of communities that nodes i and j belong to.

In order to identify overlapping community structure, they moved the border nodes around based on some local measures of improvement instead of computing the increasing value of Q_o to help decrease the computational time. While the algorithms proposed by [96] and [99] shared the same concept, we will discuss only the algorithm proposed by [96], since it is easier in terms of implementation.

Let $\mathbf{U}$ be a partition matrix of N rows and c columns, where N and c are total numbers of nodes and communities. In the non-overlapping case, $\mathbf{U}(i,k)$ takes only a binary value, that is, $\mathbf{U}(i,k) = 1$ if node i is a member of community k, and zero otherwise; but, in the overlapping case, we have $0 \leq \mathbf{U}(i,k) \leq 1$, where $\mathbf{U}(i,k)$ reflects the membership of node i in community k.

Notice that not all nodes could be members of multiple communities, but, generally, the border ones, i.e. nodes having connections with other communities. Based on this

observation, we can enhance the algorithmic performance by focusing only on this kind of nodes. Formally, we define border nodes of community c by Equation (57).

$$B_c = \{\{j\} | (i,j) \in E, \{i\} \in c, \{j\} \notin c\} \tag{57}$$

If we move a border node into different communities, we must ensure that the modularity value increases, or, at least, some well-defined local measures reflecting community improvement do. In their setting, [96] used *community strength* as a local measure of community improvement, whose mathematical expression was shown by Equation (58).

$$S(c) = \frac{\sum_{i \in c} l_i^{in}}{\left(\sum_{i \in c} l_i\right)^r}, \tag{58}$$

where

- $S(c)$ denotes the strength of community c,
- l_i^{in} denotes total internal degrees of node i within community c,
- l_i denotes total degrees of node i,
- r is a tuning parameter of the overlapping extent, i.e. the lower the value of r, the greater the extent of overlapping structure. As suggested by [96], r is typically set around 0.8 - 1.0.

Since a community is strong in the sense that its members are all well connected within, the contribution of a node to the community strength is sufficient to define its membership in such a community. Mathematically, the strength of community c with respect to the presence of node i might be evaluated by Equation (59).

$$F(c,i) = S(c \cup \{i\}) - S(c \setminus \{i\}), \tag{59}$$

where $S(c \cup \{i\})$ and $S(c \setminus \{i\})$ are the strength of community c with and without node i, respectively. If $F(c,i)$ is positive, node i should belong to community c; however, in order to avoid unstable soft partitions, a specific threshold for the normalized $F(c,i)$ might be set, i.e. node i is a member of community c if the normalized value of $F(c,i)$ is greater than the threshold t.

Algorithm 5 summarizes the aforementioned community adjusting algorithm based on community strength criterion.

Algorithm 5 The Community Adjusting Algorithm

Input: Partition Matrix $\mathbf{U}_{in}$ of size N by c, where N and $c > 0$.
For each community c, find border nodes $\mathbf{B}_c$.
while the border node set is not empty **do**
    For each of the border nodes i in $\mathbf{B}_c$, for all $c \in C$,
    if i is in community k **then**
        $\widehat{C}_k = C_k \setminus \{i\}$
    else
        $\widehat{C}_k = C_k \cup \{i\}$.
    end if
    Calculate $F(\widehat{C}_k, i)$.
    if $F(\widehat{C}_k, i) > 0$ **then**
        $\widehat{U}(i,k) = F(\widehat{C}_k, i)$.
    end if
end while
Normalize membership vector $\widehat{U}$ and store it back to $\widehat{U}$.
Set a threshold t and construct the finalized partition matrix, $\mathbf{U}_{out}$, where $\mathbf{U}_{out}(i,k) = 1$ if and only if $\widehat{U}(i,k) > t$.
return Overlapping community structure $\mathbf{U}_{out}$, with the modularity value

In the literature, such as [65] and [92], we can define another class of centrality measures based on the modularity value, called *community centrality*, where a node that mostly contributes to the modularity value is considered as the most important one. Intuitively, high community centrality node is a node acting like the center of its neighborhood.

3.4 Community Structure Comparison

In the literature, there exist numerous methodologies to identify community structure in a network, such as *mixed integer programming* [100], *tabu search* [55], *simulated annealing* [53], and the spectrum-based methods previously discussed. While these methods provide varieties of community structures with different modularity values, the best community structure could be determined by the one giving the maximum modularity value. However, by relying on such a value, we would not know whether these community structures are alike, or unlike, to what extent.

In order to quantify the difference between community structures, [102] proposed intuitive measures of similarity and dissimilarity by counting co-appearing elements between two different community structures, called the *similarity value* S.

Based on [102], similarity measure s and dissimilarity measure d of sets A and B are defined by Equations (62) and (61).

$$s = \frac{|A \cap B|}{|A \cup B|} \tag{60}$$

$$d = \frac{(|A \cap B'|) \cup (|A' \cap B|)}{|A \cup B|} \tag{61}$$

Since $|A \cup B| = |A \cap B| + (|A \cap B'| \cup |A' \cap B|)$, it is enough to consider one of them as a measure of similarity for comparison. For convenience, we will use the similarity measure s for the development of the similarity value.

In the context of community detection, given two set of community structures $\{A_1, A_2, \ldots, A_K\}$ and $\{B_1, B_2, \ldots, B_M\}$ over the same set of nodes in the network, where $|K|$ does not necessarily equal to $|M|$. The similarity between all pairs of A_i and B_j could be calculated by Equation (62).

$$s_{ij} = \frac{|A_i \cap B_j|}{|A_i \cup B_j|}, \text{ for all } i \in K \text{ and } j \in M \tag{62}$$

The similarity value (S) between two community structures is then defined as the summation of all pairwise similarity values, which could be written as Equation (63).

$$S = \frac{\sum_{i=1}^{max(k,m)} s_i}{max(k,m)}, \tag{63}$$

where $k = |K|$ and $m = |M|$. Notice that it might require a re-ordering for index sets i and j since community matching between these two sets must have been done. In order to maximize similarity value defined by Equation (63), we have to solve a matching problem, which is done by a so-called *Greedy Algorithm* in the original and their following research papers ([28], [29], and [102]). However, this problem is indeed an assignment problem, which could be solved efficiently by simple optimization techniques, such as simplex method. Thus, instead of using greedy algorithm, we solve this problem as if it were an assignment problem.

Algorithm 6 summarizes the calculation of the similarity value (S), which is consequently used in our research for comparison purpose.

Algorithm 6 The Calculation of Similarity Value

1: **Input**: Two sets of community structures $\{A_1, A_2, \ldots, A_K\}$ and $\{B_1, B_2, \ldots, B_M\}$ over the same set of nodes in the network, where $|K|$ does not necessarily equal to $|M|$.
2: For each pair of communities (i, j), calculate $s_{ij} = s_{ij} = \frac{|A_i \cap B_j|}{|A_i \cup B_j|}$.
3: Solve an assignment problem, by maximizing total pairwise similarity values.
4: **return** similarity value (S) and re-ordering index sets

Observation 3.4.1 *Since k does not necessarily equal to m, it might be the case that some communities in one set have no counterparts in the other, though their pairwise similarity values between these two set are positive.*

Observation 3.4.2 *Theoretically, the similarity value defined by Equation* (63) *lies in the range of 0 to 1, where the maximum value of one is attained only when two community structures are the same.*

3.5 Conclusions

In this Chapter, we provide a detailed discussion of a community structure identification algorithms called the *spectrum-based methods* — where eigenvectors are used as guidelines for partitioning a network into communities. In the *leading eigenvector method*, only the principal eigenvector is used to maximize the *modularity value* — a generally accepted measure of community structure wellness, while in the *multi-eigenvector method*, we use as many eigenvectors as possible to identify community structure.

In many cases, nodes might have connections with many communities, which, in turn, makes them as part of several communities. Unfortunately, both the leading and the multi-eigenvector methods are incapable of revealing this kind of structure. In such cases, we may apply a community adjusting algorithm to the network, where a hard partition of non-overlapping community structure is adjusted into a soft partition of the overlapping one by moving border nodes around without hurting the modularity value.

At the end of this chapter, we also provide a discussion of *similarity value* which could be used to quantify the structural difference between community structures.

In Chapter 4, we will reveal the community structure inherited within the *Global Container-Shipping Network* (GCSN) by means of the leading eigenvector method, where

a community is referred to as *trading community*. Based on the resulting community structure, we are able to uncover several interesting facts about the GCSN, such as the patterns of world trade and the strategic roles of terminal ports within a community.

CHAPTER IV

THE CONTAINER PORT CONNECTIVITY INDEX

In this Chapter, we establish a new measure of port importance, called the *Container Port Connectivity Index* (CPCI), to rank global container ports in the *Global Container-Shipping Network* (GCSN). The CPCI is derived based on the *Hyperlink-Induced Topic Search* (HITS) algorithm, which is primarily used for web page ranking. This measure has several advantages over the existing measures, such as the *Liner Shipping Connectivity Index* (LSCI), the *Logistics Performance Index* (LPI), and the three traditional centrality measures in social science. Firstly, while the aforementioned measures are based either on network topology or economic information, the CPCI is capable of satisfactorily integrating both. In addition, it provides separate scores for inbound and outbound, which could be consequently used to analyze the strategic position that terminal ports serve. We also conduct an experiment on the GCSN about how well these container ports connect and form communities using the *Maximization Modularity Method*. Our study reveals that trading communities are less related with geography, but interrelated with trade connections.

4.1 Measures of Port Attractiveness

What makes a container port attractive as a logistics hub? From an operational point of view, a port derives importance from three main factors. The first is the infrastructure required to move containers, such as cranes, quays, hinterland transportation, and so on. Another important factor is location, which includes geography, and, in particular, distance from other ports. Finally, there is connectivity within the network of container shipping: to what degree do shipping liners call at the port?

A traditional measure of port importance is the annual number of TEUs handled. However, this number is merely a local statistic that reflects handling and not patterns of trade flow. Others have proposed more systematic measures of port importance that reflect

something about the position of the port in the network of global container shipping. Examples include *degree centrality*, *closeness centrality*, *betweenness centrality*, or the number of origin-destination pairs the port serves (The *Network Connectivity Index*, NCI [85], and the *Port Cooperative Index*, PCI [54]). While all these measures emphasize connectivity, they do not directly reflect economics.

In terms of economics, the *United Nations Conference on Trade and Development* (UNCTAD) has established an interesting measure for comparing countries' trade competitiveness with respect to maritime logistics and transportation called the *Liner Shipping Connectivity Index* (LSCI). The LSCI is an aggregation of the following five statistics: (i) number of liner services calling, (ii) number of liner companies, (iii) number of ships, (iv) combined capacity of ships in TEUs, and (v) the largest capacity of ships calling [71], computed by a simple normalization scheme. More specifically, for each component, each country's value is normalized by the maximum value of its kind, and the LSCI is then defined by the normalized value of country's average over these five statistics multiplied by 100. Since the LSCI focuses on the accessibility of a country to global trade, economists have found it useful as a joint measure of trade facilitation and maritime connectivity. The LSCI is also found to be strongly correlated with the *Logistics Performance Index* (LPI), which is another index relying on a comprehensive survey of perceptions reported annually by the *World Bank* ([6] and [71]).

While meaningful to some extent, the LSCI is of limited use, especially in a more detailed analysis, as it treats each country as if it were a single location and the entire rest of the world is its counterpart trading partner. In other words, the world container network is reduced to a two-node network, as in Figure 13.

To utilize this idea at a more granular level, we develop a new trade intensity between ports, using the same calculation like that of the LSCI, except for ports rather than the countries. With the LSCI-like measure defined as link weights reflecting direct connectivity between ports, we can establish a network model of container shipping called the *Global Container-Shipping Network* (GCSN), as in Figure 14, in which there is a link from port i to j if there is direct service from port i to j and the weight of such a link indicates rate of

Figure 13: The visualization of the LSCI from network perspective, when we consider the computation of such an index for the United States.

capacity movement between them.

Advantageously, we can use the GCSN to better understand the patterns of world trade, i.e. trading communities, and the relative importance of various ports therein, based on a new measure of port importance called the *Container Port Connectivity Index* (CPCI).

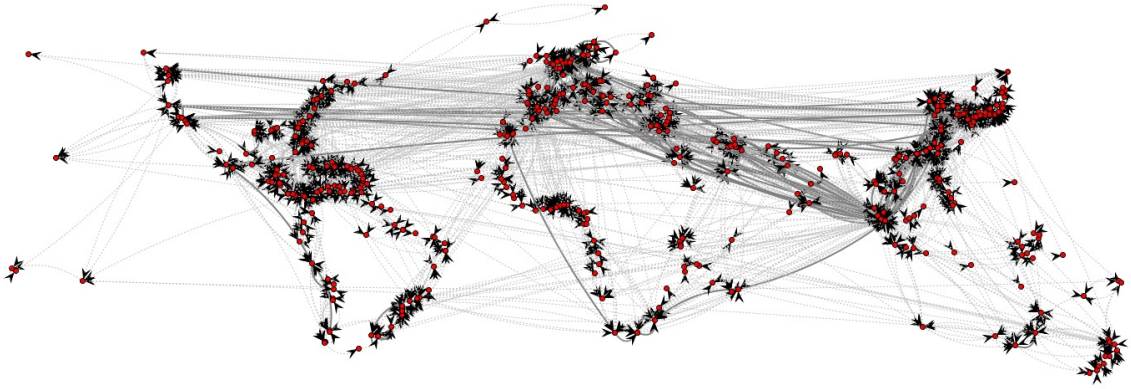

Figure 14: The Global Container-Shipping Network (GCSN), which is constructed based on the LSCI-like measure. In this network, nodes represent ports, links represent rates of container movement between ports, or trade intensity, where the darker the link, the higher the LSCI-like measure.

4.2 The Global Container-Shipping Network

Prior to the establishment of a new index for measuring port importance, we would like to clarify detailed construction of the GCSN and discuss its properties compared with another network of container shipping studied by [44]. While their study concerns the structure of general cargo-shipping network and its subnetworks of containers, tankers, and dry bulk, based on traces of each cargo vessels, ours will focus only on the movement of container

vessels.

In both networks, each node represents a unique container port, but the meaning of a link differs due to different data sources and research objectives. More specifically, in [44], a directed link from port i to j indicates the existence of ships traveling from port i to j at any time during 2007, as reported by `www.sea-web.com`; but, in our network, such a link indicates the existence of mainline, or a scheduled container service traveling from port i to j, as reported by `www.compairdata.com` on 25 September 2011. In other words, our network is a snapshot of container vessel movements on 25 September 2011, while that of [44] is a time-exposure network aggregating all ship movements for a year. Although, the network studied in [44] may include more ephemeral services, such as variants of seasonal services that typically do not co-exist, it does make sense for the bio-invasion problem in which the authors were interested. In contrast, our network suits the objective of studying the nature of container movements, which is more operational.

Based on the aforementioned, we refer to the subnetwork of container vessel movements described by [44] and the snapshot of the scheduled services presented in this work as the *Time-Aggregated Container Network* (TAC network) and the *Scheduled Container Network* (SC network) respectively. While the TAC network and the SC network are similar in general, they differ in serval ways.

Firstly, while both networks have almost the same number of ports, that is, 378 in the TAC network versus 409 in the SC network, the number of links in the TAC network is significantly greater, or about 6,059 links. As a consequence, the mean degree of a port in the TAC network is undoubtedly much greater than that of the SC network, reported as 32.4, where the diameter[1] of the TAC network is reported to be 8 links.

The SC network is rather sparser, with only 2,312 links; it is nevertheless strongly connected[2], with mean degree of 11.3 and diameter of 11 links[3]. Interestingly, with almost 4,000 fewer links, the diameter of the SC network is just three links above that of the TAC

[1]The longest length of the shortest path between any two ports.

[2]For any two ports u and v, u is reachable by some directed path from v, and vice versa.

[3]From Maizuru (Japan) to Fortaleza (Brazil) passing ports of Niigata (Japan), Tomakomai (Japan), Hachinohe (Japan), Busan (South Korea), Savannah (United States), Kingston (Jamaica), Port of Spain (Trinidad and Tobago), Degrad des Cannes (French Guiana), and Belem (Brazil).

network. This difference is likely and it could be explained by the construction of the TAC network. As a time-exposure network, those additional links may come from both seasonal and unplanned service routes of local small feeder lines and short-sea services, which are not expected to significantly reduce network diameter. Because our dataset includes transit times, we can also report the diameter of the SC network measured by travel at sea (ignoring time spent at ports) as 56 days [4].

The mean shortest path in the TAC network is reported as 2.76 links, while in the SC network we can compute it as 4.02 links, with a median of 4 links. Similarly, we can find the time-shortest path of the SC network as 18.6 days, with the median of 19 days. The global clustering coefficient, i.e. the average of local clustering coefficient of all ports, which is a measure of how connected are the immediate neighbors in the network, is also calculated for both networks and reported as 0.52 and 0.40, respectively.

The last but most important difference between these two networks is the definition of link weight. In the TAC network, the weight of a link is simply the sum of gross tonnage of all ships traversing that link in 2007; but, in the SC network, the weight of a link is trade intensity between ports computed by the pairwise-port LSCI previously described. Table 1 lists the twenty links of greatest weight computed by the LSCI-like measure. Interestingly, links among East Asian ports constitute all but one. Notably, Shanghai figures in six of these links, three times as an origin and three times as a destination.

In conclusion, Table 2 gives the summary of the standard topological statistics of each network. Observably, these statistics provide only facts about the networks but not detailed information or insights into geography or economics.

4.3 The Container Port Connectivity Index

Based on the dimension of measurement, all of port attractiveness measures could be classified as either *Network-Based* or *Economics-Based Measure*. The measures in the first group include all three traditional social science measures, together with the NCI and the PCI,

[4]To ship from Honiara, Solomon Islands to Sortland, Norway requires 56 days and traverses 9 links. Any container must pass, en route, through Shanghai, Busan (South Korea), Cristobal (Panama), Manzanillo (Panama), New York, Halifax, Argentia (Newfoundland), and Reykjavik.

Table 1: The twenty links of greatest weight, as determined by the LSCI-like computation. Only one is outside East Asia.

From	To	Weight
Shanghai	Ningbo	1.000
Ningbo	Shanghai	0.987
Hong Kong	Yantian, Shenzhen	0.834
Port Klang	Singapore	0.635
Busan	Shanghai	0.605
Singapore	Hong Kong	0.556
Yantian, Shenzhen	Hong Kong	0.528
Shanghai	Busan	0.523
Hong Kong	Shekou, Shenzhen	0.515
Singapore	Port Klang	0.519
Qingdao	Shanghai	0.505
Ningbo	Hong Kong	0.477
Shanghai	Hong Kong	0.462
Kaohsiung	Hong Kong	0.459
Rotterdam	Hamburg	0.454
Yantian, Shenzhen	Tanjung Pelepas	0.438
Chiwan, Shenzhen	Hong Kong	0.423
Shekou, Shenzhen	Hong Kong	0.421
Qingdao	Ningbo	0.410
Qingdao	Busan	0.408

Table 2: Summary of the comparison statistics of two network models (degree = total number of links, CC = clustering coefficient, Dia. = diameter measured in links, SP = shortest path measured in links).

Network	Ports	Links	Link weight	Avg degree	CC	Dia.	Avg SP
TAC network	378	6,059	Gross tonnage	32.4	0.52	8	2.76
SC network	409	2,312	LSCI-like	11.3	0.40	11	4.02

which require only information regarding network topology, but not the economics, for the computation. In contrast, the measures in the latter group, including the LSCI and the LPI, are based on economics, but not the network structure. While none of the existing measures is capable of reflecting port importance taking both into account, we are able to establish one, which we called the *Container Port Connectivity Index* (CPCI).

The computation of the CPCI is based on the *Hyperlink-Induced Topic Search* (HITS) algorithm [46], which is an eigenvector-based method primarily used for web page ranking[5]. Similar to the HITS algorithm, where a web page is assigned two types of scores, namely, the *hub* and *authority scores*, reflecting its importance as hub and authority page, the CPCI assigns two types of importance scores to each container port, referred to as the *inbound* and *outbound scores*.

In the context of container shipping, a port with high inbound score has greater power to aggregate goods; and, a port with high outbound score has greater power to distribute goods. In addition, a port receives a higher inbound score if many services call from many other ports with high outbound scores, or it is located not too far downstream from them, while a port receives a higher outbound scores if many services depart to many other ports with high inbound scores. For example, St. Vincete, a container port in Cape Verde, receives a relatively high inbound score due to direct service originated from Algeciras, a regional hub with a relatively high outbound score. Although, such a service continues on to Praia, another container port of the Cape Verde islands, it has comparatively lower inbound score since it is located further away from Algeciras.

As measured by the CPCI, Figure 15 visualizes the importance of 409 container ports in the GCSN in terms of inbound.

Our proposed measure of port importance has several advantages over the existing ones.

[5]See Chapter 2 for more details. It is worth noting that while the concept of both the HITS and the Google's PageRank algorithms is the same, where importance scores are derived based on the principal eigenvector, the underlying assumption in each algorithm is quite different. In the PageRank algorithm, we assume that, at a particular page, the user could move freely to any other pages with a specific probability vector, known as the *random-surfer assumption*. In terms of network, this vector may be regarded as link weight vector connecting a web page to the rest. As a consequence, the user at each web page is treated equally important. This assumption does not hold in the GCSN where trade intensity between ports are of different importance.

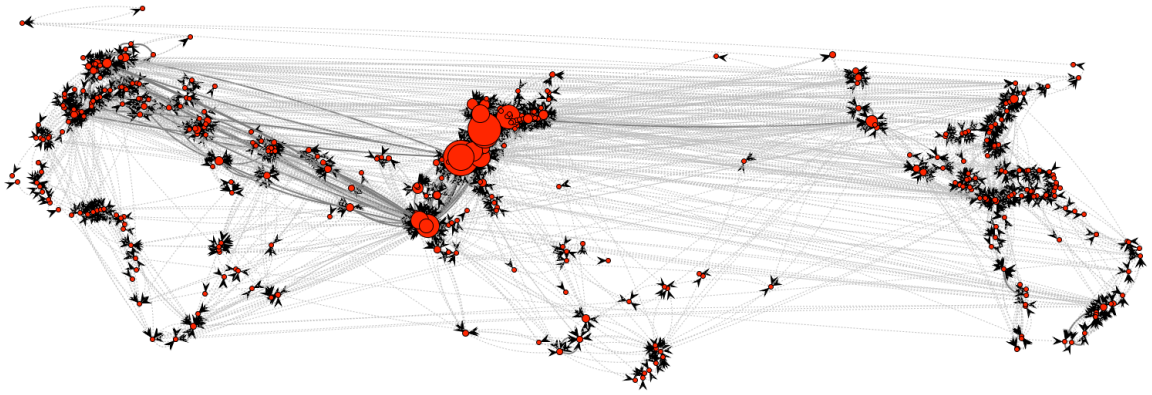

Figure 15: The visualization of the CPCI in the GCSN containing 409 ports. Ports represented by larger disks are scored proportionally higher according to the new measure of port connectivity described in terms of inbound.

Firstly, it is capable of satisfactorily integrating both network structure and economics; and, it is the only one, to the best of our knowledge. In addition, it provides separate scores for inbound and outbound, which could be consequently used to analyze the strategic position that terminal ports serve. It also allows us flexibility to study the relative importance of ports in alternative network settings. More specifically, we can use other interested characteristics of the network as input, and still obtain two well-defined ranked lists of ports preserving all intrinsic properties like those of the CPCI. For example, we may redefine link weights of the GCSN by using trade flow instead of capacity to properly reflect trade intensity between ports.

Later, in Chapter 5, we show that we can extract more detailed information regarding port importance by a simple disaggregation scheme, where the overall port importance score is decomposed into several components — each reflecting its contribution to the overall port importance score. This information, in turn, allows the port authority to comprehend and compare its strategic port importance with competitors' in great detail.

4.3.1 Ranking Ports by the Container Port Connectivity Index

As measured by the CPCI, the most important ports may not necessarily be the ones with the most links. For example, Cartagena receives services from 20 different ports, and Yantian receives only from 18; however, Yantain ranks much higher as scored by the CPCI

with regard to inbound in the GCSN (0.286 versus 0.0036). This is a reflection of fact that the CPCI does not depend only on the number of links but also on link quality and the scores of the ports to which they connect.

Similarly, the most important ports may not necessarily be the busiest ones. Tables 3 and 4 show the CPCI of the twenty ports that scored highest with respect to our measure of *inbound* and *outbound* connectivity, together with ranking by TEUs handled in 2010 for comparison. The ports of East Asia dominate with respect to either measure. Even though Shanghai handled more TEUs, Hong Kong ranks higher by the CPCI, presumably because it is better connected within the GCSN[6].

On the other hand, our ranking appears to neglect the high-volume European ports such as Rotterdam, Antwerp, and Hamburg, as well as the busy Mideast port of Dubai, but this is because they are more isolated from other big ports. In contrast, the big East Asian ports are well-connected with the rest of the world — and with each other, which further increases their scores based on our algorithm.

Figure 16 plots scores of all 409 ports. Several stand out for the significant differences between inbound and outbound scores, and these differences illustrate how the the CPCI can make structural distinctions about the position of a port in the network. For example, Yokohama has a higher outbound than inbound score because it receives from smaller ports but ships to major Asian ports such as Shanghai, Ningbo, Yantian, Xiamen, Kiaosiung, and Busan.

A more elaborate example is provided by Los Angeles and Long Beach, which have inbound scores that are relatively high in comparison to outbound scores. This reflects the fact that these are the two main ports of entry for products manufactured in East Asia. To reduce in-transit inventory, powerful retailers in North America insist that their freight be the last loaded out of Asia and the first unloaded in North America, and so there are many direct links from big Asian ports into Los Angeles and Long Beach. Services that have traversed the Pacific Ocean to call at Los Angeles or Long Beach then typically call

[6]The ranking by volume combines several of the Shenzhen ports, including Yantian, Chiwan, Shekou,and Da Chan Bay, into one, ranked fourth in volume.

Table 3: All but two of the twenty highest-scoring ports by the CPCI (inbound) are in Asia. (Volume rankings are based on the number of TEUs transported through the ports in 2010 [20].)

Rank	Port	Inbound	Outbound	Country	By volume
1	Hong Kong	0.4080	0.4035	China	3
2	Shanghai	0.3726	0.3475	China	1
3	Ningbo	0.3040	0.3419	China	6
4	Yantian	0.2861	0.2646	China	
5	Busan	0.2515	0.2415	South Korea	5
6	Singapore	0.2456	0.3420	Singapore	2
7	Kaohsiung	0.2054	0.2009	Taiwan	12
8	Chiwan	0.1973	0.1905	China	
9	Xiamen	0.1933	0.1841	China	19
10	Shekou	0.1859	0.1614	China	
11	Port Klang	0.1748	0.1935	Malaysia	13
12	Qingdao	0.1725	0.1593	China	8
13	Nansha	0.1369	0.1109	China	
14	Tanjung Pelepas	0.1289	0.1134	Malaysia	16
15	Gwangyang	0.1289	0.1182	South Korea	
16	Los Angeles CA	0.0927	0.0286	USA	17
17	Long Beach CA	0.0917	0.0187	USA	18
18	Xingang/Tianjin	0.0890	0.0802	China	11
19	Da Chan Bay	0.0829	0.0809	China	
20	Laem Chabang	0.0818	0.0633	Thailand	22

Table 4: All but one of the twenty highest-scoring ports by the CPCI (outbound) are in Asia.

Rank	Port	Inbound	Outbound	Country	By volume
1	Hong Kong	0.4080	0.4035	China	3
2	Shanghai	0.3726	0.3475	China	1
3	Singapore	0.2456	0.3420	Singapore	2
4	Ningbo	0.3040	0.3419	China	6
5	Yantian	0.2861	0.2646	China	
6	Busan	0.2515	0.2415	South Korea	5
7	Kaohsiung	0.2054	0.2009	Taiwan	12
8	Port Klang	0.1748	0.1935	Malaysia	13
9	Chiwan	0.1973	0.1905	China	
10	Xiamen	0.1933	0.1841	China	19
11	Shekou	0.1859	0.1614	China	
12	Qingdao	0.1725	0.1593	China	8
13	Gwangyang	0.1289	0.1182	South Korea	
14	Yokohama	0.0619	0.1147	Japan	36
15	Tanjung Pelepas	0.1289	0.1134	Malaysia	16
16	Nansha	0.1369	0.1109	China	
17	Oakland	0.0132	0.0883	USA	
18	Da Chan Bay	0.0829	0.0809	China	
19	Xingang/Tianjin	0.0890	0.0802	China	11
20	Cai Mep	0.0517	0.0750	Viet Nam	28

at Oakland before returning to the large ports of Asia. Consequently, Oakland has a high outbound score in comparison to its inbound score. This is a general pattern that may be observed along many service loops; ports that are immediately downstream from important ports tend to have higher inbound scores, while ports toward the end of the loop tend to have higher outbound scores.

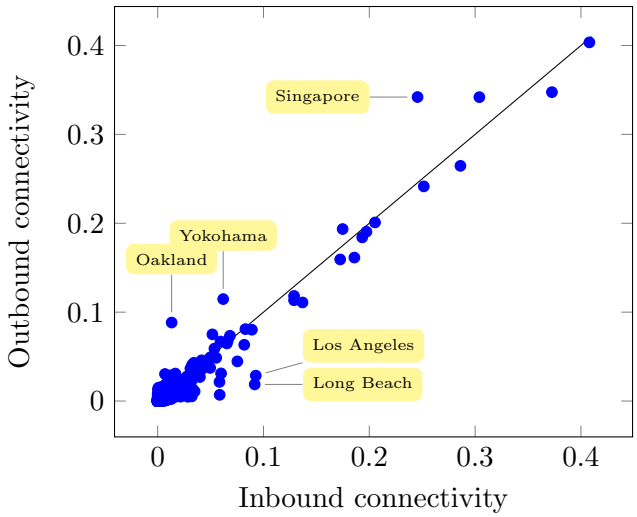

Figure 16: As computed by the CPCI, those container ports for which inbound and outbound scores fall in the lower right are inbound-dominant and those in the upper left are outbound-dominant.

4.3.2 North American Ports

Table 5 shows that, among the ports of North America, the west coast ports, led by Los Angeles and Long Beach, dominate by the measure of inbound connectivity, reflecting the many services that come directly from the great manufacturing centers of East Asia. Moreover, many of the west coast ports score much higher with respect to inbound connectivity than to outbound.

New York is the only port on the east coast to score highly with respect to inbound scores. But Table 6 shows that east coast ports such as Savannah are more competitive with respect to outbound scores. It will be interesting to see how these rankings change after the widening of the Panama Canal is completed in 2014.

Table 5: All but one of the top ten North American ports measured by the CPCI (inbound) are on the west coast.

Rank	Port	Inbound	Outbound
1	Los Angeles CA	0.0927	0.0286
2	Long Beach CA	0.0917	0.0187
3	New York NY/NJ	0.0586	0.0070
4	Lazaro Cardenas, MEX	0.0349	0.0108
5	Manzanillo, MEX	0.0325	0.0406
6	Tacoma WA	0.0305	0.0084
7	Prince Rupert BC	0.0285	0.0048
8	Vancouver BC	0.0260	0.0249
9	Seattle WA	0.0231	0.0207
10	Oakland CA	0.0132	0.0883

Table 6: Four of the top ten North American ports ranked by the CPCI (outbound) are on the east coast.

Rank	Port	Inbound	Outbound
1	Oakland CA	0.0132	0.0883
2	Manzanillo, MEX	0.0325	0.0406
3	Savannah GA	0.0122	0.0289
4	Los Angeles CA	0.0927	0.0286
5	Vancouver BC	0.0260	0.0249
6	Seattle WA	0.0231	0.0207
7	Long Beach CA	0.0917	0.0187
8	Boston MA	0.0007	0.0150
9	Wilmington NC	0.0008	0.0133
10	Miami FL	0.0030	0.0125

4.3.3 Panamá as a Transshipment Hub

The ports of Panama lead their region in terms of connectivity: Balboa has scores of 0.0291 and 0.0208 for inbound and outbound respectively; Manzanillo has scores of 0.0184 and 0.0213; and Cristobal has scores of 0.0182 and 0.0082.

The Panama Canal Authority currently operates a transcontinental railroad that makes it possible to move containers between the Panamanian ports on the Pacific and Atlantic sides. Currently, it takes at least three hours to move containers from one port stack to another (one hour to load the train; one hour of travel time; one hour to unload the train); and because of the delay between trains, eight hours is more typical. If the transit time could be reliably reduced, the ports at each end of the Canal might be considered as one, in which case the inbound and outbound scores of the aggregated port would become 0.0455 and 0.0313 making it be one of the highest scoring outside East Asia (specifically, thirty-sixth in inbound and forty-second in outbound). Furthermore, its connectivity would dominate that of the regional competitors such as Kingston, Jamaica (0.0037 and 0.006) and Freeport, Bahamas (0.0026 and 0.0044).

4.3.4 Comparison With Other Measures

Fundamentally, we may evaluate the centrality of a vertex within a network by *degree centrality*, which, in our context, tells from how many other ports a port receives direct shipments (in-degree) or to how many others it sends direct shipments (out-degree). Tables 7 and 8 report the twenty most central ports measured by in-degree and out-degree centrality, together with the CPCI ranking. While interesting, these measures neglect economic issues, such as the volume of trade along each link and interrelationship among ports within the network. Literally, it merely records the fact of trade, but not the importance of ports in the GCSN.

Another fundamental means of evaluating port centrality is by distance: *is a port close to other ports?* Shorter travel times mean less operating cost for the shipping company and less in-transit inventory for the shipper or consignee. In such a case, *closeness centrality*, the reciprocal of the sum of shortest distances from a vertex to all other vertices, may be

Table 7: The twenty most central ports measured by in-degree centrality, together with the CPCI ranking.

Port	**Country**	**In-Degree**	**Outbound**	**Inbound**
Singapore	Singapore	56	3	6
Hong Kong	China	44	1	1
Port Klang	Malaysia	41	8	11
Busan	South Korea	39	6	5
Shanghai	China	35	2	2
Kaohsiung	Taiwan	35	7	7
Algeciras	Spain	30	32	44
Tanjung Pelepas	Malaysia	30	15	14
New York NY/NJ	United States	28	113	28
Rotterdam	Netherlands	27	24	24
Jeddah	Saudi Arabia	25	26	31
Tokyo	Japan	24	22	23
Ningbo	China	23	4	3
Antwerp	Belgium	23	37	42
Keelung	Taiwan	22	23	27
Dubai, Jebel Ali	United Arab Emirates	22	28	30
Qingdao	China	22	12	12
Cartagena	Colombia	20	146	127
Tanger	Morocco	20	84	51
Yokohama	Japan	20	14	25

Table 8: The twenty most central ports measured by out-degree centrality, together with the CPCI ranking.

Port	**Country**	**Out-Degree**	**Outbound**	**Inbound**
Singapore	Singapore	53	3	6
Shanghai	China	41	2	2
Hong Kong	China	40	1	1
Port Klang	Malaysia	40	8	11
Busan	South Korea	40	6	5
Kaohsiung	Taiwan	33	7	7
Tanjung Pelepas	Malaysia	33	15	14
Valencia	Spain	27	71	74
Jeddah	Saudi Arabia	24	26	31
Yantian	China	24	5	4
Algeciras	Spain	23	32	44
Ningbo	China	23	4	3
Antwerp	Belgium	23	37	42
Le Havre	France	23	41	48
Cartagena	Colombia	22	146	127
Oakland CA	United States	22	17	80
Tanger	Morocco	21	84	51
Kobe	Japan	21	21	22
Tokyo	Japan	20	22	23
Dubai, Jebel Ali	United Arab Emirates	20	28	30

considered as an appealing measure. Table 9 shows the twenty most central ports measured by closeness. Interestingly, most container ports have approximately the same closeness centrality. Although closeness centrality may be interesting as it includes time as part of centrality, it neglects the fact that container flow does not always follows the shortest distance. In addition, it treats all the links from either big or small ports with equal weight, which seems questionable in practice.

Table 9: The twenty most central ports measured by closeness centrality, together with the CPCI ranking.

Port	**Country**	**Closeness** (10^{-4})	**Outbound**	**Inbound**
Singapore	Singapore	9.2937	3	6
Port Klang	Malaysia	9.1996	8	11
Tanjung Pelepas	Malaysia	8.9606	15	14
Hong Kong	China	8.8968	1	1
Kaohsiung	Taiwan	8.7566	7	7
Le Havre	France	8.7566	41	48
Yantian	China	8.7184	5	4
Savannah GA	United States	8.7184	46	85
Rotterdam	Netherlands	8.6356	24	24
Manzanillo	Panama	8.5543	56	71
Valencia	Spain	8.5034	71	74
Algeciras	Spain	8.4317	32	44
Port Said	Egypt	8.3963	29	35
Antwerp	Belgium	8.3542	37	42
Busan	South Korea	8.3333	6	5
Chiwan	China	8.2305	9	8
Shanghai	China	8.2237	2	2
Bremerhaven	Germany	8.2102	43	76
Jeddah	Saudi Arabia	8.0906	26	31
Ningbo	China	8.0645	4	3

The last benchmarking centrality measure for container ports is betweenness, i.e. the number of shortest paths within the network on which the vertex lies, as reported in Table 10. We find that the twenty ports of greatest betweenness centrality in the SC network is quite different from those of the TAC network, as shown in Table 11.

A systematic difference seems to be that some among the twenty ports of highest betweenness in the TAC network are ranked much lower in the SC network. Consider, for

example, the following ports, where the first ranking is that within the TAC network and the second is that within the SC network: Jebel Ali 5 (20), Barcelona 8 (49), Bremerhaven 9 (26), Hamburg 10 (58), Tacoma 11 (313), Malaga 12 (162), Antwerp 13 (34), Piraeus 17 (160), Felixstowe 19 (40), Colombo 20 (63). We speculate that these ports had seasonal services, which would have added artificially to their betweenness by suggesting paths that did not actually exist.

Table 10: The twenty most central ports measured by betweenness centrality, together with the CPCI ranking.

Port	**Country**	**Betweenness** (10^{-2})	**Outbound**	**Inbound**
Singapore	Singapore	13.4482	3	6
Algeciras	Spain	9.0277	32	44
Busan	South Korea	8.9076	6	5
Shanghai	China	8.5991	2	2
Hong Kong	China	6.5738	1	1
Cartagena	Colombia	6.3407	146	127
Port Klang	Malaysia	6.2749	8	11
Balboa	Panama	5.6483	60	55
Tanjung Pelepas	Malaysia	5.4653	15	14
New York NY/NJ	United States	5.4225	113	28
Valencia	Spain	5.0959	71	74
Port Said	Egypt	4.8993	29	35
Kingston	Jamaica	4.8179	129	124
Savannah GA	United States	4.8110	46	85
Manzanillo	Panama	4.3594	56	71
Santos	Brazil	4.2839	61	52
Le Havre	France	4.0957	41	48
Rotterdam	Netherlands	3.9718	24	24
Tanger	Morocco	3.8974	84	51
Dubai, Jebel Ali	United Arab Emirates	3.7566	28	30

In comparison with the LSCI defined for countries, we can only compare the rankings from our indices with those of countries having a single dominant port. In doing so, we identified 64 container ports that were, within our data source, unique within their country, and then compared rankings by the 2011 LSCI and the inbound and outbound versions of the CPCI. The results appear in Table 12 and are generally consonant: those ranked among the top ten by LSCI are among the top twenty by the CPCI, either inbound or outbound.

Table 11: The twenty most central ports measured by betweenness centrality of the SC network comparing with those of [44].

Port	**Country**	**SC Network**	**TAC Network**
Singapore	Singapore	1	4
Algeciras	Spain	2	6
Busan	South Korea	3	18
Shanghai	China	4	1
Hong Kong	China	5	
Cartagena	Colombia	6	3
Port Klang	Malaysia	7	
Balboa	Panama	8	3
Tanjung Pelepas	Malaysia	9	
New York NY/NJ	United States	10	
Valencia	Spain	11	
Port Said	Egypt	12	14
Kingston	Jamaica	13	
Savannah GA	United States	14	
Manzanillo	Panama	15	3
Santos	Brazil	16	15
Le Havre	France	17	7
Rotterdam	Netherlands	18	16
Tanger	Morocco	19	
Dubai, Jebel Ali	United Arab Emirates	20	5

The differences in ranking between Gothenburg and Gdansk again illustrate how our suggested index captures the global structure of the network. Gdansk ranks relatively high in inbound strength because it receives shipments directly from Hamburg but ships only to the lesser port of Aarhus, which accounts for its relatively lower ranking in outbound strength. On the other hand, Gothenburg receives freight only from Aarhus, but it ships to the more significant port of Bremerhaven, from which it derives a higher outbound score.

Table 12: Ranks among those countries represented by a single port, the LSCI, and the CPCI, are in general agreement.

Port	**by LSCI**	**by The CPCI (inbound)**	**by CPCI (outbound)**
Singapore	1	1	1
Rotterdam	2	2	2
Colombo	3	3	3
Malta	4	6	11
Beirut	5	4	10
Piraeus	6	7	6
Buenos Aires	7	18	26
Karachi	8	8	5
Gothenburg	9	35	20
Gdansk	10	15	57

4.4 Properties of the CPCI

Evidently, the CPCI has been proven to be a useful tool in a new ranking scheme as it allows us to draw a systematic inference about the importance of a port, as well as the patterns of trade flow within the network. In this section, we will provide some interesting properties of the CPCI which might be useful for further inferences.

4.4.1 Degree, Distance, and Connectedness

One interesting property of the CPCI is that, among degree, distance, and connectedness, port connectedness is the most crucial factor driving the CPCI — this is the reason why we name such an index as the connectivity one. In order to explore how degree, distance, and connectedness could affect the CPCI, as well as other classical centrality measures, let us

consider the network shown in Figure 17, where the links shown are bidirectional with equal weights. Port S_m is the center of the star graph whose degree is m, and each path of S_m comprises a line graph of l links connected with a complete graph K of size n. In addition, we define port c, a member of the complete graph that is connected with the line graph, as the *connection port* which serves as a gateway from the outside world to a well-connected and dense subgraph.

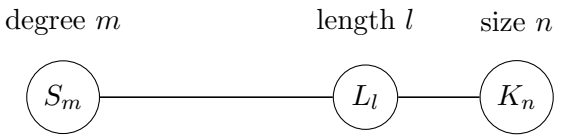

Figure 17: A theoretical network of ports comprising of three different graphs, that is, a star graph of degree m, m line graphs of l links, and m complete graphs of size k. Since the underlying network is symmetric and all m paths connected with port S_m have the same structure, each path will be scored equally position-wise.

By construction, the center port is initially set as the most central one in terms of degree. In addition, as it is located at the center of the whole network, both its betweenness and closeness would also be the highest. For simplicity, we denote the configuration of the underlying network by the triplets (S_m, L_l, K_n), and define an importance ratio as the relative importance of the connection port c to that of the center port S_m — more specifically, the higher the ratios, the more important the connection port.

Any changes in the CPCI ratio, betweennness ratio, and closeness ratio, are observed when the parameters m, l, and n, have been altered. Interesting observations are as follows.

i. When the length l is fixed, as the complete graph grows larger, i.e. n has been increased, the CPCI of the connection port quickly dominates that of the center port, especially when the length l is also increased (Figures 18 – 20).

   Betweenness and closeness ratios also increase as the complete graph grows larger, which is expected, since the connection port is just one link away from a new member of the complete graph, but it is l links away from the center port. However, these ratios decrease as the length l increases, since it would make each path farther away

from the others (Figures 21 – 26).

ii. Similarly, we can infer that, when the complete graph is considerably large, the greater the length of the line graph, the smaller the CPCI of the center port.

iii. Given that the degree of the center port is the same as the size of the complete graph, the center port tends to significantly lose its importance to the connection port as the degree of the center port and the size of the complete graph grow at the same level (Figure 27). In contrast, both betweenness and closeness ratios keep decreasing as the network grows larger (Figures 28 and 29).

iv. It requires a considerable number of degree for the center port to regain its rank back, while it requires only a very few number increasing in either the length of the line graph or the size of the complete graph to outrank the center port.

Based on the aforementioned results, we can conclude that port connectedness, or port connectivity, is the one that drives the CPCI, not the degree. This distinct property of the CPCI clearly distinguishes itself from other measures and, unquestionably, is the reason why we name such a measure as the *Container Port Connectivity Index*.

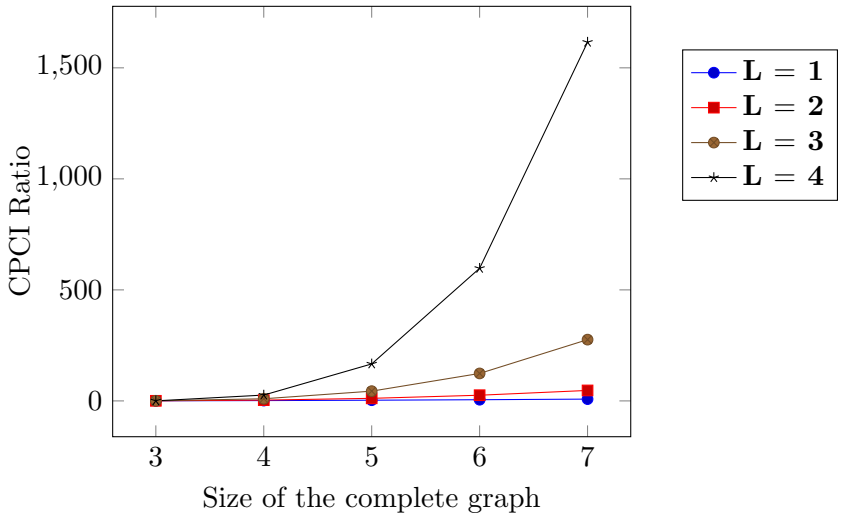

Figure 18: Relationship between the CPCI ratio and the size of the complete graph when the degree of star graph is $2(n-1)$.

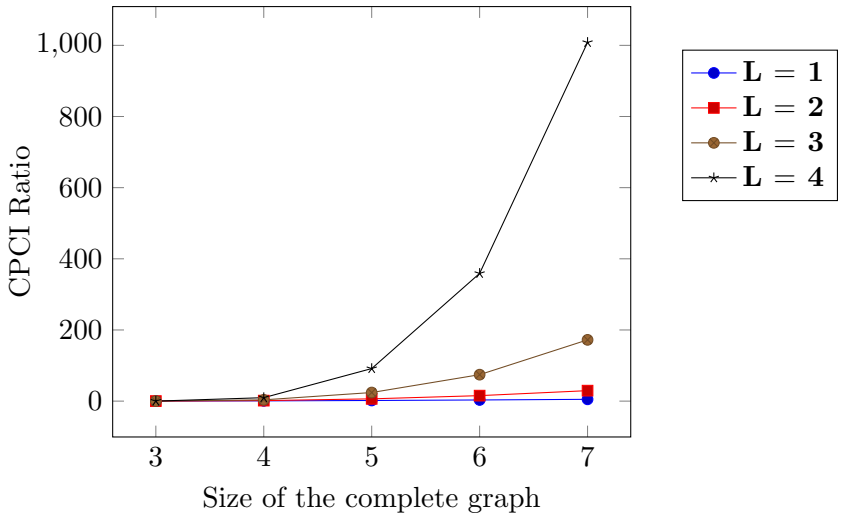

Figure 19: Relationship between the CPCI ratio and the size of the complete graph when the degree of star graph is $3(n-1)$.

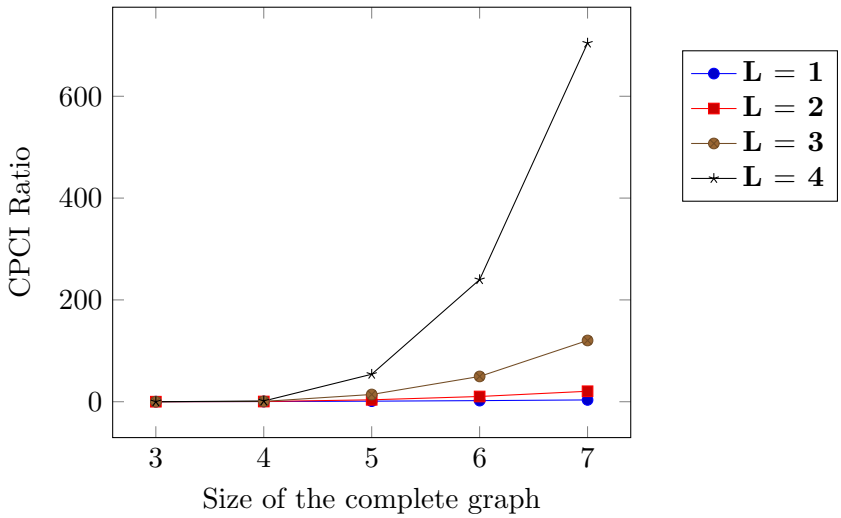

Figure 20: Relationship between the CPCI ratio and the size of the complete graph when the degree of star graph is $4(n-1)$.

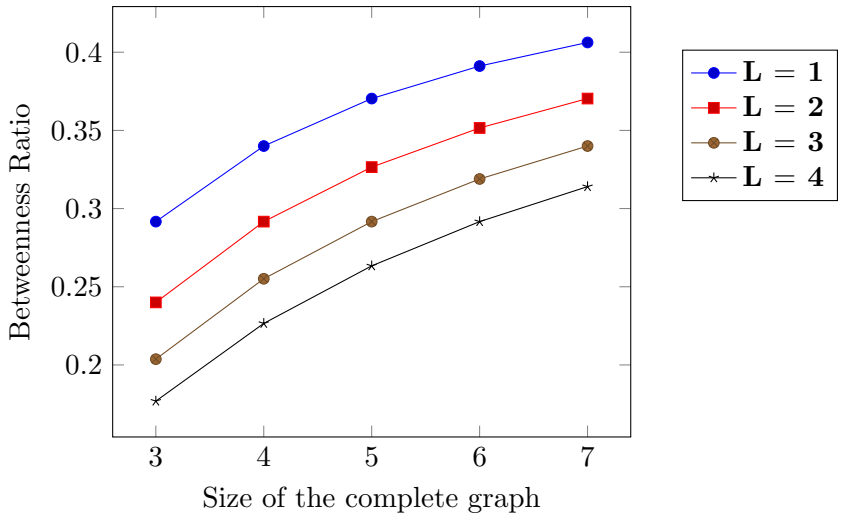

Figure 21: Relationship between betweenness ratio and the size of the complete graph when the degree of star graph is $2(n-1)$.

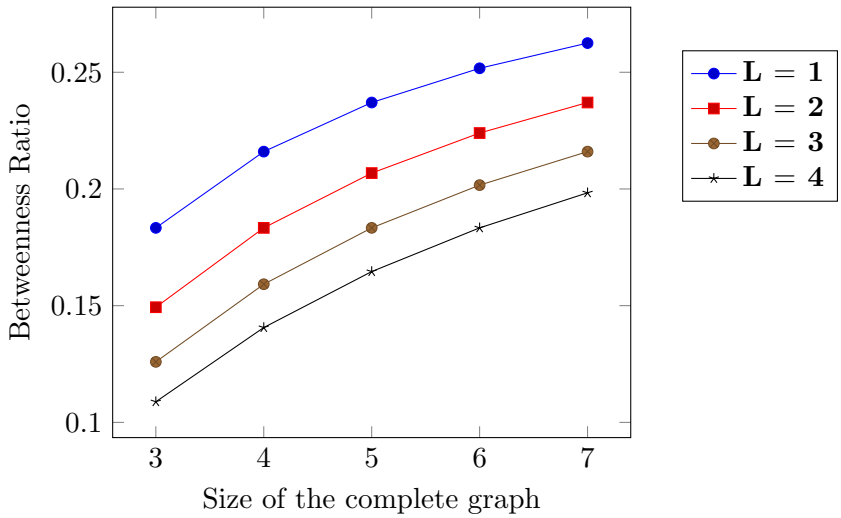

Figure 22: Relationship between betweenness ratio and the size of the complete graph when the degree of star graph is $3(n-1)$.

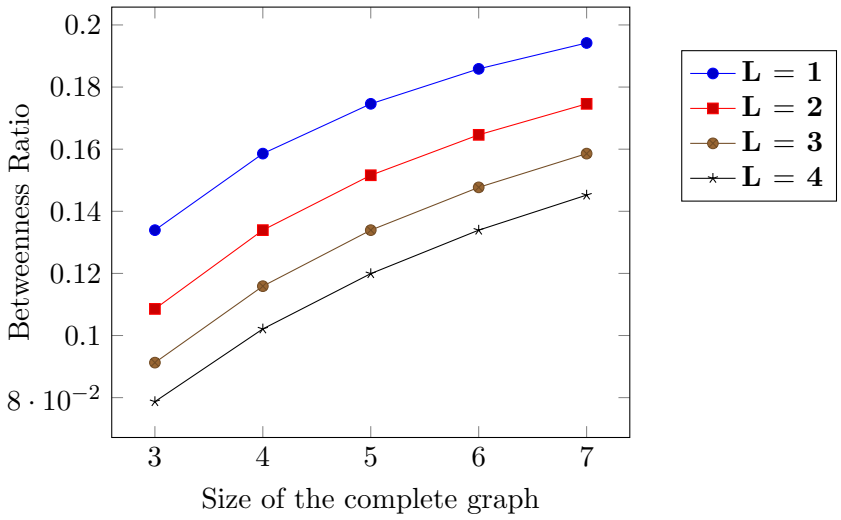

Figure 23: Relationship between betweenness ratio and the size of the complete graph when the degree of star graph is $4(n-1)$.

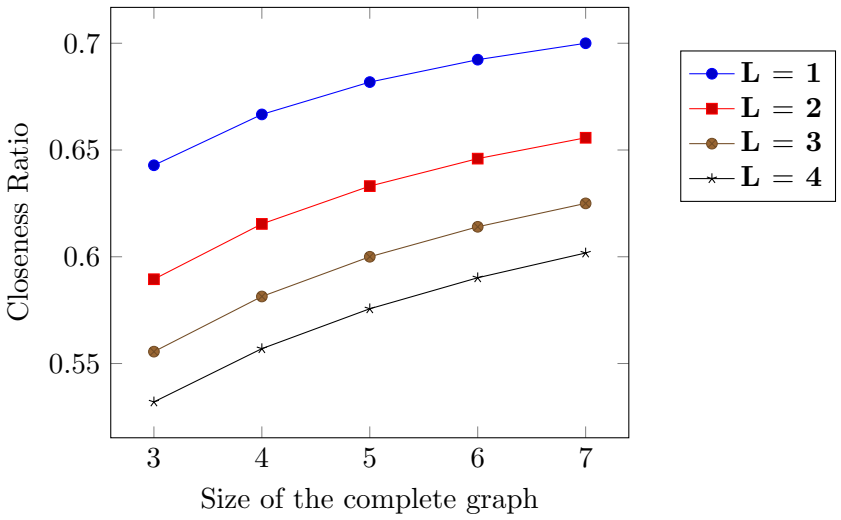

Figure 24: Relationship between closeness ratio and the size of the complete graph when the degree of star graph is $2(n-1)$.

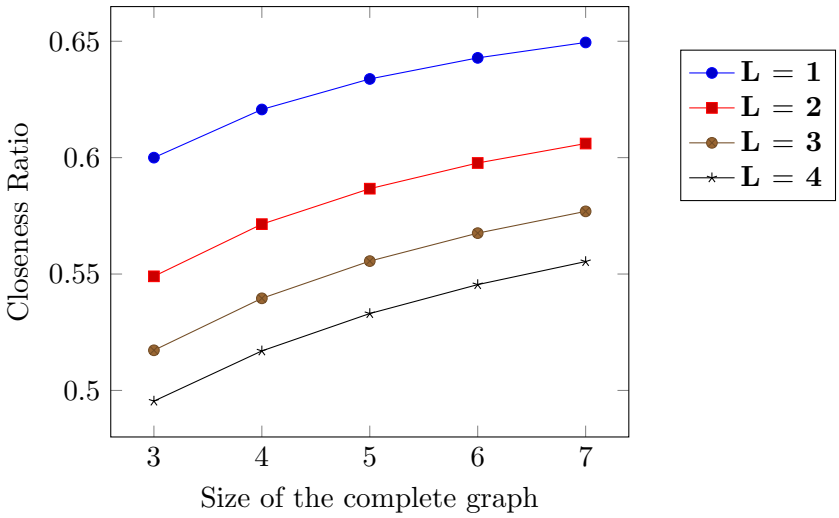

Figure 25: Relationship between closeness ratio and the size of the complete graph when the degree of star graph is $3(n-1)$.

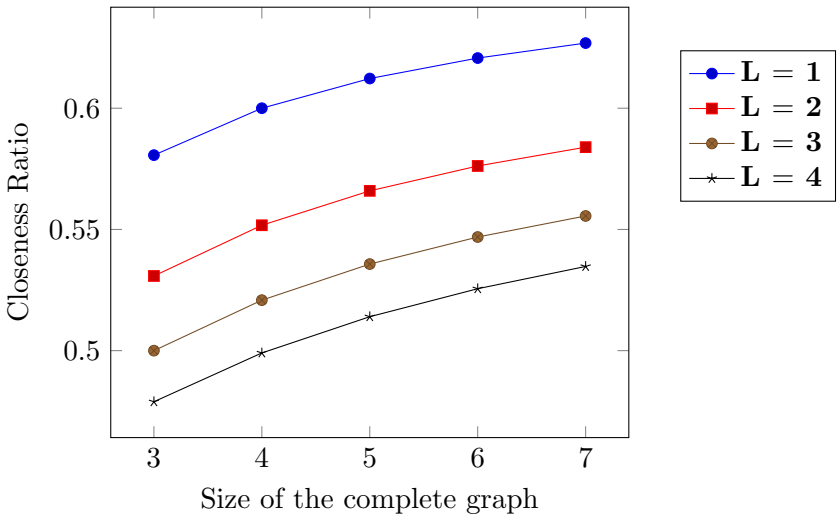

Figure 26: Relationship between closeness ratio and the size of the complete graph when the degree of star graph is $4(n-1)$.

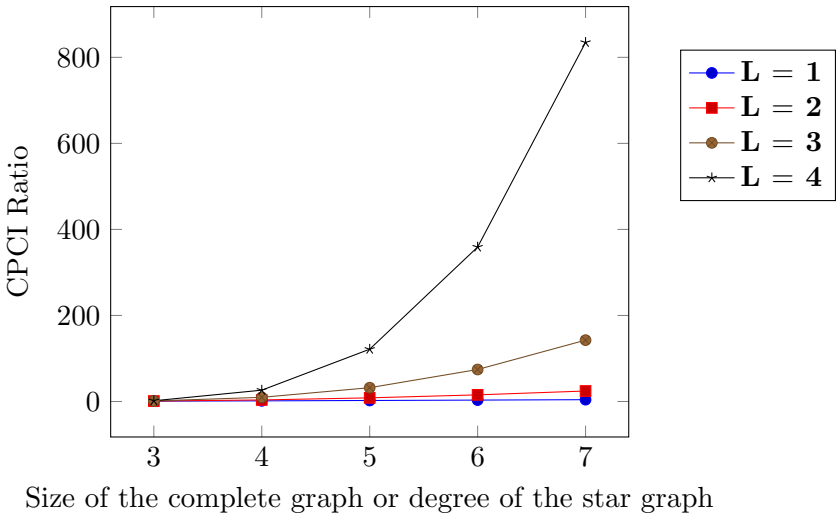

Figure 27: Relationship between CPCI ratio and the size of the complete graph, or the degree of the star graph.

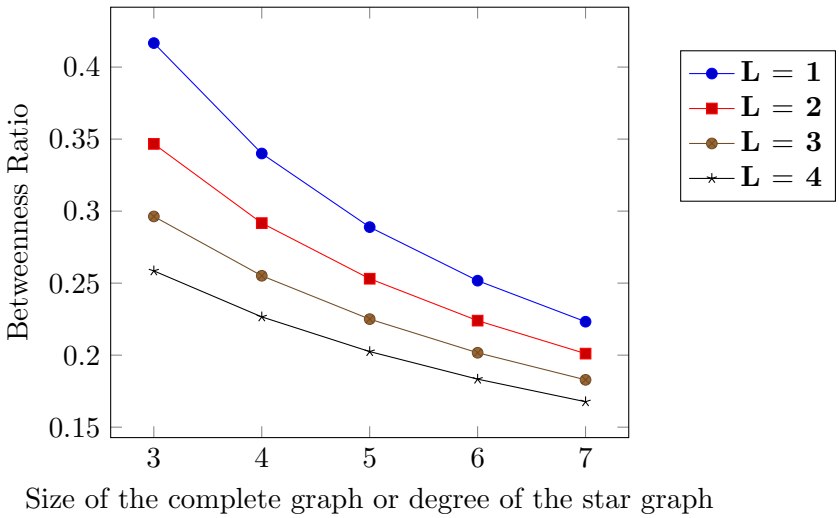

Figure 28: Relationship between betweenness ratio and the size of the complete graph, or the degree of the star graph.

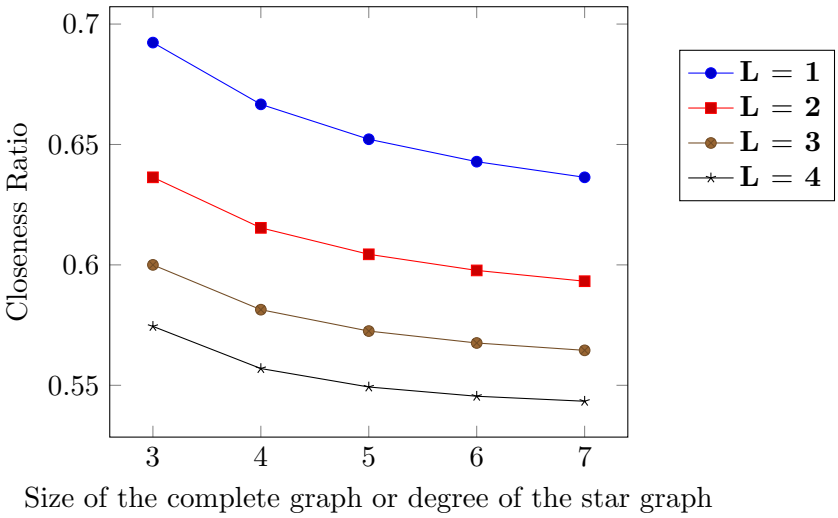

Figure 29: Relationship between closeness ratio and the size of the complete graph, or the degree of the star graph.

4.4.2 Link Modification

Another interesting property of the CPCI concerns the change of the CPCI as links have been modified. Typically, when a particular link has been added or removed, the CPCI is expected to change, not only those of the ports directly connected with such a link but also those of the rest, since the CPCI depends on the global structure of the network.

For example, consider a network shown in Figure 30, where link $(3, 8)$ is the one to be removed. V_1 and V_2 show the connectivity scores of all ports, i.e. before and after the removal of link $(3, 8)$.

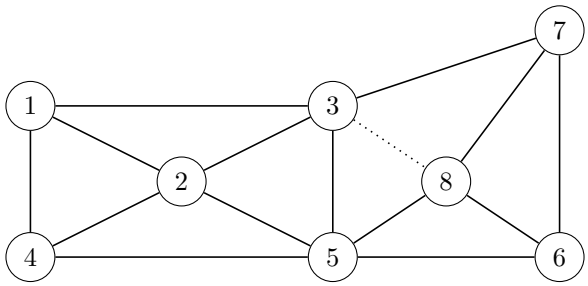

Figure 30: An example network for evaluating the effect of the removal of link $(3, 8)$, where all links are bidirectional with unity link weight.

$$V_1 = [0.2819\ 0.3732\ 0.4492\ 0.2819\ 0.4492\ 0.2819\ 0.2819\ 0.3732]$$

$$V_2 = [0.3181\ 0.4197\ 0.4051\ 0.3324\ 0.4715\ 0.2790\ 0.2647\ 0.2790]$$

As each of these vectors is a unit vector, we can systematically define and compare the effect of link modification by the difference between the squared value of these two vectors. Table 13 shows the result of such a procedure.

Table 13: The observed differences of the squared value of the two different CPCI vectors, given that link $(3, 8)$ is the one to be removed from the network shown in Figure 30.

Ports and Scores	V_4^2	V_1^2	$V_4^2 - V_1^2$
1	0.1012	0.0795	0.0217
2	0.1762	0.1393	0.0368
3	0.1641	0.2017	-0.0376
4	0.1105	0.0795	0.0310
5	0.2223	0.2017	0.0205
6	0.0779	0.0795	-0.0016
7	0.0701	0.0795	-0.0094
8	0.0779	0.1393	-0.0614
Sum	1	1	

From Table 13, with the removal of link $(3, 8)$, port 5 has become the most central port in the network as connections between the rightmost and the leftmost ports have found themselves convenient by passing port 5, while port 8 significantly loses its importance due to direct connectivity loss with port 3.

Based on the aforementioned comparison, one may evaluate and identify the most important link to any interested port by a sequential link removal evaluation. Interestingly, we have found that some indirect links may have greater effect than that of the direct ones. For example, consider the network shown in Figure 31, where, in this example, we are identifying the most influential link associated with port 13.

As ports 14 and 15 are well-connected, these two ports are unsurprisingly important ports in the network with the importance scores of 0.324 and 0.533, respectively.

By sequentially removing direct links of port 13, that is, (9,13), (12,13), and (13,14), we

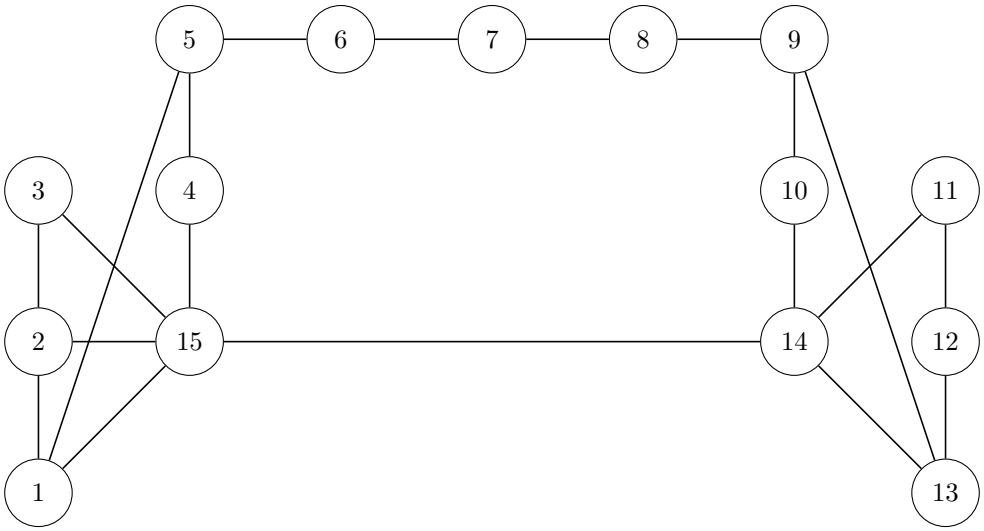

Figure 31: An example network for identifying the most influential link to port 13.

can evaluate the effect of these link removals to the importance score of port 13 as reported below.

Port	**(9,13)**	**(12,13)**	**(13,14)**
13	-0.0164	-0.0144	-0.0306

Since port 14 may be regarded as a hub port, by removing link (13,14), the connectivity of port 13 is significantly reduced — port 13 would be located at greater distance from the rest of the network. In contrast, deleting link (12,13) has less effect on port 13 since port 12 itself is far less important compared to that of port 14. In addition, port 13 could still be reached from well-connected ports like port 9 or 14.

However, we have found that some indirect links might pose greater threats to port 13 than the direct ones. More specifically, the removal of link (14,15), which clearly reduces connectivity of port 13 as flow is required to travel a longer distance between the left and right of the network. Based on our computation, indirect link (14,15) has been found as the most influential link to port 13 with the removal effect of -0.0316.

Let us consider another example shown in Figure 32, where we are identifying whether the most important link to port 15 is direct or indirect. For better visualization, we will use the network shown in Figure 32b to represent the original network shown in Figure 32a. In

addition, the darker link is the one that is identified as the most influential link to port 15.

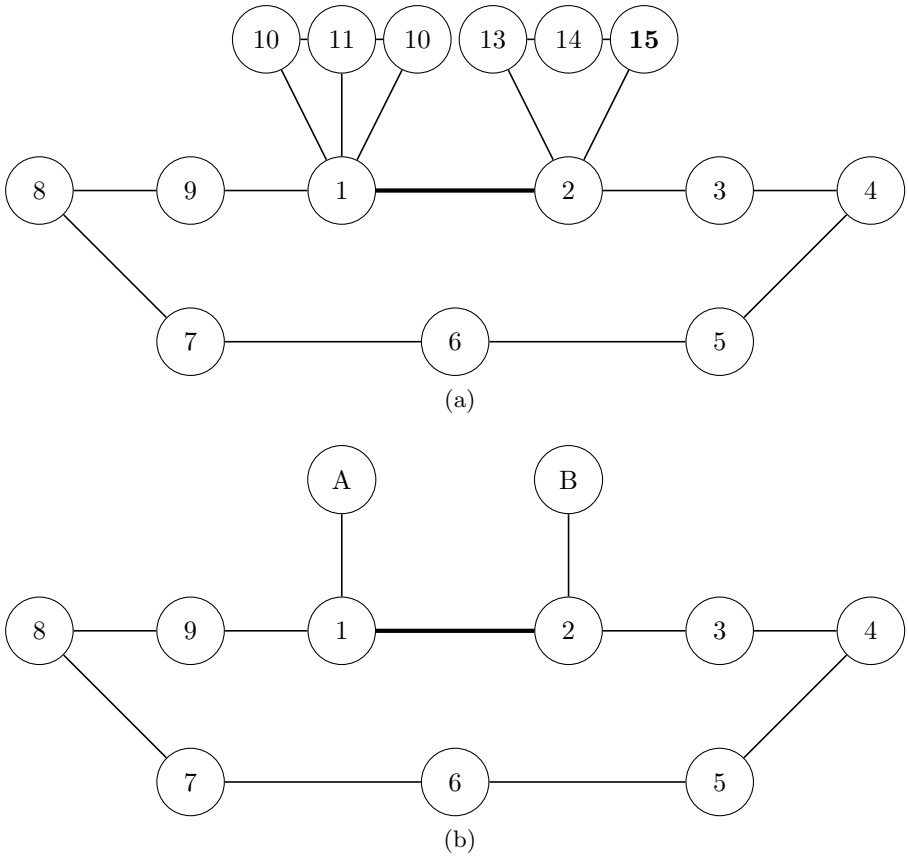

Figure 32: A network of 15 ports used to identify the most influential link to port 15 (the darker link), where Figure 32b represents Figure 32a by replacing groups of nodes as A and B.

Figure 33 shows the changes of the most influential link to port 15 as the position of B changes. Interestingly, the most influential link tends to be the one that is crucial for the flow moving from port 15 to a more important port 1. This result reflects that fact that the CPCI depends on global structure of the network, and not on the local connectivity to its immediate neighbors.

4.5 Trading Communities

Beside the CPCI which ranks the container ports around the world based on their inbound and outbound connectivity, one might be interested in how the GCSN is arranged and resolved into communities based on trade patterns, which is herein referred to as *Trading*

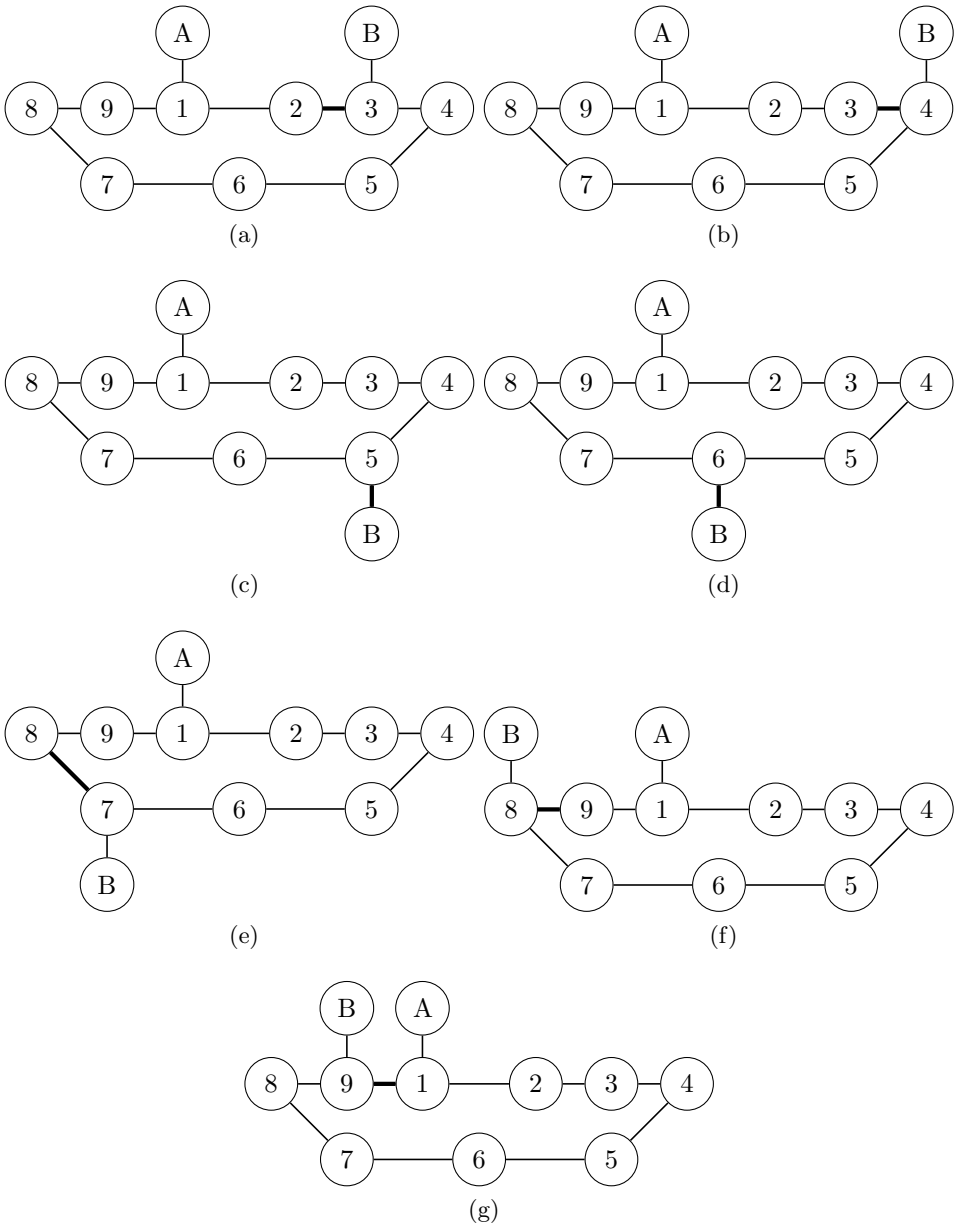

Figure 33: The changes of the most influential link (darker link) to port 15 as the position of B changes.

Community.

4.5.1 Identifying Trading Communities

The concept of trading community in this context is similar to that of community structure in social science's network analysis. More specifically, a *community* within a network is a collection of vertices with dense and strong connections among themselves but sparser and

weaker connections to other vertices. Although there exist several community detection algorithms in the literature[7], we will rely on the *Modularity Maximization Method* [66]. In this method, the modularity Q is defined as the difference between actual and expected links within a community. Clearly, the modularity value is high when there is more total weight contributed by links within the communities than might be expected by chance [63]. More formally,

$$Q = \frac{1}{m} \sum_{ij} \left(A_{ij} - \frac{\left(\sum_k A_{ik}\right)\left(\sum_k A_{kj}\right)}{m} \right) \delta_{c_i,c_j},$$

where A_{ij} has value w_{ij} if there is a link of weight w_{ij} from vertex (port) i to vertex (port) j, $m = \sum_{ij} A_{ij}$, δ_{ij} is the Kronecker delta symbol, and c_i is the label of the community to which vertex (port) i is assigned.

To identify communities in a network one must search over all partitions $\{c_i\}$ of the vertices to find one that maximizes the modularity Q. We used the same heuristic search method as [44] devised by [66][8], which is known to work well, under which the GCSN is resolved into eight communities based on links weighted by the LSCI; (i) Asia-Pacific and Trans-Pacific, (ii) Trans-Atlantic, (iii) South Asia and Mideast, (iv) West and South Africa, (v) Southeastern United States, Caribbean, and Pacific South America, (vi) Southeastern Latin America, (vii) New Zealand, and (viii) Southern Europe, as shown in Figure 34. Interestingly, the communities we identify differ greatly from those of [44], where there are about 12 communities in their container subnetwork[9]. In addition, the first five largest communities are:

- Middle East, South and East Asia, and South Africa,
- Eastern United States, Caribbean, and Northern Latin America,
- Mediterranean, Black Sea, and Western Europe,
- Northern Europe,

[7] Interested readers could find a detailed discussion of community structure and community detection algorithms in Chapter 3.

[8] See Algorithm 4 in Chapter 3 for more details.

[9] In their study, the community detection algorithm was applied on directed unweighted network, where information about economic information, such as trade flow or freight capacity, is neglected.

- Trans-Pacific.

As supported by [29] that link weight may help improve community detection contrast, our computation clearly recognized important global patterns, including trans-Pacific trade (Figure 34a), as well as trans-Atlantic (Figure 34b), and intra-American trade (Figure 34e). Other interesting observations are as follows.

- Figure 34a: This community is the most strongly-defined in the sense that it includes the ports that contribute most to the total modularity.

  It may seem surprising that this Pacific-spanning community also includes the Caribbean port of Colon, Panama (all the other Panamanian ports are, as would be expected, in the Caribbean community of Figure 34e). But this makes sense because services from Asia to the US East Coast find it convenient to tranship at Colon for subsequent disbursement throughout the Caribbean.

- Figure 34b: Rotterdam and Hamburg are the core ports of this community.

- Figure 34c: The Mideast trading community includes East Africa above the ports of Tanzania and the Comoros and Seychelles Islands.

- Figure 34d: The East African ports below Tanzania, including the large ports of South Africa, are better connected to the West African trading community than to others. Tanjung Pelepas is the easternmost member, reflecting its role as point of distribution of manufactured goods to Africa. The few European members are connected primarily through the ports of Tanger or Algeciras.

- Figure 34e: The Caribbean community includes two outliers inviting comment. Wilmington, Delaware, in the US, has strong ties to Central America because of its specialization in the handling of tropical fruits and fruit juices. On the west coast, San Diego is more strongly connected to Latin America than to East Asia because the Asian services prefer to call at Los Angeles or Long Beach for their larger regional market and superior hinterland storage and transportation infrastructure.

- Figure 34f: Port-of-Spain (Trinidad) is the northernmost member. Services travel from it into this community.

- Figure 34g: This community is an artifact of geography, in this case, the fact that New Zealand is far from trading partners. This community consists of the New Zealand regional ports of Lyttelton, Napier, Port Chalmers, and Wellington, which have very few direct international connections. They are better connected amongst themselves than to the rest of the world. The international connections to New Zealand call mainly at Auckland and Tauranga which are members of the Asia-Pac and trans-Pacific trading community.

- Figure 34h: This is another community determined by the geography of the Mediterranean Sea. These ports are locally connected but all significant connections to the outside world are mainly through a few ports near the exit to the Atlantic Ocean.

The ports that contribute most to the modularity score are overwhelmingly Asian and especially Chinese, with the top ten being Shanghai, Ningbo, Hong Kong, Busan, Rotterdam, Yantian, Hamburg, Port Klang (Malaysia), and Qingdao. The ports that contribute most within the Trans-Atlantic community are Rotterdam, Hamburg, and Savannah; within the South Asia/Mideast community: Port Klang, Jeddah, and Dubai; within the West/South Africa: Tanjung Pelepas, Cape Town, and Durban; and within the southeastern US, Caribbean, and Pacific South American community: Callao (Peru), Manzanillo (Panama), and Balboa (Panama).

It is worth noting that Singapore is not among the ten largest contributors to the modularity. It is a member of the powerful Asia-Pac and trans-Pacific community, but it does not have dense local connections as do the big China ports. Instead, it serves more as a transshipment hub, with services to and from other ports that may not be directly connected themselves. In fact, the *clustering coefficient* of Singapore, which measures how connected to each other as its immediate neighbors, is very low among all container ports.

Lastly, when we allow ports to be assigned in multiple trading communities[10], we have

[10]This is known as an overlapping trading community structure, see Algorithm 5 in Chapter 3 for more

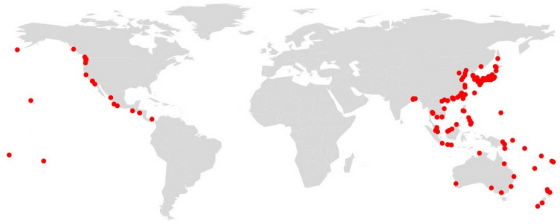

(a) Asia-Pac and trans-Pacific

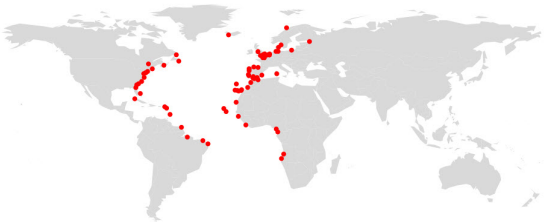

(b) Trans-Atlantic

(c) South Asia and Mideast

(d) West and south Africa

(e) Southeastern United States, Caribbean, and Pacific South America

(f) Southeastern Latin America

(g) New Zealand

(h) Southern Europe

Figure 34: Trading communities identified by maximizing total LSCI weight of links within groups (rather than between groups), with reported modularity value of 0.5085.

found that there are about 32 ports that could be assigned in alternative communities without hurting the modularity value, as reported in Table 14. Most of the ports are generally small, located at the border of their original trading communities, having weak connections within both their original trading communities and the alternative ones.

4.5.2 Comparing Trading Communities Across Networks

It is evident from the studies of [9] and [91] that trading communities evolve over time as trade patterns change, mostly from the shift of demand and supply all around the globe. In [91], it was found that the community structure of the *World Trade Web* (WTW), consisting of 178 nations, has been changed greatly from a dispersed island structure to a more centric one reflecting an increase in intercontinental services across the globe. [9] also found several interesting observations in a study of the evolution of community structure in the *Multi-Layer World Trade Web* as follows.

- The community structure of commodity specific networks usually differs from that of the aggregated one over the period of study. More specifically, the number of communities obtained from the aggregated network keeps increasing, but this is not a typical trend for most of commodity specific networks — which is quite stable. This implies that the structural change within specific commodity networks is less volatile.

- By using the *Normalized Mutual Information Measure* (NMI) as a measure of similarity comparison, they have found that geographical distance is more related with the formation of community, which is surprisingly irrelevant with trade.

In this study, by using the *Similarity Value*[11] as a measure for community structure comparison, we can identify the evolution of trading communities in the GCSN over time, as well as the structural difference between the GCSN and its counterpart networks. However, as our data set is quite limited and does not include trade information during economic downturns, we can only compare the community structure of the GCSN with those of

details.

[11] See Algorithm 6 in Chapter 3 for more details.

Table 14: A list of ports that could be assigned in multiple trading communities without hurting the modularity value.

Port	**Country**	**Original**	**Alternative**
Gibraltar	Spain	2	5
Pointe-a-Pitre	Guadeloupe	4	5
San Pedro, Ivory Coast	Ivory Coast	4	2
Jacksonville FL	United States	2	5
Pasir Gudang, Johor	Malaysia	1	3
Izmit	Turkey	4	3
St Johns, Antigua	Antigua and Barbuda	2	5
Montoir	France	4	2
Freetown	Sierra Leone	4	2
Bintulu, Sarawak	Malaysia	1	4
Vitoria	Brazil	7	5
Degrad des Cannes	French Guiana	2	7
Lobito	Angola	2	4
Monrovia	Liberia	2	4
Longoni,	Comoros	3	4
Izmir	Turkey	3	6
Havana	Cuba	2	6
Bridgetown	Barbados	2	5
Malabo	Equatorial Guinea	2	6
Melilla	Spain/N Af	2	5
Agadir	Morocco	2	6
Salerno	Italy	6	2
Cagliari	Italy	2	3
Tanger	Morocco	4	2
Miami FL	United States	5	2
Casablanca	Morocco	2	6
Motril	Spain	2	5
Marina di Carrara	Italy	3	6
Colon	Panama	1	2
Alicante	Spain	2	6
Malaga	Spain	4	2
Taranto	Italy	3	6

its adjacency counterpart network, and the continent-based network, where each port is assigned a community based on its geographic location over seven continents.

The result has been reported in Table 15, where we found that the community structure detected in the GCSN was less related with geographic location, but more with trade connection, which is quite different from the observation of [9].

Table 15: The results obtained from the comparison study of three different community structures detected from three different networks, namely, the GCSN, the adjacency counterpart network, and the continent-based network.

Network 1	**Network 2**	**Similarity Value**
GCSN	Adjacency	0.3962
GCSN	Continent-based	0.2958
Adjacency	Continent-based	0.2697

4.6 Conclusions

The Container Port Connectivity Index (CPCI) is a *descriptive* index summarizing how each port is connected to others within the larger network. Importantly, the CPCI expresses more than local connectivity to immediate neighbors but also neighbors-of-neighbors, and so on, with all links weighted by the Liner Shipping Connectivity Index (LSCI). Furthermore, the CPCI allows inbound and outbound strengths to be studied independently, and this gives a more detailed look at the economic roles played by each port. Finally, the CPCI supports what-if analysis in a way that survey-based indices, like the Logistics Performance Index (LPI), cannot.

Any index of logistics performance is an attempt to summarize a complex environment. The LSCI may be criticized for the rather arbitrary way that data is agglomerated, and the LPI criticized for its reliance on perception rather than measurement. The CPCI has weaknesses as well. In particular, because it uses an LSCI-like computation, it inherits any criticism of that. In addition, while the CPCI scores are based on connectivity, they are not based on geography, and so do not explicitly account for travel time between ports.

It should be remarked that neither our network model nor that of [44] captures anything

about transshipment. Even though there may be direct links from port A to port B and from port B to port C, to transport a container from A to C may require transshipment. In this case ports A and C are further apart in both time and cost than they might appear in these models. Nevertheless, the CPCI has many useful properties. In particular, it is based on link weights that are computed just like the LSCI; and because the LSCI has been vetted by economists as capturing intensities of trade, our index inherits that descriptive power and exercises it at a more granular level.

It is worth noting that link weights could be plausibly generated in other ways than the LSCI-type computation suggested herein. The LSCI represents shipping *capacity* but ideally one would like to assign weights to the links in some way that reflects the actual number of TEUs transported, rather than TEU capacity. Unfortunately, data at this level of detail is not generally available. Yet the mechanism we use to generate the CPCI supports any relevant alternative of link weight assignment, depending on the focal point of the research. For example, we may assign link weight as the reciprocal of the typical travel time so that the strength of a port would be determined by how close its neighbors are, which could be used in a study that focused on speed of freight flow rather than volume.

We expect the CPCI to be useful in some of the same ways as the LSCI. This may include explaining how the container-shipping network changes over time or using the link weights and port scores as explanatory variables for economic phenomena. We believe these finer-grained statistics will be easier to understand and to explain because they directly reflect immediate decisions of primary actors such as shipping companies.

CHAPTER V

AN EXTENSION OF THE CONTAINER PORT CONNECTIVITY INDEX

In Chapter 4, we provided a detailed discussion of a new ranking scheme that ranks container ports based on a new index of port importance called the *Container Port Connectivity Index* (CPCI). In that setting, the CPCI takes the *Liner Shipping Connectivity Index* (LSCI) as input and returns two separate scores, namely the *inbound* and *outbound scores*, for port ranking. In this chapter, we will show an interesting modification of such an index by exercising alternative input, that is, the container flow. In doing so, we simply assume that a port derives its importance based on the container flow it handles. In practice, a port, with little demand or supply, could become a strategic hub due to a great number of transshipped containers, such as the port of Singapore. By using the CPCI as a tool in a disaggregation fashion, where the importance score of a port is decomposed into components, each reflects its contribution to the overall port importance score, we can explore how each type of flow affects port importance and why a particular port has become important. This would allow the port authority to realize its strategic port importance compared to those of competitors. Following the same idea, we can also establish *route* and *leg importance scores* by help of hyperedges, reflecting multidimensional relationship between ports, routes, legs, and container flow circulating within the network.

5.1 A Simple Disaggregation Scheme

In the *Global Container-Shipping Network* (GCSN), we use the *Container Port Connectivity Index* (CPCI) to quantify port attractiveness in terms of inbound and outbound connectivity based on rate of capacity movement between ports, or *trade intensity*. While the CPCI tells us which port is important based on the connections with other ports, it does not explain why such connections affect port importance in detail. In order to answer this question properly, we propose an extension of the CPCI in a disaggregation fashion, where the

overall port importance score is computed and decomposed into components, each reflects its contribution to the overall port importance score.

Instead of using capacity, we alternatively use container flow to define link weights. In doing so, we simply assume that a port derives its importance based on the container flow it handles. For better understanding, we will show this procedure in a two-phase fashion. In the first phase, we construct an optimization model to help shipping lines decide the optimal channel of container flow through ports. Such a solution is then arranged into a proper matrix form used subsequently for the computation of port importance scores, in the second phase.

Depending on the metric spaces used, the construction of both the optimization model and the container-flow matrix may vary. In order to show such a difference, two different metric spaces, namely the *link* and the *route metric spaces*, will be discussed. In the link space model, there is a link from port i to j if there exist services from port i to j, while, in the route space model, port j is connected from port i if there exist routes containing leg (i, j).

Since we do not track the number of containers carried in each route but rather the number of containers traversing each link in the link space model, we may simply categorize the container flow into three groups, that is, (i) direct shipment, which is defined as the total number of pick-up and drop-off containers reflecting demand and supply at ports, (ii) indirect shipment, defined as the total number of containers passing through ports which are not their destinations, i.e. the transshipment hubs or other intermediary ports in service loops, and (iii) empty container shipment preserving container balancedness. By applying the HITS algorithm to proper matrix arrangements, the overall port importance score and its components could be revealed. We can then use these resulting scores to answer *why a particular port has become important*

In the *route space model*, the importance of a particular port might depend not only on the flow it handles but also on the importance of routes and legs to which it belongs. For example, a port which is a member of important routes should be treated differently from those of the trivial ones. In such a case, we need to modify the flow matrix such that the

relationship between ports, routes, and legs is included. With proper modifications, we can also establish route and leg importance scores in addition to port importance score by help of hyperedges and their associated incidence matrix representation.

In order to visualize such concepts, the detailed discussion of both link and route space models is provided, followed by an example illustrating how we construct both the optimization model and the flow matrix in each case.

5.2 The Link Space Model

In this section, we show how to extend the CPCI using container flow to define link weights instead of capacity in a disaggregation fashion under the link metric space. For simplicity, we will restrict ourselves with three types of container flow, that is, (i) direct shipment, (ii) indirect shipment, and (iii) empty container shipment. In Phase 1, we establish a simple optimization model to find the optimal flow of containers satisfying sets of practical constraints, including demand, supply, and capacity constraints. Once solved, we then use the solution of such a model to construct a flow matrix used subsequently for the computation of port importance score and its components, in the second phase. The computation of the importance scores in this extension is the same as that of the CPCI, except for different matrix representations.

5.2.1 The First Phase

Given a set of ports V and a set of directed links E comprising a network G, together with all demand and supply of containerized goods from ports to ports, the main objective of this phase is to find the optimal flow of containers that minimizes liner shipping operational costs, constrained by sets of practical restrictions. For simplicity, we will focus on a simple model where all demand must be satisfied and there must be sufficient empty containers to load goods at all ports. In addition, there exist link capacities, which the total number of containers moved on any links, both full and empty ones, must not exceed. In this setting, the containers passing by intermediary ports, i.e. ports which are not their destinations, are counted as indirect shipment. It is worth noting that, in the link space model, we do not take account for the transshipment of containers. More specifically, while the containers

might be carried by their original vessels or transshipped to the others, we treat them as the same.

Sets

- C denotes a set of all commodities, where each commodity is defined as an origin-destination pair of containers represented by a tuple of two ports, i.e. (k, l).
- E denotes a set of directed links.
- V denotes a set of ports.

Parameters

- t_{ij} denotes time, or cost, of moving a container from port i to j.
- u_{ij} denotes capacity of link (i, j).
- S^{kl} denotes total supply amount of commodity (k, l) measured in containers.
- D^{kl} denotes total demand amount of commodity (k, l) measured in containers.

Decision Variables

- x_{ij}^{kl} denotes full containers of commodity (k, l) moved on link (i, j).
- y_{ij} denotes total number of empty containers moved on link (i, j), where y_{ii} represents empty containers available at port i.

At the moment, we assume that port importance score depends mostly on the container flow from ports to ports. Since such flow is mainly controlled by shipping lines, thus, our objective function might be properly defined as a cost minimization supposedly solved by the shipping lines,

$$min \sum_{(k,l)\in C} \sum_{(i,j)\in E} t_{ij} x_{ij}^{kl} + \sum_{(i,j)\in E} t_{ij} y_{ij}. \tag{64}$$

In the case where profits of fulfilled demand are known, we may instead redefine the objective function to profit maximization.

Constraints

- Supply amount of commodity (k, l) must be originated from port k.

$$\sum_{j \in V} x_{kj}^{kl} = S^{kl}, \text{ for all } (k, l) \in C \tag{65}$$

- Demand of each commodity must be fulfilled at its destination.

$$\sum_{i \in V} x_{il}^{kl} = D^{kl}, \text{ for all } (k, l) \in C \tag{66}$$

- Capacity constraint on each link (i, j).

$$\sum_{(k,l) \in C} x_{ij}^{kl} + y_{ij} \leq u_{ij}, \text{ for all } (i, j) \in E \tag{67}$$

- Empty containers at port k must be sufficient for loading goods and for repositioning to other ports.

$$y_{kk} \geq \sum_{(k,l) \in C} S^{kl} + \sum_{j \in V} y_{kj}, \text{ for all } k \in V \tag{68}$$

- Empty-container balancing constraints reflecting the availability of empty containers at ports.

$$y_{ll} = \sum_{(k,l) \in C} \sum_{i \in V} x_{il}^{kl} + \sum_{i \in V} y_{il}, \text{ for all } l \in V \tag{69}$$

- Indirect-shipment balancing constraints, i.e. if port j is not the destination of commodity (k, l), the containers will only pass by port j.

$$\sum_{i \in V} x_{ij}^{kl} = \sum_{i \in V} x_{ji}^{kl}, \text{ for all } (k, l) \in C, \text{ and for all } j, l \in V \text{ where } j \neq l \tag{70}$$

- Other technological constraints imposed on the network, i.e. traffic control constraint at each port.

- Non negativity and integrity constraints for all decision variables.

5.2.2 The Second Phase

In this phase, the overall port importance score is computed based on the resulting container flow from Phase 1, using the HITS algorithm. Recall that, from the establishment of the CPCI, a port is assigned two types of importance scores, namely the inbound and outbound scores, which are computed by Equations (15) and (16). Similar to the LSCI-based CPCI, in this setting, we still get those two scores, with additional capability of quantifying the contribution of each flow type to each of those connectivity scores. This piece of information could consequently be used to explain why some ports, with little demand or supply like the port of Singapore, is considered as the world logistics hub, while there are many more ports with relatively high demand or supply that have been ranked much lower.

Regarding its computation, assume that we have the optimal flow of containers in matrix form, denoted as F, which is the composition of (i) direct shipment from the ports of origin to the ports of destination without passing by any intermediary ports (D), (ii) indirect shipment from the ports of origin passing by a series of intermediary ports before reaching its final destination (I), and (iii) empty container shipment between ports (E). Since the overall port importance score is structurally contributed by these three components, one can calculate the inbound (x) and outbound scores (y) of all ports by Equations (71) and (72).

$$\lambda x = (D + I + E)^T y \Longrightarrow \lambda^2 x = (D + I + E)^T (D + I + E)x, \tag{71}$$

$$\lambda y = (D + I + E)x \Longrightarrow \lambda^2 y = (D + I + E)(D + I + E)^T y. \tag{72}$$

Notice that once the overall inbound and outbound scores have been calculated, we could substitute these values into Equations (71) and (72) to obtain the contribution of each flow type. With this approach, the port authority would be able to comprehend and benchmark its importance in terms of (i) direct freight forwarding/receiving ability, (ii) strategic intermediary, and (iii) empty repositioning ground, with competitors, which would be crucial for the planning of its future course of operations.

5.2.3 An Example of the Link Space Model

Let us consider a small example consisting of four ports and seven commodities shown in Figure 35, where its associated demand and supply information is provided in Table 16. For simplicity, we assume that all links have the same transportation cost per container and capacity of one and 10, respectively.

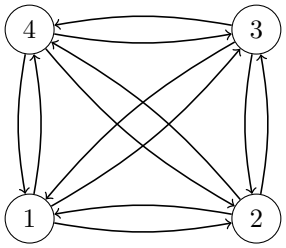

Figure 35: An example of four fully connected ports with transportation cost of one unit per container, and each link has capacity of 10 containers.

Based on the three traditional centrality measures, all ports are equivalently important since they all have the same number of degrees, and the same shortest path length connecting with each other. However, with flow information, ports 1 and 2 are expected to be the most important ports, since they are expected to handle more containers than the rest. Some might also suggest that port 3 would be the least important one, since it only requires goods from port 1 and produces nothing to supply the rest; however, this might not always be the case. In practice, terminal ports like port 3 might be a lot more important than it seems, due to its transshipment or empty repositioning function, which would only be revealed once the first phase has been solved.

Table 16: Demand and supply information of all commodities

From/To	1	2	3	4
1		15	10	
2	5	5		5
3				
4	5	5		

According to the aforementioned information, the optimal flow of container and its

associated disaggregation obtained from phase 1 is shown in Equation (73). The left hand side of Equation (73) is the aggregated flow, which is decomposed into three flow types, that is, (i) direct shipment, (ii) indirect shipment, and (iii) empty repositioning shipment, on the right hand side.

$$\begin{bmatrix} 0 & 10 & 10 & 5 \\ 10 & 0 & 5 & 5 \\ 10 & 0 & 0 & 5 \\ 5 & 10 & 0 & 0 \end{bmatrix} = \begin{bmatrix} 0 & 10 & 10 & 0 \\ 5 & 0 & 5 & 5 \\ 0 & 0 & 0 & 0 \\ 5 & 10 & 0 & 0 \end{bmatrix} + \begin{bmatrix} 0 & 0 & 0 & 5 \\ 0 & 0 & 0 & 0 \\ 0 & 0 & 0 & 0 \\ 0 & 0 & 0 & 0 \end{bmatrix} + \begin{bmatrix} 0 & 0 & 0 & 0 \\ 5 & 0 & 0 & 0 \\ 10 & 0 & 0 & 5 \\ 0 & 0 & 0 & 0 \end{bmatrix} \quad (73)$$

If we apply the HITS algorithm to the direct decomposition above, we can compute inbound and outbound scores of all four ports as shown in Tables 17 and 18. In terms of outbound connectivity, from Table 18, port 1 is the most important hub, which is mostly contributed by its direct shipment component. Although, port 3 is the least important hub port, as expected, interestingly, its outbound score is comparable to that of port 4 which has more activities due to a considerable amount of empty repositioning containers. Regarding consolidation, or inbound connectivity, from Table 17, port 1 is also the most important, not port 2, which requires more incoming containerized goods compared to port 1. The reason behind this controversy is the empty repositioning activity at port 1. Since demand at port 1 is less than its supply, it must draw empty containers from other ports nearby to satisfy the availability of empty containers. This is evident from Equation (73) and Table 17, where the main contribution of port 1's inbound score comes from empty reposition; while the inbound score of port 2 is derived solely from its direct shipment.

Table 17: The inbound scores of all ports.

	1	2	3	4
Inbound scores	0.5911	0.5374	0.4509	0.3981
Direct shipment	0.2459	0.5374	0.4509	0.1351
Indirect shipment	0	0	0	0.1579
Empty repositioning	0.3452	0	0	0.1051

In practice, container ports are of different sizes and capacities. Without a scaling

Table 18: The outbound scores of all ports.

	1	2	3	4
Outbound scores	0.6124	0.5238	0.4075	0.4296
Direct shipment	0.5097	0.3714	0	0.4296
Indirect shipment	0.1027	0	0	0
Empty repositioning	0	0.1524	0.4075	0

scheme, it might be cumbersome to apply the HITS algorithm to the decomposition of flow matrix directly — this might cause a precision problem in the calculation of port importance score since the sum of port importance squared is preserved at unity. However, not all scaling schemes are appropriate in this setting. For example, consider the unity row sum scaling scheme mimicking the Google's Pagerank algorithm as shown in Equation (74), i.e. the sum of each row equals one.

$$F \Longrightarrow \begin{bmatrix} 0 & 0.5 & 0.5 & 0 \\ 0.33 & 0 & 0.33 & 0.33 \\ 0 & 0 & 0 & 0 \\ 0.33 & 0.67 & 0 & 0 \end{bmatrix} + \begin{bmatrix} 0 & 0 & 0 & 1 \\ 0 & 0 & 0 & 0 \\ 0 & 0 & 0 & 0 \\ 0 & 0 & 0 & 0 \end{bmatrix} + \begin{bmatrix} 0 & 0 & 0 & 0 \\ 1 & 0 & 0 & 0 \\ 0.67 & 0 & 0 & 0.33 \\ 0 & 0 & 0 & 0 \end{bmatrix} \tag{74}$$

If we apply the HITS algorithm to Equation (74), we can compute inbound and outbound scores of all ports as reported in Tables 19 and 20. With this scaling scheme, port 2 has now become the most important hub instead of port 1. Even worse, ports 1 and 3 are now equally important, which is preposterous. This contradiction is caused by neglecting flow magnitude, where all outgoing containers from each port are treated as equally important. A better scaling scheme would be one that scales all values at the same rate, such as the LSCI-like measure.

Table 19: The inbound scores of all ports when container flow is scaled by row sum.

	1	2	3	4
Inbound scores	0.8079	0.2166	0.2733	0.4751
Direct shipment	0.1976	0.2166	0.2733	0.1506
Indirect shipment	0	0	0	0.2453
Empty repositioning	0.6102	0	0	0.0791

Table 20: The outbound scores of all ports when container flow is scaled by row sum.

	1	2	3	4
Outbound scores	0.4203	0.7743	0.4068	0.2415
Direct shipment	0.1430	0.3028	0	0.2415
Indirect shipment	0.2773	0	0	0
Empty repositioning	0	0.4716	0.4068	0

5.3 The Route Space Model

In the previous section, we have demonstrated the extension of the CPCI using container flow as link weights to compute the overall port importance score and its components under the link metric space. Observe that, in that setting, we neglect all information about vessel routes, which allows containers to be moved freely between ports. In this section, we will show how to incorporate route information into the computation of the importance scores using hyperedges to reflect multidimensional relationship between ports, routes, and legs, as well as the container flow circulating within the network. With more embedded information, we can extract not only the inbound and outbound scores but also the *route* and *leg importance scores*.

5.3.1 The First Phase

As opposed to the link metric space, in the route metric space, we need to modify the model to capture more detailed information about the container flow on each leg of all routes. In order to do so, we need one more set R representing the set of all routes, and we need to redefine the decision variables as follows.

- $x_{ij,r}^{kl}$ denotes the number of full containers of commodity (k, l) moved on leg (i, j) of route r.
- z_i denotes the number of empty containers available at port i.
- $y_{ij,r}$ denotes the number of empty containers moved on leg (i, j) of route r.

The objective function of the route space model is quite similar to that of the previous one, as shown in (75), except the inclusion of route index in the decision variables. At the

moment, we assume that we have information of all available routes and their associated capacities.

$$min \sum_{(k,l)\in C} \sum_{r\in R} \sum_{(i,j)\in E} t_{(i,j),r} x_{ij,r}^{kl} + \sum_{r\in R} \sum_{(i,j)\in E} t_{ij,r} y_{ij,r} \tag{75}$$

Constraints

- Supply amount of the commodity (k,l) must be originated at port k and transported through all possible routes r having leg (k,j) as their comprising leg.

$$\sum_{r\in R} \sum_{j\in V} x_{kj,r}^{kl} = S^{kl}, \text{ for all } (k,l) \in C \tag{76}$$

- Demand of each commodity must be fulfilled at its destination.

$$\sum_{r\in R} \sum_{i\in V} x_{il,r}^{kl} = D^{kl}, \text{ for all } (k,l) \in C \tag{77}$$

- Capacity constraint on leg (i,j) of route r.

$$\sum_{(k,l)\in C} x_{ij,r}^{kl} + y_{ij,r} \leq u_{ij,r}, \text{ for all } (i,j) \in E, \text{ and for all } r \in R \tag{78}$$

- The number of empty containers at port k must be sufficient for loading goods and for empty repositioning.

$$z_k \geq \sum_{(k,l)\in C} S^{kl} + \sum_{r\in R} \sum_{j\in V} y_{kj,r}, \text{ for all } k \in V \tag{79}$$

- Empty-container balancing constraints.

$$z_l = \sum_{(k,l)\in C} \sum_{r\in R} \sum_{i\in V} x_{ij,r}^{kl} + \sum_{r\in R} \sum_{i\in V} y_{il,r}, \text{ for all } l \in V \tag{80}$$

- Constraints regarding transshipment and indirect shipment at ports, i.e. if port j is not the destination of commodity (k,l) transported on the leg (i,j) of route r, those containers will just pass by port j.

$$\sum_{r\in R} \sum_{i\in V} x_{ij,r}^{kl} = \sum_{r\in R} \sum_{i\in V} x_{ji,r}^{kl}, \text{ for all } (k,l) \in C, \text{ and for all } j,l \in V \text{ where } j \neq l \tag{81}$$

- Other technological constraints imposed on the network, i.e. traffic control constraint at each port.

- Non negativity and integrity constraints for all decision variables.

Before proceeding to Phase 2, observe that the solution to the modified phase-one problem is route-based optimal flow, which is impossible to represent by a flow-through matrix, since the relationship between ports, routes, and their comprising legs, together with their associated flow, could not be fitted in. In order to capture such information, we instead use a hypergraph, i.e. a network consisting of hyperedges, and its associated incidence matrix, for network representation. With the presence of hyperedges, multidimensional relationships concerning more than two entities, such as a buyer-seller-broker transaction described in Chapter 2, could be described and properly defined in matrix form. Since the resulting incidence matrix contains more information, we can extract two more interesting importance scores, namely the *route* and *leg importance scores*, as the output[1].

In order to visualize this concept, let us consider the same example shown in Figure 35; but, in this case, we restrict the containers to be moved only on 8 available routes shown in Table 21.

Table 21: Information of all eight available routes for the underlying network shown in Figure 35.

Route Number	**Direction**
1	1-2-1
2	1-3-1
3	1-4-1
4	2-3-2
5	2-4-2
6	3-4-3
7	2-1-4-2
8	2-3-4-2

With the aforementioned information, the solution to the modified phase-one problem is shown in Table 22. For simplicity, we do not further classify container flow by commodity; but this could be done when importance scores are suspected to be commodity dependent.

[1]Recall that the computation of these scores is similar to that of the multidimension centrality described in Chapter 2.

Table 22: The solution to the modified phase-one problem.

Route Number	Direction	Leg	Full Container	Empty Container
1	1-2-1	(1,2)	10	0
		(2,1)	5	5
2	1-3-1	(1,3)	10	0
		(3,1)	0	5
3	1-4-1	(1,4)	0	0
		(4,1)	5	0
4	2-3-2	(2,3)	5	0
		(3,2)	0	0
5	2-4-2	(2,4)	5	0
		(4,2)	5	0
6	3-4-3	(3,4)	0	0
		(4,3)	0	0
7	2-1-4-2	(2,1)	0	5
		(1,4)	5	0
		(4,2)	5	0
8	2-3-4-2	(2,3)	0	0
		(3,4)	0	0
		(4,2)	0	0

5.3.2 The Second Phase

The most crucial modification for this second phase is the construction of an incidence matrix, where port-route-flow relationship must be captured. For better understanding, we will show a step-by-step development of this modification starting from the most general case, where all information takes only binary value reflecting membership, to the most sophisticated one, where we blend both binary and canonical information together.

Firstly, let us consider a modification where all information takes only binary value, i.e. either 0 or 1, indicating whether there exists member-wise relationship between two interested entities. In particular, this incidence matrix captures all affiliated relationship between ports, routes, and legs, as shown in Equation (82), where rows of A represent legs and columns of A represent ports (N) and routes (R). In other words, matrix A is a concatenation of columns representing ports followed by the columns representing routes. For simplicity, let $A_k(i,j)$ be the element of A corresponding to the row of edge (i,j) in column k. If $k \in N$, let $A_k(i,j) = N_k(i,j)$, and $A_k(i,j) = R_k(i,j)$ otherwise. For any edge connecting ports i and j, we have $N_i(i,j) = N_j(i,j) = 1$. Similarly, for any route $r \in R$, if

$(i,j) \in r$, then we have $R_r(i,j) = 1$, and $R_r(i,j) = 0$ otherwise.

$$A = \begin{bmatrix} | & | & | & | & | & | & ... & | \\ N_1 & N_2 & N_3 & N_4 & R_1 & R_1 & ... & R_8 \\ | & | & | & | & | & | & ... & | \end{bmatrix} \tag{82}$$

For purposes of construction, we assume that (i) leg importance score is a function of ports and routes, and (ii) both port and route importance scores are functions of legs. However, since we do not incorporate flow information into such a matrix, the resulting importance scores will be primarily derived based on membership, which might mislead their true importance. In addition, when some routes are not being used, i.e. routes 6 and 8, their route importance scores should be zero; however, with this setting, they will remain in the positive side due to the existence of route-leg relationship. In order to alleviate these effects, we need to modify matrix A in such a way that both membership and flow information are well blended.

The easiest way to modify matrix A is to use container flow instead of binary parameter $R_r(i,j)$. Based on this modification, we can decompose such flow into full and empty containers as shown in Equation (83).

$$A' = \begin{bmatrix} N & R \end{bmatrix} = \begin{bmatrix} \bar{N_1} & R_C \end{bmatrix} + \begin{bmatrix} \bar{N_2} & R_E \end{bmatrix}, \tag{83}$$

where $\bar{N_i}$ is the i^{th} weighted submatrix preserving row sum unity, and R_C, R_E are full and empty container submatrices.

With this disaggregation scheme, we would obtain port, route, and leg importance scores, where, (i) leg importance score is a function of connected ports and the container flow it handles from various routes, (ii) port importance score is a function of legs having ports of interest as members, and (iii) route importance score is a function of container flow moving on their comprising legs.

In the aforementioned modification, the assumption that port and route importance scores are functions of only legs may seem incorrect since both port and route importance scores should also depend on the flow of containers. Thence, we might further modify matrix A' to $\bar{A}$ by adding rows of ports in addition to the existing rows of legs as shown in

Equation (84).

$$\bar{A} = \begin{bmatrix} F_1 & C_1 \\ C_2 & F_2 \end{bmatrix}, \tag{84}$$

where (i) the first $|V|$ rows and the rest $|E|$ rows of $\bar{A}$ represent ports and legs in the network, (ii) the first $|V|$ columns and the rest $|R|$ columns of $\bar{A}$ represent ports and all available routes, (iii) F_1 denotes container flow submatrix among ports, which is the same as the flow-through matrix used in the link space calculation, (iv) F_2 denotes a submatrix of container flow moved on each leg of all routes, (v) C_1 denotes leg-route membership matrix, and (vi) C_2 denotes port-leg connectivity matrix. Similar to the previous modification, we can apply a simple disaggregation scheme to $\bar{A}$, where the result is shown in Equation (85).

$$\bar{A} = \begin{bmatrix} F_{1C} & \bar{C_1} \\ \bar{C_2} & F_{2C} \end{bmatrix} + \begin{bmatrix} F_{1E} & \bar{C_1} \\ \bar{C_2} & F_{2E} \end{bmatrix}, \tag{85}$$

where F_{ix} denotes the i^{th} weighted submatrix of container flow type x and $\bar{C_i}$ is the i^{th} weighted membership submatrix. With this modification, both membership and flow information is properly captured and we could obtain all importance scores and the contribution from each flow type as designed.

5.3.3 An Example of the Route Space Model

In this section, we will illustrate the aforementioned concepts of the importance score computation that take multidimensional information into account. We begin the discussion with the simplest model, where only affiliated information among ports, routes, and their comprising legs is considered. Based on Table 22 and Equation (82), we can construct the incidence matrix A as shown in Table 23, where Table 24 summarizes the resulting port, route, and leg importance scores derived from such a matrix. Since importance scores depend solely on port-leg and route-leg memberships, ports with high degree and legs appearing in many routes are expected to have relatively high scores. In addition, the longer the routes, the higher the route importance scores, regardless of the container flow circulating on such routes, for example, routes 6 and 8 containing more legs than the rest are expected to have high importance scores, though there are no containers carrying within.

In order to make the result more informative, we replace binary relationship between legs and routes with actual container flow. Based on Equation (83), matrix A' could be constructed as shown in Table 25, where Tables 26 and 27 show its decomposition based on the type of container flow. After applying the HITS algorithm to matrix A', port, route, and leg importance scores are extracted, as reported in Tables 28 and 29. Unsurprisingly, since most activities have occurred at ports 1 and 2, we would expect high port importance scores on these two ports. Additionally, legs connecting these two ports, i.e $(1, 2)$ and $(2, 1)$, are also expected to have higher scores than the rest since higher ranked ports are connected by these legs. Consequently, route 1 has become the most important. On the contrary, since routes 6 and 8 have no flow, their route importance scores are undoubtedly zero. It is worth noting that, in this decomposition, $\bar{N}_1$ and $\bar{N}_2$ are set to be the same. This implies that the importance of full and empty containers handled is equally important, i.e. each type of flow will have the same score.

In the last modification, where port importance score is a function of both legs and flow, we can construct matrix $\bar{A}$ based on Equation (84), as shown in Table 30. With this construction, we expect to obtain better results since both membership and flow are being utilized; however, there are several issues needing clarification. Firstly, observe that since membership is part of importance score calculation, there would be no entity with zero importance score. For example, while routes 6 and 8 have zero importance score in the previous alteration, in this alteration these two routes would receive some positive importance scores contributed by route-leg relationship (see Table 33). Similarly, from Table 34, ports 1 and 4 have not generated any empty containers; however, their empty container scores are not zero due to the same relational effect. Lastly, legs $(3, 2), (3, 4)$ and $(4, 3)$ as parts of the unused routes have fairly high importance scores due to the contribution of route-leg relationship. For better interpretation, empty routes should be discarded before proceeding to the calculation of importance scores, though in practice, empty routes are quite rare.

After removing empty routes and their associated legs, the updated matrix $\bar{A}$ and its decompositions are shown in Tables 35 – 37, while the updated importance scores are

reported in Tables 38 and 39. This result is much clearer since all relational effects previously discussed have been removed.

One interesting feature about the extension of the CPCI in the route space model is that the constructed matrix is not required to be a symmetric matrix for the derivation of all importance scores, since the multiplication between the constructed incidence matrix and its transpose is always symmetric. And, therefore, all importance scores are well-defined, and always exist.

5.4 Conclusions

Other than the LSCI-like measure defined as link weights, we show that the CPCI can take alternative input, such as container flow, for the computation of port importance score. We also show that, with proper modification, we can extract detailed information about route and leg importance scores in addition to that of a port. These importance scores, in turn, allow us to understand why a port has become important, though it is neither the world's largest manufacturer nor consumer, such as the port of Singapore.

The computation of these scores is quite similar to that of the CPCI, except for different matrix representations. In the link space mode, the overall port importance score and its components are computed based on a flow-through matrix, while, in the route space model, they are computed based on an incidence matrix, where hyperedges are used to represent multidimensional relationship between ports, routes, legs, and container flow circulating within the network.

Based on our illustration, it is evident that the crucial step for the derivation of importance scores lies on the construction of the flow matrix. Such relationship may vary from one to another application, making the construction of the flow matrix more like an art rather than a science. Nevertheless, we believe that the extension of the CPCI presented here gives several insights into the construction of meaningful measures for ranking network's entities other than nodes or links.

Table 23: Matrix A.

Legs	1	2	3	4	R1	R2	R3	R4	R5	R6	R7	R8
(1,2)	1	1			1							
(1,3)	1		1			1						
(1,4)	1			1			1				1	
(2,1)	1	1			1						1	
(2,3)		1	1					1				1
(2,4)		1		1					1			
(3,1)	1		1			1						
(3,2)		1	1					1				
(3,4)			1	1						1		1
(4,1)	1			1			1					
(4,2)		1		1					1		1	1
(4,3)			1	1						1		

Table 24: Importance scores derived from matrix A.

Legs	Unscaled Scores	Scaled Scores	Ports and Routes	Unscaled Scores	Scaled Scores
(1,2)	0.2518	0.0737	1	0.4027	0.2345
(1,3)	0.2317	0.0679	2	0.4558	0.2655
(1,4)	0.3173	0.0929	3	0.4027	0.2345
(2,1)	0.3173	0.0929	4	0.4558	0.2655
(2,3)	0.3173	0.0929	R1	0.1431	0.1037
(2,4)	0.2718	0.0796	R2	0.1165	0.0844
(3,1)	0.2317	0.0679	R3	0.1431	0.1037
(3,2)	0.2518	0.0737	R4	0.1431	0.1037
(3,4)	0.3173	0.0929	R5	0.1696	0.1229
(4,1)	0.2518	0.0737	R6	0.1431	0.1037
(4,2)	0.4029	0.1180	R7	0.2609	0.1890
(4,3)	0.2518	0.0737	R8	0.2609	0.1890

Table 25: Matrix A'.

Legs	1	2	3	4	R1	R2	R3	R4	R5	R6	R7	R8
(1,2)	1	1			10							
(1,3)	1		1			10						
(1,4)	1			1							5	
(2,1)	1	1			10						5	
(2,3)		1	1					5				
(2,4)		1		1					5			
(3,1)	1		1			5						
(3,2)		1	1									
(3,4)			1	1								
(4,1)	1			1			5					
(4,2)		1		1					5		5	
(4,3)			1	1								

Table 26: Matrix A'_F.

Legs	1	2	3	4	R1	R2	R3	R4	R5	R6	R7	R8
(1,2)	0.5	0.5			10							
(1,3)	0.5		0.5			10						
(1,4)	0.5			0.5							5	
(2,1)	0.5	0.5			5							
(2,3)		0.5	0.5					5				
(2,4)		0.5		0.5					5			
(3,1)	0.5		0.5									
(3,2)		0.5	0.5									
(3,4)			0.5	0.5								
(4,1)	0.5			0.5			5					
(4,2)		0.5		0.5					5		5	
(4,3)			0.5	0.5								

Table 27: Matrix A'_E.

Legs	1	2	3	4	R1	R2	R3	R4	R5	R6	R7	R8
(1,2)	0.5	0.5										
(1,3)	0.5		0.5									
(1,4)	0.5			0.5								
(2,1)	0.5	0.5			5						5	
(2,3)		0.5	0.5									
(2,4)		0.5		0.5								
(3,1)	0.5		0.5			5						
(3,2)		0.5	0.5									
(3,4)			0.5	0.5								
(4,1)	0.5			0.5								
(4,2)		0.5		0.5								
(4,3)			0.5	0.5								

Table 28: Leg importance score derived from matrix A', and its decomposition.

Legs	Unscaled Scores	Scaled Scores	Full Container	Empty Container
(1,2)	0.6352	0.3667	0.6282	0.0070
(1,3)	0.0181	0.0105	0.0146	0.0036
(1,4)	0.1218	0.0703	0.1176	0.0041
(2,1)	0.7487	0.4322	0.3176	0.4311
(2,3)	0.0082	0.0047	0.0045	0.0036
(2,4)	0.0272	0.0157	0.0230	0.0042
(3,1)	0.0127	0.0073	0.0036	0.0091
(3,2)	0.0073	0.0042	0.0036	0.0036
(3,4)	0.0016	0.0009	0.0008	0.0008
(4,1)	0.0093	0.0054	0.0052	0.0041
(4,2)	0.1407	0.0812	0.1365	0.0042
(4,3)	0.0016	0.0009	0.0008	0.0008

Table 29: Port and route importance scores derived from matrix A', and their decomposition.

Port and Routes	Unscaled Scores	Scaled Scores	Full Container	Empty Container
1	0.1036	0.4462	0.0518	0.0518
2	0.1050	0.4524	0.0525	0.0525
3	0.0033	0.0143	0.0017	0.0017
4	0.0202	0.0872	0.0101	0.0101
R1	0.9272	0.6896	0.6764	0.2508
R2	0.0164	0.0122	0.0122	0.0042
R3	0.0031	0.0023	0.0031	0
R4	0.0027	0.0020	0.0027	0
R5	0.0563	0.0419	0.0563	0
R6	0	0	0	0
R7	0.3387	0.2520	0.0879	0.2508
R8	0	0	0	0

Table 30: Matrix $\bar{A}$.

Ports and Legs	1	2	3	4	R1	R2	R3	R4	R5	R6	R7	R8
1		10	10	5	1	1	1				1	
2	15		5	5	1			1	1		1	1
3	5					1		1		1		1
4	5	10					1		1	1	1	1
(1,2)	1	1			10							
(1,3)	1		1			10						
(1,4)	1			1							5	
(2,1)	1	1			10						5	
(2,3)		1	1					5				
(2,4)		1		1					5			
(3,1)	1		1			5						
(3,2)		1	1									
(3,4)			1	1								
(4,1)	1			1			5					
(4,2)		1		1					5		5	
(4,3)			1	1								

Table 31: Matrix $\bar{A_F}$.

Ports and Legs	1	2	3	4	R1	R2	R3	R4	R5	R6	R7	R8
1		10	10	5	0.5	05	0.5				0.5	
2	5		5	5	0.5			0.5	0.5		0.5	0.5
3						0.5		0.5		0.5		0.5
4	5	10					0.5		0.5	0.5	0.5	0.5
(1,2)	0.5	0.5			10							
(1,3)	0.5		0.5			10						
(1,4)	0.5			0.5							5	
(2,1)	0.5	0.5			5							
(2,3)		0.5	0.5					5				
(2,4)		0.5		0.5					5			
(3,1)	0.5		0.5									
(3,2)		0.5	0.5									
(3,4)			0.5	0.5								
(4,1)	0.5			0.5			5					
(4,2)		0.5		0.5					5		5	
(4,3)			0.5	0.5								

Table 32: Matrix $\bar{A_E}$.

Ports and Legs	1	2	3	4	R1	R2	R3	R4	R5	R6	R7	R8
1					0.5	05	0.5				0.5	
2	10				0.5			0.5	0.5		0.5	0.5
3	5					0.5		0.5		0.5		0.5
4							0.5		0.5	0.5	0.5	0.5
(1,2)	0.5	0.5										
(1,3)	0.5		0.5									
(1,4)	0.5			0.5								
(2,1)	0.5	0.5			5						5	
(2,3)		0.5	0.5									
(2,4)		0.5		0.5								
(3,1)	0.5		0.5			5						
(3,2)		0.5	0.5									
(3,4)			0.5	0.5								
(4,1)	0.5			0.5								
(4,2)		0.5		0.5								
(4,3)			0.5	0.5								

Table 33: Inbound score and route importance score derived from matrix $\bar{A}$, and their decomposition.

Ports and Routes	Unscaled Scores	Scaled Scores	Full Container	Empty Container
1	0.6359	0.3483	0.2672	0.3687
2	0.4678	0.2562	0.4530	0.0148
3	0.4228	0.2316	0.4147	0.0080
4	0.2993	0.1639	0.2905	0.0088
R1	0.2313	0.2978	0.1546	0.0767
R2	0.0965	0.1243	0.0626	0.0340
R3	0.0578	0.0744	0.0359	0.0219
R4	0.0523	0.0673	0.0327	0.0196
R5	0.0872	0.1122	0.0621	0.0251
R6	0.0266	0.0343	0.0133	0.0133
R7	0.1671	0.2152	0.0810	0.0861
R8	0.0580	0.0746	0.0290	0.0290

Table 34: Outbound score and leg importance score derived from matrix $\bar{A}$, and their decomposition.

Ports and Legs	Unscaled Scores	Scaled Scores	Full Container	Empty Container
1	0.5232	0.3012	0.5100	0.0132
2	0.6565	0.3780	0.3385	0.3180
3	0.1630	0.0938	0.0056	0.1574
4	0.3942	0.2270	0.3848	0.0095
(1,2)	0.1632	0.1630	0.1368	0.0264
(1,3)	0.0967	0.0966	0.0714	0.0253
(1,4)	0.0846	0.0845	0.0623	0.0223
(2,1)	0.2031	0.2029	0.0816	0.1215
(2,3)	0.0550	0.0550	0.0338	0.0213
(2,4)	0.0575	0.0574	0.0391	0.0183
(3,1)	0.0736	0.0735	0.0253	0.0483
(3,2)	0.0425	0.0425	0.0213	0.0213
(3,4)	0.0345	0.0345	0.0172	0.0172
(4,1)	0.0585	0.0584	0.0361	0.0223
(4,2)	0.0974	0.0973	0.0791	0.0183
(4,3)	0.0345	0.0345	0.0172	0.0172

Table 35: Updated matrix $\bar{A}$.

Ports and Legs	1	2	3	4	R1	R2	R3	R4	R5	R7
1		10	10	5	1	1	1			1
2	15		5	5	1			1	1	1
3	5					1		1		
4	5	10					1		1	1
(1,2)	1	1			10					
(1,3)	1		1			10				
(1,4)	1			1						5
(2,1)	1	1			10					5
(2,3)		1	1					5		
(2,4)		1		1					5	
(3,1)	1		1			5				
(4,1)	1			1			5			
(4,2)		1		1					5	5

Table 36: Updated matrix $\bar{A_F}$.

Ports and Legs	1	2	3	4	R1	R2	R3	R4	R5	R7
1		10	10	5	0.5	05	0.5			0.5
2	5		5	5	0.5			0.5	0.5	0.5
3						0.5		0.5		
4	5	10					0.5		0.5	0.5
(1,2)	0.5	0.5			10					
(1,3)	0.5		0.5			10				
(1,4)	0.5			0.5						5
(2,1)	0.5	0.5			5					
(2,3)		0.5	0.5					5		
(2,4)		0.5		0.5					5	
(3,1)	0.5		0.5							
(4,1)	0.5			0.5			5			
(4,2)		0.5		0.5					5	5

Table 37: Updated matrix $\bar{A_E}$.

Ports and Legs	1	2	3	4	R1	R2	R3	R4	R5	R7
1					0.5	05	0.5			0.5
2	10				0.5			0.5	0.5	0.5
3	5					0.5		0.5		
4							0.5		0.5	0.5
(1,2)	0.5	0.5								
(1,3)	0.5		0.5							
(1,4)	0.5			0.5						
(2,1)	0.5	0.5			5					5
(2,3)		0.5	0.5							
(2,4)		0.5		0.5						
(3,1)	0.5		0.5			5				
(4,1)	0.5			0.5						
(4,2)		0.5		0.5						

Table 38: Inbound score and route importance score derived from the updated matrix $\bar{A}$, and their decomposition.

Ports and Routes	Unscaled Scores	Scaled Scores	Full Container	Empty Container
1	0.6392	0.3502	0.2685	0.3707
2	0.4678	0.2563	0.4538	0.0140
3	0.4201	0.2302	0.4147	0.0054
4	0.2979	0.1633	0.2907	0.0072
R1	0.2354	0.3361	0.1858	0.0495
R2	0.0974	0.1391	0.0796	0.0178
R3	0.0581	0.0829	0.0581	0.0000
R4	0.0525	0.0750	0.0525	0.0000
R5	0.0879	0.1254	0.0879	0.0000
R7	0.1692	0.2415	0.1196	0.0495

Table 39: Outbound score and leg importance score derived from the updated matrix $\bar{A}$, and their decomposition.

Ports and Legs	Unscaled Scores	Scaled Scores	Full Container	Empty Container
1	0.5241	0.3020	0.5241	0.0000
2	0.6582	0.3792	0.3516	0.3066
3	0.1605	0.0925	0.0072	0.1533
4	0.3927	0.2263	0.3927	0.0000
(1,2)	0.1660	0.1844	0.1394	0.0265
(1,3)	0.0975	0.1084	0.0721	0.0254
(1,4)	0.0855	0.0950	0.0630	0.0225
(2,1)	0.2066	0.2295	0.0830	0.1236
(2,3)	0.0552	0.0613	0.0339	0.0213
(2,4)	0.0578	0.0642	0.0394	0.0184
(3,1)	0.0742	0.0824	0.0254	0.0488
(4,1)	0.0589	0.0654	0.0364	0.0225
(4,2)	0.0984	0.1093	0.0800	0.0184

CHAPTER VI

MARKET STABILITY OF A LOGISTICS HUB

It might be true that a strategically located port with advanced and efficient infrastructure may attract more liners and container flow, and consequently create opportunities for freight consolidation or transshipment. Yet there are several threats that might affect the stability of such a hub, for example, the competition among ports in the region, connectivity loss, and hub relocation. In this chapter, we show that these risks are closely related and they should all be recognized in a unified framework. In doing so, we establish an analytical framework for assessing market stability of a logistics hub, which could also be used to predict the behavior of shipping lines in a competitive/cooperative setting. With this analytical scheme, it is possible for the port authority to comprehend and evaluate the expected loss from shipping lines' defection with respect to the actions executed by competitors. This piece of information, in turn, allows the port authority to devise counter strategies protecting its business from competing ports, such as strengthening its relationship with the customers anticipated to leave.

6.1 Shipping Lines and Market Stability of a Logistics Hub

Among all members of the container-shipping industry, ports and shipping lines might be considered as the most crucial players — since a port acts as a gateway for containerized goods to be distributed, while a shipping line is the one that physically transports them from the origins to the destinations via its service network. In practice, shipping lines usually form an alliance to help enhance their vessel capacity. This also gives them opportunities for serving more destinations by integrating their service networks with those in the same alliance via transshipment at a logistics hub. Interestingly, it is shipping lines, not a hub, that provide this connectivity. And, a popular hub with great connectivity usually induces more liners, which consequently helps it remain popular.

From the port's perspective, in order to become a logistics hub, a port must possess at

least two important characteristics. The first is the infrastructure that allows shipping lines to operate at lower cost but with higher speed. The latter is its geographical location, or *centrality*. A hub possessing these two characteristics, such as ports of Singapore and Hong Kong, usually attracts more liners, container flow, and so achieves connectivity for freight consolidation or transshipment. Yet there are several threats that might affect the stability of such a hub.

The first is the competition among ports in the vicinity. Obviously, ports in the vicinity possess approximately the same importance in terms of centrality. Therefore, a port with better infrastructure, as well as other external factors, such as lower port charges or lower labor costs, generally attracts shipping lines to camp their operations at such a port. As a consequence, a dramatic change in container-shipping patterns is evident. For example, in 1991, Port of Hong Kong was the first and only container port in the *Pearl River Delta* which served as the gateway to the southern region of China. The port of Hong Kong became the world's busiest container port several years before the emerging of the port of Shenzhen, located in the same region. The port of Shenzhen began its container operation with capacity of less than a million TEUs in 1991, which was far less than one tenth of Hong Kong's at the same period. However, with lower cost of operation and its location close to the world manufacturer, China, the port of Shenzhen has become more and more important, with a huge leap of both throughput and capacity. During 1991 – 2008, although ports of Hong Kong and Shenzhen have increased both their throughput and capacity dramatically, market share of the port of Hong Kong significantly dropped from 99% in 1991 to 53% in 2008, which is opposite to that of Shenzhen's [56].

Another prominent example of port competition is the emerging of the port of Tanjung Pelepas in Southeast Asia. It is well known that port of Singapore is one of the most efficient container ports in the world, with designed capacity of over 24 million TEUs. The port of Singapore, together with Port Klang and port of Tanjung Pelepas, is major port accounting for 68.2% of container throughput in this region. Additionally, in terms of transshipment, these three major ports account for almost 100% of transshipment traffic [48]. However, based on the study of [48], they found that the annualized slot capacity

called at the port of Tanjung Pelepas increased dramatically from 1999 to 2004, while the exclusive market share of the port of Singapore decreased from 64.6% to 47.8% during the same period. Apparently, a fierce competition among ports in the vicinity inevitably affects market stability of logistics hubs.

Since ports themselves are static entities that cannot move freely, they are more vulnerable to any decisions made by other players, especially the shipping lines. Without container flow fed by the liners, a port is merely a gigantic monument located along the shore. Having that in mind, port authorities have generally tried to bind shipping lines to operate at their complexes by a wide range of strategies, such as providing dedicated terminals to their best customers or contracting the minimum container amount to be handled to ensure lower port fees charged. By having more operating lines at a port, it will become popular and remain popular by help of its customers that provides port connectivity. Therefore, losing a customer implies a reduction of both port connectivity and its attractiveness as a logistics hub at the same time. In the worst case, this may trigger a series of defections by others whose transshipment opportunities have been reduced. A transshipment hub is especially vulnerable to this threat due to its smaller demand and supply, which might not otherwise justify port calls made by the liners.

One prominent example demonstrating this risk is the competition between the ports of Singapore and Tanjung Pelepas, Malaysia [10]. While Tanjung Pelepas and Singapore are located on the opposite side of the *Johor Strait*, next to each other, labor cost at the port of Tanjung Pelepas is much lower. In order to secure lower operational costs, in 2000, Maersk Sealand, the largest operating line at port of Singapore, moved its operating hub from the port of Singapore to the port of Tanjung Pelepas. Afterward, in 2002, Evergreen, the second biggest line, also moved to the port of Tanjung Pelepas. Under economic pressure on small shipping lines, some have to establish connection services to the port of Tanjung Pelepas in order to transship their containers with those who moved, and the others have followed them to the port of Tanjung Pelepas. By this succession of moves, the port of Singapore has lost millions of TEUs of container flow to its competitor. Ironically, the most important customer is also the greatest threat to the hub itself since it could abandon the current hub

and easily move to a competing one, which increases economic pressure on the rest to follow its move.

Based on the aforementioned, it might be true that, in order to maintain its status, as well as its market share, a logistics hub must improve not only its operational performance but also the relationship with its customers. Unfortunately, such a claim is not quite complete since the container-shipping industry is more dynamic and such stability depends not only on the hub's decision itself but also on other players'.

In order to capture the whole picture of such a system, we establish a unified framework for analyzing the effect of external forces on market stability of a logistics hub in a competitive environment, taking account of both ports' and shipping lines' decisions. In this setting, ports decide on their infrastructure which consequently defines shipping lines' operational costs. With this cost function, shipping lines then decide on their operational plans directing their container flow through these ports in a competitive/cooperative setting. Once the system reaches stability, where no shipping line is better off moving its business away to competing ports, each shipping line's value of cooperation is determined and used as base solution for the hub to devise counter strategies or policies preventing a defection.

6.2 Literature Review

There are several research streams associated with port and shipping line operations ranging from planning to operations in both non-cooperative and cooperative settings. Network optimization is regarded as one major research stream concerning shipping line's best response in a non-cooperative setting. The problems in this class mostly focus on shipping line's operational improvement, such as network design or ship scheduling. In [2], ship scheduling and network design problems were modeled simultaneously by means of a time and space network to help minimize liner shipping operational costs. In [94], the authors developed a cost minimization model to help identify ship types and their associated numbers in each shipping route to maintain the desired service level at minimal cost. In [93], liner shipping schedule design and container routing problems were combined and solved for the optimal

shipping plan that minimized total transshipment cost and penalty cost associated with longer transit times at ports. Lastly, in [95], an interesting method of cost minimizing path generation taking into account practical operational constraints, such as maritime cabotage and maximum allowable transit time, was presented.

In order to make the model more realistic and practical, many researchers have incorporated an implicit cost, such as queuing or congestion, into their models. For example, in [40], a multiserver queuing model was embedded within the optimization model to help find the optimal number of open gate lanes that minimize total operating costs at marine container terminals for trucking services.

In a large-scale optimization, the liner shipping network may be integrated with the rail line or trucking network, reflecting intermodal transportation, such as those sea-land networks studied in [27], [42], and [43]. In [43], they studied an integrated model of liner shipping and rail line networks taking both transportation and inventory costs into account. The objective of their research model was to identify the optimal channels of shipment from the origin located somewhere in Asia to the Regional Distribution Centers (RDCs) in the US. For modeling simplicity, several assumptions were imposed. For example, the demand at each RDC was set to be proportional to the purchasing power in the region that such a RDC served. In addition, each RDC was served only by one port using one channel of transportation, where there was no capacity constraint at ports or rail line terminals, as well as the minimum contractual volume. In [42], they revised their previous model by (i) including the minimum contractual volume at each port and (ii) using the result from a so-called short-run model presented by [52] to update the parameters of the revised model, reflecting the fluctuation of transit times with seasonality.

Similarly, in [25] and [27], the studies of the North American container flow diversion in a competitive environment were conducted. In their studies, congestion was considered as part of shipping line's operating costs modeled by means of a *piecewise linear function*. The result from their model indicated the optimal routes, ship sizes, ports, and hinterland shipping channels, that satisfied demand and capacity constraints at minimal cost. According to their model, demand units were referred to as the *Business Economic Areas* (BEAs), which were

defined as geographical groups that were relevant for economic analysis. They also used such a model to evaluate the impacts of the Panama Canal Expansion and the change of infrastructure at the port of Prince Rupert on the North American container flow diversion. In [26], they extended their previous works to analyze the diversion of container flow in the US ports caused by congestion. They concluded that congestion existed at most ports in the US; and in some cases, flow diversion might be required to lower the cost of transportation.

Besides network optimization whose primary objective is to improve shipping line's operational performance, several researchers have instead focused more on the behavioral study of players in the container-shipping industry. From the shipping line's perspective [88], an empirical study of port selection was conducted based on a survey of major lines in Singapore and Malaysia. Their study concluded that, among seven factors, only *port charges* and a *wide range of services* were the most influential factors in the selection process. Similar studies were done by [69] and [87], but from different players' perspective. From freight forwarders' perspective, [87] concluded that, among seven factors, *efficiency*, *shipping frequency*, and *infrastructure*, were the top three influential factors in the selection process, while *cost* and *time related factors* were the most significant ones from the shippers' side [69]. In [84], the authors performed a detailed analysis of port selection incorporating shipper size and other external factors under the control of port management. They found that the most influential factors for different sizes of shippers were not the same. More specifically, larger shippers focused more on the factors associated with *delivery speed*, while the smaller ones focused more on *costs*. Although we can explain player's behavior through these sophisticated statistical methods, unfortunately they are too subjective and heavily dependent on the design of the survey.

Observe that most of the literature discussed so far focuses on the performance of an individual player, such as shipping lines or shippers, without considering the mechanism between the player itself and others. In the case where the resulting outcome depends on the decisions of several players, game theory might be used as a tool for explaining the behavior of those involved players, where port competition is one of the active studies relying on such a concept.

The competition between Busan and Shanghai ports for transshipment container flow was conducted by [3]. In their study, the payoff received by a port was assumed to depend not only on the investment it made in its infrastructure but also on the investment made by its competitor. In order to defend its market share, the key decision for a port was to decide whether to invest, as well as the extent of such an investment, taking the strategies of its competitor as factors for making a decision. In [56], the competition between the ports of Hong Kong and Shenzhen was studied based on a two-stage game concerning price and capacity of the competing ports as factors for decision making.

Recently, [57] investigated the duopolistic competition of transshipment ports using a game-theoretic approach. This problem was motivated by a series of shipping line's defections from the port of Singapore to the port of Tanjung Pelepas mentioned earlier. In their study, the relationship between shipping line's operating costs and the number of transshipped containers at ports was captured by a two-stage game solved by a traditional backward induction. Though their study is interesting in several aspects, their model is unrealistic since it heavily relies on speculative assumptions. For example, the demand function used in their study assumes the same number of transshipment containers for all shipping lines. In addition, transshipment volumes are assumed to depend on port connectivity, or port efficiency, which is merely a conceptually undefined quantity. Objectively, these assumptions are imposed solely for problem characterization and the derivation of model's solution.

Although both ports and shipping lines are each competing with their rivals within the same business, interestingly, the cooperation among themselves has found to be useful and it is widely used for enhancing their operational performance. From the shipping line's perspective, vessel capacity is time sensitive, and unfilled capacity is considered as loss. Capacity sharing within a cooperative group of shipping lines, or the *alliance*, could help improve member's vessel utilization. Additionally, within an alliance, each member would have more opportunities to serve more destinations by combining its network with others via transshipment.

Since the contribution of each member to the formed alliance is not the same, the main

issue that might arise in that setting is *how to secure the stability of such an alliance*. Cooperative game theory then comes into sight. In the literature, we can model this kind of problem by using the concept of cooperative game theory to find a condition that stabilizes the formed coalition. Theoretically, such a condition is a fair sharing of cost or benefit based on a specific set of allocation rules. There are three prominent solution strategies for such an allocation in the literature, that is, the *core solution*, the *Shapley value*, and the *nucleolus*.

The *core solution* is defined as an allocation such that no one is better off outside the coalition. While the core solution is outstanding in terms of stability, unfortunately, in many cases, it is not uniquely defined, or it might be empty. In order to alleviate this problem, attention has been turned to another allocation concept called the *Shapley Value*. The Shapley value is axiomatically characterized based on three properties, that is, (i) *dummy*, (ii) *symmetry*, and (iii) *additivity*. Intuitively, one can interpret the Shapley value as the marginal contribution of a player to the coalition. The Shapley value has several appealing properties over the core, including that it is uniquely determined. Lastly, the *nucleolus* is defined as the allocation rule such that player's dissatisfaction is minimized.

In the container-shipping industry, cooperation between liners is common, but not for the ports. Yet it is conceptually possible. For example, [77] studied a two-stage game involving cooperative structures among container terminals of the port of Karachi that directly competed with another terminal of the port of Qasim. In the first stage, each terminal decided whether to join the coalition non-cooperatively. Once the coalition was formed, those who joined the coalition cooperatively determined the price in order to maximize the coalition surplus in the second stage. In their model, market share of each terminal was solely a function of price set by terminals. Such a function was derived from the *multinomial logit model* and the equilibrium price was then determined by backward induction. As an extension to their previous work, [78] used the same model to explain the effects of different concession contracts on the coalition formation.

Lastly, [7] developed a game theoretic model to study the competition and cooperation among three parties in the network of container shipping, that is, two major hub ports and

the shipping companies. In that setting, market share of a hub port was a function of its utility and such a utility function was solely based on its handling charge and that of its competitors — and not the congestion. While their study, as well as their associated model, is quite similar to ours in several aspects, our framework is more operational and, plausibly, more beneficial for both ports and shipping lines. In particular, our framework properly and better explains the mechanism between ports and shipping lines, in both competitive and cooperative settings, without any further assumptions on port's market share. It also supports what-if analysis in such a way that their model, or the aforementioned models discussed so far, could not.

Besides the applications of cooperative game theory in the container-shipping industry, [36] showed that a significant decrease in the systemwide cost of the southern Sweden forestry industry could be achieved by a cooperation within the forestry companies. Similar to [36], but with different setting of cooperation, [8] proposed a methodology to answer one interesting question: *how should the collaborating group be formed?* They answered such a problem by modeling it as a transferable utility game in an extensive form, where a subset of players in the *leading companies* (LC) was considered as the first and central decision maker offering the proposition of bilateral agreement to the rest in the *non-leading companies* (NLC), one at a time. Each players in the NLC decided whether to accept or reject the proposal offered by the LC, whose proposition was offered only once. Once the coalition formation ended, a set of potential solution paths would be revealed, together with their associated payoff vectors. The optimal path was then determined based on the concept of *subgame perfect Nash equilibrium* (SPNE) using backward induction.

Interested readers should refer to [79] and [30] for the comprehensive review of cooperative game theory in coalition games, and a detailed discussion of the general framework for cost allocation.

6.3 The Structure of Stability

Conceptually, a community of customers at a hub is stable if no customer is better off moving his business to the competing ports. This means that the hub is resistant to the

external forces from both its competitors and customers. In particular, we can analyze the stability of a logistics hub by the following steps (see Figure 36).

- Step 1: Given infrastructure of ports in a competition and a set of actions to be executed by competitors, we establish a model called the *Liner Shipping Cooperative Model* to predict the diversion of container flow made by shipping lines in a cooperative setting.

  Conceptually, we use such a model to minimize total operating costs of a group of shipping lines taking both port infrastructure and other cost factors into account. Such a model is then sequentially solved from a singleton containing one particular shipping line to the grand coalition constituting all lines. At each step, shipping lines are assumed to work as a single entity planning for a centralized operational plan that benefits them as a whole. As the coalition grows larger, shipping lines are expected to perform better; and, the grand coalition is the most desirable state for all lines with the largest surplus. In our study, market stability is reached when the grand coalition has been formed.

- Step 2: At stability, we compute value of cooperation for each shipping line based on the Shapley value. In this context, value of cooperation indicates incentive that a shipping line expects to receive from cooperation.

- Step 3: From the logistics hub's perspective, the grand coalition may be regarded as the expected outcome caused by competitors, and the value of cooperation is the condition that stabilizes it.

  A hub can comprehend how container flow has been shifted from one to another state during the formation in Step 1, as well as the condition sustaining the stable community of shipping lines from Step 2. This information, in turn, allows the hub to destabilize undesirable outcomes by devising and evaluating counter strategies or policies preventing market share loss — by repeating these three steps.

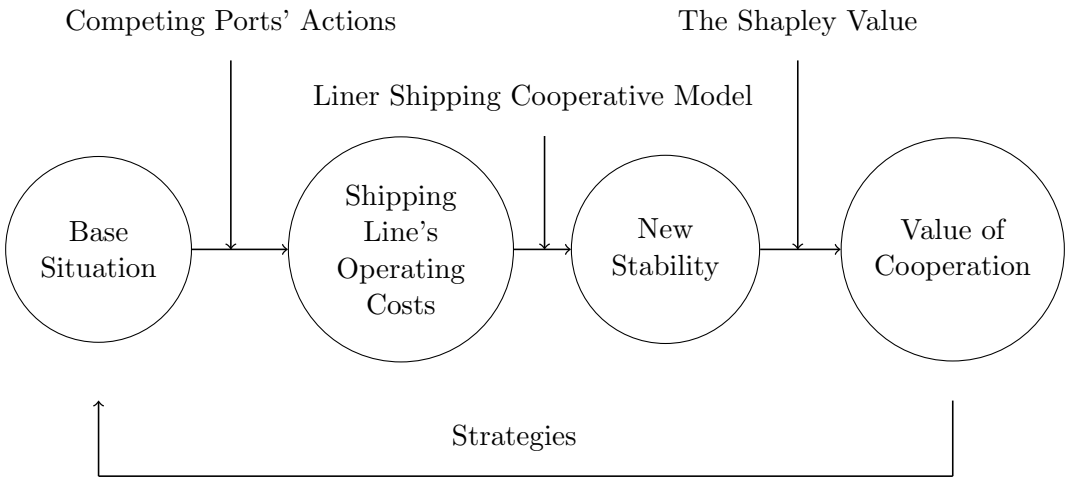

Figure 36: An analytical framework for investigating the stability of a logistics hub in a competitive environment.

Our proposed methodology differs from the existing research in three ways. Firstly, while most of the existing models may incorporate both explicit and implicit costs into consideration, an implicit cost, such as waiting or congestion, is improperly captured. Particularly, such a function is modeled by means of $G/G/m$ queuing model [41], where the distribution of container processing time and interarrival time of the containers at ports are assumed to be general with m operating cranes. As a consequence, given port infrastructure, we can compute the average waiting time that each container must wait in the steady state.

In general, as container flow reaches port capacity, the average waiting time abruptly increases. This means that shipping lines who operate at congested or highly utilized ports will suffer more from this implicit cost. In the literature, we may model this cost by a piecewise linear function, where such a cost is linearized into several connected segments as an approximation of the original function. However, there is a pitfall with regard to this particular technique; containers are assessed with different average waiting times, which is improper to reflect the congestion at busy ports as they handle a great number of containers at all times.

In our proposed cooperative model, we address this issue by using an alternate approach called the *piecewise-affine cost function* introduced by [89], which assigns only one cost rate

to all containers, modeled as a mixed integer program.

Secondly, to the best of our knowledge, we are the first to tackle this problem by means of an optimization-based cooperative game theoretic approach. More precisely, instead of defining relationship between interested quantities, we take advantage of the optimization model to explain such a mechanism, without need of any further assumptions for the characterization of the model's solution.

Lastly, the structure of our proposed methodology allows us opportunity not only to investigate the behavior of shipping lines taking port information into account but also to provide insights into the changes in container-flow patterns. This information, in turn, allows a logistics hub to comprehend and quantify the threats posed by its competitors, which is crucial for devising counter strategies or policies attaining its stability in the future.

It is worth noting that, depending on the structures of cooperation, we may use variants of the Shapley value for the evaluation of shipping line's value of cooperation in Step 2. And since there exist several variants that might be useful for our study, we will next review the concept of cooperative game theory and the Shapley value, together with its variants and applications, in Chapter 7, while the detailed discussion of liner shipping cooperative model and its results will be presented in Chapter 8.

Interestingly, as the concept of the Shapley value is gradually built, the connection between the Shapely value and centrality measures will become more apparent. At the end of Chapter 7, by using network expansion as a criterion, we show that the Shapley value might be used as a centrality measure to identify key operational lines at ports.

CHAPTER VII

THE SHAPLEY VALUE, CENTRALITY MEASURES, AND KEY OPERATIONAL LINES

In complex systems, where the interaction among members affects their decisions and welfare, *Game Theory* is regarded as a proper tool for the behavioral study of those rational decision makers. In a non-cooperative game, each player independently chooses the strategy that maximizes its own welfare assuming that other players would react to its action rationally. On the contrary, if players are allowed to cooperate, we call such a game a *cooperative game*, where a group of cooperating players is usually referred to as a *coalition*, or an *alliance* in the context of shipping liners. While cooperation could help increase systemwide welfare, and so better payoff, one question needs to be answered: *How would this surplus be fairly allocated to each member of the coalition?* In this chapter, we will discuss one prominent solution strategy for such an allocation, called the *Shapley Value*. And, as the concept of the Shapley value is gradually built, the connection between the Shapley value and centrality measures will be more apparent. This suggests that the Shapley value may be used as a centrality measure to identify key players in cooperative games. Based on this observation, we show that the most influential shipping lines at a port, or *Key Operational Lines*, could be revealed by such a value.

7.1 The Shapley Value

In cooperative game theory, we define N as a non empty set of players and any subset $s \in N$ is called a *coalition*, where the *grand coalition* is the one that constitutes all players. Given a coalition s, the coalition value $v(s)$ is defined as total worth gained from such a structure — which is usually referred to as a *characteristic function* — and by definition $v(\phi) = 0$. If total worth could be divided and allocated to the coalition members freely, i.e. there is no restriction on the distribution of total worth among members, such games are called games with *transferable utility* (TU), else the games are *nontransferable* (NTU). Since our focus

lies on the TU games, from here on, unless specified, all games are considered TU games.

The Shapley value is one of the solution strategies that allocates total worth $v(s)$ to the coalitional members based on three axioms: *dummy*, *symmetry*, and *additivity*, where the allocation vector $\phi_i(v)$ denotes the worth each member $i \in s$ receives.

Axiom 7.1.1 *Dummy (Carrier): Define a coalition s as a carrier of game v if and only if $v(s \cap t) = v(s)$ for all $s \subseteq N$. It follows that, for any game v and coalition s, if s is a carrier of v, then $\sum_{i \in s} \phi_i(v) = v(s)$.*

Intuitively, the first axiom states that dummy players, i.e. any players who are not the carrier, contribute nothing to the coalition. Therefore, they should not get any worth from the allocation.

Axiom 7.1.2 *Symmetry: Let v be a game and π be a one-to-one permutation function mapping N onto N, where $\pi(i) = j$. Moreover, for any game v and coalition s, let πv be the game such that $\pi v\{\pi(i)|i \in s\} = v(s)$ for all $s \subseteq N$, we have $\phi_{\pi(i)}(\pi v) = \phi_i(v)$.*

This axiom states that the role of player i in v, and $\pi(i)$ in πv, are essentially the same. In other words, relabeling does not change total worth of the coalition.

Axiom 7.1.3 *Additivity (Linearity): For any games v and w, $\phi(v + w) = \phi(v) + \phi(w)$.*

Prominently, Shapley has shown that, given a game v, there exists a unique function ϕ, or the *Shapley value*, satisfying those three axioms.

Theorem 7.1.1 *The Shapley value: There exists a unique function ϕ mapping coalition vector v to R^N which satisfies all three axioms, i.e. dummy, symmetry, and additivity axioms. For each $i \in N$, such a function could be defined as Expression* (86)*.*

$$\phi_i(v) = \sum_{s \subseteq N, i \in s} \frac{(|s| - 1)!(|N| - |s|)!}{|N|!} \left(v(s) - v(s - \{i\})\right) \tag{86}$$

Interestingly, the Shapley value has a nice interpretation in terms of a probabilistic model. Suppose that all players are going to form the grand coalition at a specific place.

However, each player can enter the place one at a time. Clearly, there would be $|N|!$ combinations of queues possible. Further assume that the next player to enter the place is player i and the resulting coalition to be formed is s. Without player i, the total worth would be $v(s-\{i\})$ and the marginal contribution of player i to the coalition s is $v(s)-v(s-\{i\})$. Since $\frac{(|s|-1)!(|N|-|s|)!}{|N|!}$ is the probability that player i would find itself in the coalition s once it enters the place, the Shapley value is indeed the expected payoff that player i obtains under this randomization scheme.

Besides the Shapley value, we will briefly discuss other prominent solution strategies called the *core* and the *nucleolus*[1]. The core of a game is defined as the set of allocated payoffs that no member is better off in any coalitions. Mathematically, if $x \in \mathbb{R}^N$ is an allocation vector, where $\sum_{i\in n} x_i = v(N)$, x is in the core if and only if $\sum_{i\in s} x_i \geq v(s)$, $\forall s \subseteq N$. Although the core solution is appealing in terms of stability, researchers have found that the core might be empty and finding the core solution is as hard as solving an $\mathcal{NP}$-complete problem (as cited in [79]). Additionally, the core is not uniquely defined and the allocations that lie in the core might not be fair to all players.

The nucleolus of a game is defined as the allocation vector that minimizes player dissatisfaction. More formally, given a coalition s, the excess $e(x,s) = v(s) - \sum_{i\in s} x_i$, is defined as a measure of dissatisfaction of the allocation vector x in coalition s, and $O(x)$ is the excess vector of x arranged in a non-increasing order. The allocation vector x such that $O(x)$ is lexographically less than $O(\delta)$, for any allocation δ, is called the nucleolus. While the nucleolus is quite an interesting solution concept, it has been rarely studied due to its computational complexity.

7.2 Variants of the Shapley Value

7.2.1 Graph-Restricted Games

According to the calculation of the Shapley value, all coalitions are assumed to be equiprobable. Yet, in practice, some coalitions might not even exist. For example, let us consider a three-player game, where (i) player 1 desires to cooperate with both players 2 and 3, (ii)

[1]Interested readers may find detailed discussion about the core and the nucleolus in [61] and [79].

player 2 prefers to cooperate with only player 1, and (iii) player 3 wants to cooperate with only player 1. This dilemma would make coalitions $\{123\}$, $\{12, 3\}$, and $\{13, 2\}$ seem implausible. However, if we consider the cooperation between members as cooperative links, this puzzle is immediately solved, and the graph shown in Figure 37 properly reveals their cooperation preferences. In the literature, we refer to this kind of games, where the coalition is represented by a restricted cooperative graph as *graph-restricted games*.

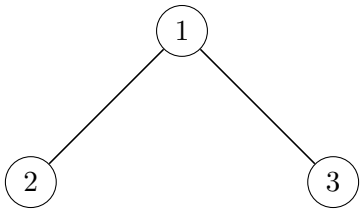

Figure 37: A graph representing cooperative preference of a three-player game, where (i) player 1 desires to cooperate with both players 2 and 3, (ii) player 2 prefers to cooperate with only player 1, and (iii) player 3 wants to cooperate with only player 1 [59].

To establish a fair allocation, let N be a non empty set of players and CL be the set of all coalitions formed by members of N, i.e. $CL = \{s|s \subseteq N, s \neq \phi\}$. A graph-restricted game is defined as vector v in R^{CL}; and, for any game $v \in R^{CL}$ and coalition $s \in CL$, we define $v(s)$ as total transferable utility of coalition s.

In addition, let g be the network containing a list of unordered pairs, or links, connecting nodes i and j, denoted as ij. If we let g^N be the complete graph, i.e. graph containing all links connecting all nodes, then $G = \{g|g \in g^N\}$ represents the set of all possible graphs generated by N players.

For simplicity, from here on, we denote the symbol $\backslash$ as the removal operation. For example, given a coalition s and node j, $s\backslash j$ denotes the removal of node j from coalition s, i.e. $s\backslash j = \{i \in N|i \in s, i \neq j\}$. Similarly, $g\backslash nm = \{ij|ij \in g, ij \neq nm\}$. Lastly, given a graph g and coalition s, $g|s$ denotes the resulting graph after removing all links except those connecting nodes within s, i.e. $g|s = \{ij|ij \in g \text{ and } i, j \in s\}$, while $s|g$ denotes the partition of s on g, or the collection of smaller coalitions of s induced by graph g. In other words, the symbol $|$ denotes the division of the first component based on the structure of

the second component.

Let $Y_i(g)$ be the expected payoff of player i under cooperative graph structure g, [59] shown that the payoff vector $Y(g)$ could be axiomatically derived the same way as that of the Shapley value, but with two allocation rules, (i) component balanced condition and (ii) equal bargaining power condition.

Definition 7.2.1 *Component Balanced Condition: An allocation Y is component balanced if for any graph $g \in G$ and any coalition $s \in g|N$, $\sum_{i \in s} Y_i(g) = v(s)$. In other words, for any connected component of g, total worth of s, denoted as $v(s)$, should be allocated only to the members of s. In addition, this allocation rule is independent of connected structures.*

Definition 7.2.2 *Equal Bargaining Power Condition: An allocation Y is equal bargaining power if for any graph $g \in G$ and $ij \in g$, $Y_i(g) - Y_i(g \backslash ij) = Y_j(g) - Y_j(g \backslash ij)$. In other words, players i and j equally benefit or lose from the removal of cooperative link ij.*

As proven by [59], there exists a unique fair allocation Y satisfying these two rules, as shown in Equation (87).

$$Y_i(g) = \sum_{s \subset N \backslash \{i\}} (v(g|s \cup \{i\}) - v(g|s)) \left(\frac{|s|!(|N| - |s|! - 1)!}{|N|!} \right) \tag{87}$$

Moreover, if $v \in R^{CL}$ is supperadditive, i.e. for any game s and t in R^{CL}, if $s \cap t \neq \phi$ and $v(s \cup t) \geq v(s) + v(t)$, the allocation vector Y is also proven to be totally stable.

Example 7.2.1 *Consider a three-player game with $v \in R^{CL}$, where $v(\{1\}) = v(\{2\}) = v(\{3\}) = 0$, $v(\{1,3\}) = v(\{2,3\}) = 1$, and $v(\{1,2\}) = v(\{1,2,3\}) = 2$. If the cooperative graph g is $\{12, 13, 23\}$, by Equation (87), $Y_1(\{12, 13, 23\})$ could be calculated as follows.*

$$Y_1(g) = \sum_{s \subset N \backslash \{1\}} (v(g|s \cup \{1\}) - v(g|s)) \left(\frac{|s|!(|N| - |s|! - 1)!}{|N|!} \right)$$

- $s = \{2\}$, *we have* $(v(g|\{1,2\}) - v(g|\{2\})) \left(\frac{|1|!(|3|-|1|!-1)!}{|3|!} \right) = \frac{1}{6}(2-0) = \frac{1}{3}$.
- $s = \{3\}$, *we have* $(v(g|\{2,3\}) - v(g|\{3\})) \left(\frac{|1|!(|3|-|1|!-1)!}{|3|!} \right) = \frac{1}{6}(1-0) = \frac{1}{6}$.
- $s = \{2,3\}$, *we have* $(v(g|\{1,2,3\}) - v(g|\{2,3\})) \left(\frac{|2|!(|3|-|2|!-1)!}{|3|!} \right) = \frac{1}{3}(2-1) = \frac{1}{3}$.

Here we have $Y_1(g) = \frac{5}{6}$. *Similarly,* $Y_2(g) = \frac{5}{6}$ *and* $Y_3(g) = \frac{2}{6}$, *and the allocation vector for graph g is* $(\frac{5}{6}, \frac{5}{6}, \frac{1}{3})$.

In this example, we find that both the core and the nucleolus lead to the same allocation vector (1,1,0) as player 3 is considered as a dummy player. However, in terms of the cooperative graph, if either player 1 or player 2 is about to break its relationship with player 3, its allocated worth would decrease, i.e. $Y(\{12, 23\}) = (\frac{1}{2}, \frac{1}{2}, 1)$ *and* $Y(\{12, 13\}) = (\frac{7}{6}, \frac{2}{3}, \frac{1}{6})$, *which implies that vector* $(\frac{5}{6}, \frac{5}{6}, \frac{1}{3})$ *is indeed stable and fair for this game.*

7.2.2 Games in Partition Function Form

Games in partition function form were firstly introduced by [86], and [60] has extended the result of the Shapley value to such games. In that setting, we assume that the payoff of any coalition depends not only on its members but also on the structure outside the formed coalition. More specifically, given a coalition s, the coalitional structure set B is defined as $B = \{s_1, s_2, s_3, \ldots, s_l\}$ such that $\forall i \neq j, s_i \cap s_j = \phi$, and $\cup_{i=1}^{i} s_i = N$, where the total worth of coalition s depends on both s and B that $s \in B$, denoted as $v(s, B)$. For example, let us consider a four-player game, where $s_1 = \{12\}$, $s_2 = \{34\}$, $s_3 = \{3\}$, and $s_4 = \{4\}$. In addition, let $B_1 = \{s_1, s_2\}$ and $B_2 = \{s_1, s_3, s_4\}$. In this game, although the coalition s_1 is a member of both partitions B_1 and B_2, as the partitions B_1 and B_2 differ, $v(s_1, B_1) \neq v(s_1, B_2)$.

In the literature, this type of effect is usually referred to as the *externality*. To model externality [60], let $\mathcal{B}$ be the set of all partitions of N, we define the embedded coalitions, denoted as ECL, as the set of coalitions that specifies the structure of the coalition formed by both players inside and outside coalition s, that is, $ECL = \{(s, q) | s \in q \in \mathcal{B}\}$.

With all of the aforementioned notations, games in partition function form are defined as vectors in R^{ECL}, and, for any game $w \in R^{ECL}$ and $(s, q) \in ECL$, $w(s, q)$ is total transferable utility of coalition s in partition q. Deriving from the same axioms as those of the original Shapley value, it was shown by [60] that there exists a unique function mapping games in partition function form to allocation vectors in R^N, denoted as $\Phi(w)$, where the

i^{th} element of such a function is calculated by Expression (88).

$$\Phi_i(w) = \sum_{(s,q)\in ECL} (-1)^{|q|-1}(|q|-1)! \left(\frac{1}{|N|} - \sum_{\tilde{s}\in q, \tilde{s}\neq s, i\notin\tilde{s}} \frac{1}{(|q|-1)(|N|-|\tilde{s}|)} \right) w(s,q) \quad (88)$$

Example 7.2.2 *Consider an arbitrary three-player game, by Expression* (88)*,* $\Phi_1(w)$ *could be calculated as follows.*

$$\begin{aligned}
\Phi_i(w) \;=\; & \frac{1}{3}w(\{1,2,3\},\{\{1,2,3\}\}) + \frac{1}{6}w(\{1,2\},\{\{1,2\},\{3\}\}) \\
& -\frac{1}{3}w(\{3\},\{\{1,2\},\{3\}\}) + \frac{1}{6}w(\{1,3\},\{\{1,3\},\{2\}\}) \\
& -\frac{1}{3}w(\{2\},\{\{1,3\},\{2\}\}) + \frac{2}{3}w(\{1\},\{\{1\},\{2,3\}\}) \\
& -\frac{1}{3}w(\{2,3\},\{\{1\},\{2,3\}\}) - \frac{1}{3}w(\{1\},\{\{1\},\{2\},\{3\}\}) \\
& +\frac{1}{6}w(\{2\},\{\{1\},\{2\},\{3\}\}) + \frac{1}{6}w(\{3\},\{\{1\},\{2\},\{3\}\})
\end{aligned}$$

Regarding the first term of this expression, we have $|q| = 1$ *and* $|\tilde{s}| = 0$*. Thus, the coefficient of* $w(\{1,2,3\},\{\{1,2,3\}\})$ *is* $(-1)^{|1|-1}(|1|-1)!\left(\frac{1}{3}-0\right) = \frac{1}{3}$*. Similarly, since both the second and the third terms appear in partition* $q = \{\{1,2\},\{3\}\}$*, we have* $|q| = 2$*, and* $\frac{1}{6}$ *and* $-\frac{1}{3}$ *are the coefficients of the second and the third terms, respectively.*

7.2.3 Games in Generalized Characteristic Function Form

If we view a coalition formation as a sequential process, the worth each player gets might depend not only on its members but also on the order of players forming such a coalition. For example, consider a three-player game raised by [70], where player 1 has two machines which are of value to him only if he could sell them. Players 2 and 3 could use these machines to produce goods for sale. Assume that both players 2 and 3 have valued the first inferior machine equally as 1 monetary unit, while players 2 and 3 have valued the second superior machine differently as 2 and 3 monetary units. While both players 2 and 3 try to buy the second machine first, player 1 is going to sell it to anyone offering the best price. In this setting, it is evident that total worth of any coalitions inevitably depends on the order of the players forming the coalitions. For example, if player 2 offers to buy the second machine and at that time player 3 has not shown up yet, $S = \{1,2,3\}$, the total worth of this coalition would be 3, $v(1,2,3) = 2+1$. However, if player 3 shows up before

player 2 does, the coalition formed would be $S = \{1, 3, 2\}$ and its associated total worth is 4, $v(1, 3, 2) = 3 + 1$.

In conclusion, we have the following.

$$v(1, 3, 2) = v(3, 2, 1) = v(2, 3, 1) = v(3, 2, 1) = 4$$

$$v(1, 2, 3) = v(2, 1, 3) = 3$$

$$v(1, 2) = v(2, 1) = 2 \text{ and } v(1, 3) = v(3, 1) = 3$$

The coalitions other than those stated above have a worth of zero. In such a case, we can alternatively say that total worth of the coalitions depends on the information each player perceived in order, and [70] defined this kind of game as games in generalized characteristic function form.

More formally, a game in generalized characteristic function form is defined as a function v that assigns a real value $v(T)$ to each of the ordered coalition $T \in \Pi(s)$, where $\Pi(s)$ is the set of all ordered coalition, and $s \subseteq N$. [70] shown that such a function, as shown by Equation (89), was uniquely determined based on the following three axioms, (i) efficiency, (ii) null player, and (iii) additivity.

$$\psi_i^{NR}(v) = \sum_{S \in N \setminus i} \sum_{T \in \Pi(S)} \frac{(|N| - |T| - 1)!}{|N|!} \left(v(T, i) - v(T)\right) \tag{89}$$

By applying Equation (89) to the described three-player game, we have $\psi^{NR}(v) = (\frac{39}{18}, \frac{12}{18}, \frac{15}{18})$, where $\psi_i^{NR}(v)$ specifies expected payoff that player i receives from this randomized bidding scheme.

Based on similar concept, [80] introduced another variant of the Shapley value for games in generalized characteristic function form by (i) modifying null player axiom introduced in [70] and (ii) adding one more axiom called the *symmetry axiom*. Regarding null player axiom, in [70], a player i is defined as a null player if $v(T, i) = v(T)$ for all ordered coalitions T not containing i, while, in [80], a player i is a null player if $v(T, i^h) = v(T)$ for all ordered coalitions T not containing i and $h \in \{1, 2, \ldots, |T| + 1\}$, where (T, i^h) denotes the ordered coalition $(i_1, i_2, \ldots, i_{h-1}, i, i_h, i_{h+1}, \ldots, i_{(|T|)})$ — this could be viewed as a stricter

version, where a null player contributes nothing independently of his position in the ordered coalitions of every game v.

For symmetry axiom, players i and j are symmetric in game v if for every ordered coalition T such that, for $i, j \notin T$, $v(T, i^k) = v(T, j^k)$ for all $k = 1, 2, \ldots, |T| + 1$. In other words, if players i and j are symmetric, total worth under games v would be the same.

According to the aforementioned axioms, [80] axiomatically characterized a variant of the Shapely value for games in generalized characteristic function form, denoted as $\psi^{SB}(v)$, by Equation (90).

$$\psi_i^{SB}(v) = \sum_{S \subset N \setminus i} \sum_{T \in \Pi(S)} \frac{(|N| - |T| - 1)!}{|N|!(|T| + 1)} \sum_{l=1}^{|T|+1} \Big(v(T, i^l) - v(T) \Big) \tag{90}$$

7.3 Applications of the Shapley Value in Cooperative Games

In the literature, cooperative game theory and the Shapley value have been intensively studied and successfully applied in many applications. Examples include communication networks, logistics and transportation systems, and bioinformatics. Due to their viability, in this section, we will present two interesting applications of the Shapley value. Based on the results of these applications, we are able to develop a game-based centrality measure for the identification of key operating lines at ports discussed in the following section.

7.3.1 Maximum Flow Games

Let $G = (V, E)$ be a network, where V represents a set of nodes and E represents a set of (directed) links. Assume that each node has control over a specific set of links, which consequently limits the flow passing each link. In logistics network, we may consider a node as a shipper, where each link denotes either shipping capacity or contracted capacity between shippers. Without cooperation, each shipper can use only its own controlled network for fulfilling their shipment, which might leave some of its capacity unfulfilled.

To visualize this, let us consider an example network from [76], shown in Figure 38, where s and t denote source and sink node. Additionally, node 1 has control over edge set {s1,1t}, node 2 has control over edge set {s2,12,32,2t}, and node 3 has control over edge set {s3,3t}, where the number shown next to an edge is its capacity.

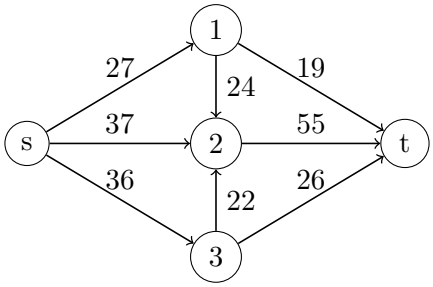

Figure 38: An example for describing the use of the Shapley value in a maximum flow game [76].

If we let $v(s)$ be the maximum flow of coalition s, under the myopic strategy, each shipper will have limited capacity of $v(1) = 19$, $v(2) = 37$, and $v(3) = 26$, or equivalently the total capacity of 82. However, they could do better in a cooperative setting, which is evident from the increase in maximum flow from source to sink as the coalition gets bigger, $v(12) = 64$, $v(13) = 45$, $v(23) = 73$, and $v(123) = 100$.

Assume further that fulfilling a unit of flow from source to sink would leave a profit of one monetary unit to a shipper, as the maximum flow is attained only from the grand coalition, every player would be tempted to form the grand coalition in order to enjoy the surplus of 18 more monetary units. [76] referred to this problem as the maximum flow game, where the Shapley value was used as an allocation rule to sustain the grand coalition.

According to the Shapley value formulation, we can calculate the payoff of player 1 as,

$$\phi_1(v) = \frac{1}{3}[v(1) - v(0)] + \frac{1}{6}[v(12) - v(2)] + \frac{1}{6}[v(13) - v(3)] + \frac{1}{3}[v(123) - v(23)] = 23.$$

Similarly, the payoffs of players 2 and 3 are $\phi_2(v) = 46$ and $\phi_3(v) = 31$. Since it is well known that the core of flow games is non-empty and we can verify whether the point $(23, 46, 31)$ lies in the core by substituting it into the definition of the core, it is not difficult to show that this allocation vector indeed lies in the core. Therefore, it is a stable solution.

7.3.2 Vertex Connectivity Rating

Another interesting application of the Shapley value in network analysis was presented by [1], where the Shapley value was used as a centrality measure for assessing the influence of

vertices in terms of their connectivity. In that setting, given a graph $G = (V, E)$, we say that G is strongly connected if for every pair of vertices $u, v \in V$ there is a path defined on E connecting u to v. In addition, for any coalition $s \subseteq V$, the characteristic function $v(s)$ is defined as total number of strongly connected components on graph G induced by a set of vertices in s. Intuitively, the smaller the value of the Shapley value, the greater the connectivity.

For later reference, let $SCC(G)$ denote the set of all strongly connected components of G and f_G be the characteristic function mapping any subsets s of V to a real number in $\mathcal{R}$, that is $f_G(s) = |SCC(G|s)|$, where $G|s$ denotes the subgraph of G induced by s for every subset $s \subseteq V$.

For example, consider a directed network G containing eight vertices as shown in Figure 39. Apparently, since G is strongly connected, we must have $f_G(V) = 1$. And, based on the aforementioned characteristic function v, we can calculate the Shapley value of all nodes as $\phi(f) = (\frac{2}{3}, \frac{-7}{10}, \frac{-7}{10}, \frac{2}{15}, \frac{2}{15}, \frac{2}{15}, \frac{5}{6}, \frac{1}{2})$.

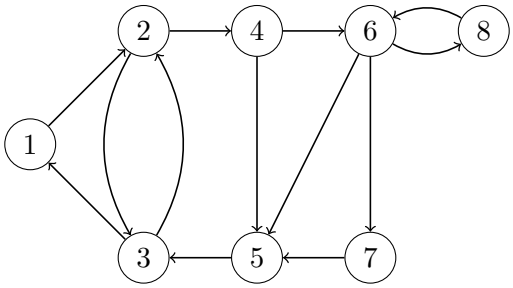

Figure 39: An application of the Shapley value for vertex connectivity rating on a directed graph G containing eight vertices [1].

Although such an application is quite interesting in many aspects, it is quite costly for both, counting the connecting subgraphs and calculating the Shapley value. Yet this application suggests how cooperative game theory could be connected with centrality measures in network analysis.

7.4 Cooperative Game-Based Centrality Measures and Their Applications

The foundation of cooperative game-based centrality measures might have originated from the study of *power* in the context of game theory, where the *Banzhaf power index* might be considered as the very first measure of power.

Consider a weighted voting game, where N denotes a set of political parties, where each political party $i \in N$ has a weighted voting power w_i, $0 < w_i \leq 1$ and $\sum_{i \in N} w_i = 1$. In such a game, a coalition is defined as *winning* if the sum of its members' weighted voting power is equal to or greater than a threshold q. A political party i is called a *decisive vote*, if its defection leads to *losing*. In the literature, the decisive vote is usually referred to as *swing* mimicking its nature, and the Banzhaf power index of the political party i, denoted as B_i, is defined as Equation (91).

$$B_i = \frac{\text{number of swings of party } i}{\text{total number of swings for all parties}} \tag{91}$$

In general, the normalized version of such an index might be preferable since it allows us to compare the players' power across networks. In order to do so, if $|N| = n$, there are 2^{N-1} possible coalitions, and, hence, we have the following.

$$B_i = \frac{\text{number of swings of party } i}{2^{N-1}} \tag{92}$$

By using the Banzhaf power index as an alternative measure of node centrality, [39] redefined the winning coalition as the existence of path connecting nodes, where node i was a decisive vote if its deviation led to the failure of the winning coalition, i.e. the coalition could not be formed when node i disappears.

Another interesting class of cooperative game-based centrality measures was introduced by [38], where the centrality of a node was defined as the difference between the Shapley values obtained from two different structures of graph games. In order to visualize this concept, let us consider a three-party voting game discussed in [38], where each party has different voting power: 40, 20, and 40 %. In addition, assume that each member of each party has agreed to vote in block. Suppose that, for passing a bill, it requires at least 2/3 of all votes, which is only possible when the first and the third parties have formed a coalition.

Since party 2 is a dummy player, and by the symmetry axiom, parties 1 and 3 would have equivalently the same bargaining power, which leads,

$$\phi_1(v) = \phi_3(v) = \frac{1}{2}, \text{ and } \phi_2(v) = 0.$$

[38] pointed out that this allocation was reasonable only if all coalitions were equally possible; however, in many cases, some coalitions might not even exist with regard to the relationship among players. For example, if parties 1, 2, and 3 are aligned from the liberal to the conservative one, it is less likely that parties 1 and 3 could reach an agreement to form a coalition without party 2. Hence, the only coalition possible now has become the grand coalition. With this information, we may model this game as graph-restricted game, and, by Equation (87), we have,

$$Y_1(g) = Y_2(g) = Y_3(g) = \frac{1}{3},$$

where $g = \{12, 23\}$. It is evident that party 2 has increased its power with regard to its position, while the power of both parties 1 and 3 have been decreased.

By exploiting the difference between these two values, [38] successfully defined a new class of centrality measures based on cooperative game theory, where the greater the difference, the better the centrality of a player. As an extension to their previous work, [21] introduced another family of centrality measures defined on directed networks by defining centrality as the difference between the allocations with and without graph restriction.

Similar to [38], [97] explored and used a cooperative game-based centrality measure as power index by defining players' power as the difference between two reference values, called the reference-point dependent measure.

Lastly, as motivated by [38], [58] have established a cooperative game-based centrality measure for assessing gene centrality in a bioinformatics application, whose objective was to investigate the most centrality, or powerful, genes causing genetic disorders. In their setting, two different sets of genes have been firstly defined, (i) a set K of key genes and (ii) a set N of interested genes supposedly affecting key genes, i.e. when genes in N interact with genes in K, some genetic disorders might occur.

If we let I be a set of interactions between genes in N and K, i.e. $I \subseteq \{\{i,k\}|i \in N, k \in K\}$, the triplet (N,K,I) represents the situation when genes in N and genes in K interact with interactions in I.

Based on the assumption that, given a set of genes $s \subseteq N$, the more interactions between genes in s and key genes K, the higher the possibility that genes in s evolves in the interested biological process, [58] define a characteristic function $v(s)$ as the number of key genes in K that *only* interacts with genes in s by interaction I. The pair (N,v) is now defined as an *association game* corresponding to the triplet (N,K,I). Since not all coalitions are possible, they define a specific network structure of interactions among genes in N prohibiting some coalitions from being formed, called the interaction network $< N, \Gamma >$, where Γ is a set of edges connecting genes in N.

With all of the aforementioned notations, the centrality measure of genes in N, defined as $\gamma_i(v,\Gamma)$, could be calculated through Expression (93).

$$\gamma_i(v,\Gamma) = Y_i(\Gamma) - \phi_i(v) \tag{93}$$

Based on their example, consider a set of key genes $K = \{a,b,c\}$, a set of genes $N = \{1,2,3,4\}$, a set of interaction $I = \{1a, 1b, 3b, 3c, 4c\}$, and a set of interaction $\Gamma = \{12, 23, 24, 34\}$, as shown in Figure 40.

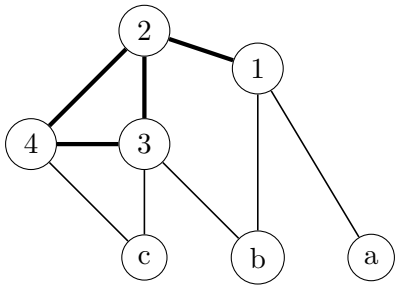

Figure 40: An example of the association game, where the interaction set I is represented by thin lines and the interaction set Γ is represented by thick lines [58].

By ignoring the interactions of genes in N, we have $v(2) = v(3) = v(4) = v(2,3) = v(2,4) = 0$, $v(1) = v(1,2) = v(1,4) = v(3,4) = v(1,2,4) = v(2,3,4) = 1$, $v(1,3) = v(1,2,3) = 2$, and $v(1,3,4) = v(1,2,3,4) = 3$. After applying the Shapley value to such a

graph, we have $\phi(v) = (\frac{3}{2}, 0, 1, \frac{1}{2})$.

Similarly, in its graph-restricted version, where the interaction Γ has been imposed on gene set N, we have $Y_i(g) = (\frac{4}{3}, \frac{1}{3}, \frac{5}{6}, \frac{1}{2})$, and the centrality of genes in N, which is the difference between these two vectors is $\gamma(v, \Gamma) = (-\frac{1}{6}, \frac{1}{3}, -\frac{1}{6}, 0)$. This implies that, with the existence of connecting edges within gene set N, gene 2 is the most influential gene, not gene 1.

7.5 An Application to Liner Services at a Port

In the shipping industry, cooperation among shipping lines is not unusual since forming an alliance with other lines helps enhance liner shipping operations in many ways [5]. Firstly, since liner shipping is a capital intensive industry and ocean vessels are getting bigger in order to take advantage of economies of scale by pooling vessels within the alliances, all lines are better off in terms of capacity utilization. This directly helps decrease each member's operational cost. In addition, by forming an alliance, shipping lines would be able to explore new markets by creating new service routes joining their core shipping networks with those of other members via transshipment.

Observe that, it is also the shipping lines that provide port connectivity for transshipment. A port may lose its connectivity, and so its competitiveness, if these customers decide to move their operations away to the competitors. In the worst case, this may trigger a series of defections by other shipping lines whose transshipment opportunities have been reduced. To survive in this situation, a port has to understand how important each of its customers is, and use this information to estimate the damage from each defection. This information would in turn allow the port authority to keep its customers, or, at least, lessen the effect of container bleeding. In order to do so, the port authority may need to identify the most influential shipping lines, or key operational lines, of the port and treat them with different standards.

For example, let us consider an integrated service network provided by four shipping lines at the port of Singapore, namely, Maersk Line, CMA CGM, APL, and Evergreen[2]. Each

[2]All information is provided on shipping lines' websites as of October, 2010.

shipping line has a different number of services, both from and to the port of Singapore, as well as total number of reachable ports, which defines the size of its core shipping network.

Table 40: Information of service routes, from and to the port of Singapore, together with total number of reachable ports of the four interested shipping lines.

Shipping Lines	**Incoming Routes**	**Outgoing Routes**	**Reachable Ports**
Maersk	27	29	183
CMA CGM	17	17	287
APL	43	43	137
Evergreen	17	15	141

From Table 40, APL may be regarded as the most powerful shipping line at the port of Singapore based on the number of routes; however, the size of its core shipping network is the lowest. If there exist bigger shipping lines that provide service services covering all ports that APL serves, losing APL will not seriously affect worldwide connectivity of the port of Singapore.

By considering worldwide connectivity shrinkage as the most important factor, the most powerful shipping line is the one whose existence increases total number of reachable ports the most. Mathematically, if we define N as a set of shipping lines, A as a set of coalitions, or liner shipping alliances, and $R(i)$ is the set of line i's reachable ports, a *connectivity game* could be defined as $v \in R^A$, where $v(s)$ is the incremental number of reachable ports from coalition s. For example, $v(i) = 0$, $\forall\ i \in N$, and $v(s) = \{\cup_{i \in s}(\cup_{i \in s} R(i) - R(i))\}$. By applying the Shapley value to this game, we have $\phi(v) = (80.75, 106.75, 65.42, 66.08)$.

According to the Shapley value, we can conclude that, with respect to worldwide connectivity shrinkage, CMA CGM is the most powerful shipping line to the port of Singapore, while both APL and Evergreen are relatively the least powerful.

Similarly, we can use another metric to identify key operational lines other than network expansion, such as origin-destination pair expansion or container flow; however, it is worth noting that the best metric should be the one that most reflects port interest.

7.6 Conclusions

In this chapter, we have provided fundamental concepts of the Shapley value and its variants, which may be considered as an alternative form of centrality measure. We adapt this idea to define key operational lines at the port of Singapore. We believe such a model can serve as a guide for assessing shipping line's incentives in a cooperative setting (see Chapter 8 for more details). With this piece of information, it is possible for the port authority to devise strategies to keep shipping lines from decamping to competing ports.

CHAPTER VIII

THE LINER SHIPPING COOPERATIVE MODEL AND THE EVALUATION OF MARKET STABILITY OF A LOGISTICS HUB

In order to evaluate market stability of a logistics hub, we develop an optimization model, called the *Liner Shipping Cooperative Model*, to predict the diversion of container flow made by the shipping lines in a cooperative setting — where the grand coalition defines the stability of a logistics hub. This model is constructed based on the assumption that shipping line's operating costs are the main driver affecting the decision of shipping lines. Once stability has been reached, we compute *value of cooperation* for each shipping line indicating its expected incentive for joining such a coalition. This information, in turn, allows a hub to devise and evaluate counter strategies for destabilizing undesirable outcomes, and to regain its market share from competitors.

8.1 The Liner Shipping Cooperative Model

Fundamentally, shipping lines decide how to transport their containers based on their total operating costs. While a portion of these costs may be observed from direct payment associated with container-shipping operations such as handling cost, the remainder are somewhat unintentional costs paid for non-value added processes, for example, the waiting time — as longer waiting time implies more operating costs for the shipping line and more in-transit inventory for the shipper.

As traffic at mega-hub ports is usually high, congestion and so longer waiting time is expected. In such a case, waiting cost may affect both shipping line's and shipper's operational costs greatly. While important, waiting cost is usually omitted during planning due to its complex nature. In particular, no individual shipping line has control over the costly waiting time as it is a result from both liner shipping uncoordinated plan and port infrastructure. However, shipping lines could plausibly avoid congestion by centralized planning, where they cooperatively re-route their container flow to nearby ports while maintaining

the connectivity of liner services.

Based on the aforementioned, and the assumption that shipping lines decide solely on their total operating costs — which include both implicit and explicit costs — we establish an optimization model, called the *Liner Shipping Cooperative Model*, to help them decide how to cooperatively re-route their container flow through ports optimally. Conceptually, our proposed model takes port infrastructure as input for constructing a waiting cost function; and, once observed, shipping lines then centrally decide on the diversion of container flow through ports such that total operating costs are minimized.

8.1.1 A Waiting Cost Function

In the literature, such as [25], [26], and [27], given port infrastructure, the average waiting cost at a port could be computed by the $G/G/m$ queuing model [41], where the distributions of both container interarrival time and container processing time at the port are assumed to be *general* with m operating cranes. Figure 41, for example, shows two congestion curves reflecting the average waiting time at ports A and B computed by such a model, where the infrastructure of both ports are given in Table 41. Observe that, as container flow reaches the port's designed capacity, the average waiting time abruptly rises. This implies that the shipping lines operating at congested or highly utilized ports are expected to pay more for waiting to be served.

Table 41: Infrastructure of fictitious ports A and B.

Ports	**Number of Cranes**	**Crane Efficiency (TEUs/hr/crane)**	**Implied Capacity (kTEUs/month)**
A	10	40	288.0
B	6	30	129.6

Though the waiting time is nonlinear in nature, we can linearlize and model it as a *piecewise linear function*, where the function of waiting cost is represented by connected linear segments. This modeling approach has been widely used in the literature for the modeling of waiting cost. Unfortunately, it has one pitfall, which is its misinterpretation. More specifically, by using a piecewise linear function, each container will be assessed with

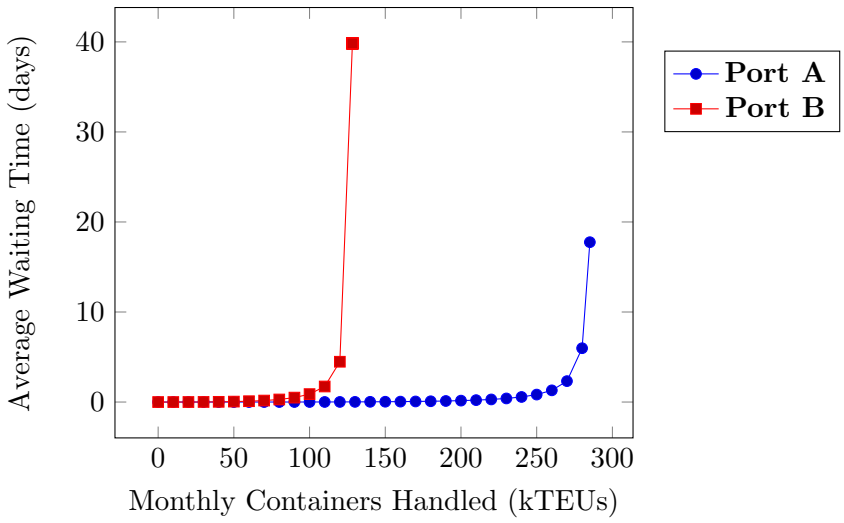

Figure 41: Congestion curves of ports A and B, up to 99% of port utilization.

different cost rates rather than one, as it should be in the steady state.

To make it clear, let us consider a port with traffic of d containers per month, where the computed average waiting time is assumed to be t_d, i.e. each container would remain in queue for t_d on average before getting served. Assume further that the average waiting time is linearized into three segments having u_1 and u_2 as breakpoints (see Figure 42). With this modeling approach, the average waiting time of the first u_1 units, the next $u_2 - u_1$ units, and the last $d - u_2$ units, will be differently calculated based on different rates, that is, rates 1, 2, and 3. This is clearly an improper estimate of congestion at busy ports as they generally handle a great number of containers at all times.

In order to address this issue, we instead use the *piecewise-affine cost function* proposed by [89]. As waiting cost is part of shipping line's operating costs, in the following sections, we will show how to model such costs using these two different modeling approaches.

8.1.2 The Modeling of Shipping Line's Operating Costs

Observe that the fundamental service of a logistics hub is to facilitate the transshipment of freight, which, in turn, allows liners to open new markets by calling at such a hub. In addition, since the majority of container traffic at major hubs, such as port of Singapore, is transshipment, and shipping lines have no direct control over demand or supply at any

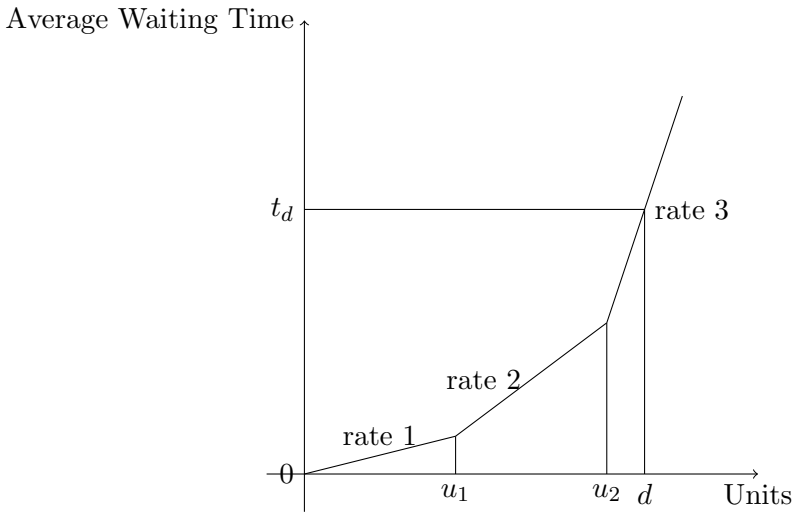

Figure 42: An illustration of the approximated piecewise linear function of the average waiting time at a fictitious port with d containers.

ports, we therefore assume that shipping line's operating costs are mainly constituted of transshipment related and congestion costs. More specifically, in this work, shipping line's operating costs consist of (i) handling cost at ports, (ii) cost of unfilled demand due to insufficient capacity, possibly caused by connectivity loss, and (iii) congestion cost reflected by waiting at ports.

In order to describe these cost components properly, we need the following sets, parameters, and decision variables.

Sets

- L is a set of shipping lines, where $|L| = l$.
- K is a set of ports, where $|K| = k$.

Parameters

- F^{ij} denotes the required number of containers to be transshipped from shipping line i to j, where a pair (i, j) might be referred to as commodity.
- $LCap^i$ denotes total capacity of shipping line i.
- $PCap^k$ denotes total capacity of port k.
- c_k^i denotes the handling cost per container that port k charges shipping line i.

- CW_k denotes the waiting cost per container per time unit at port k.
- TL^{ij} denotes loss per container of the commodity (i, j)'s unfilled demand.

Decision Variables

- x_k^{ij} is the number of containers to be transshipped from shipping line i to j at port k (see Figure 43, for example).

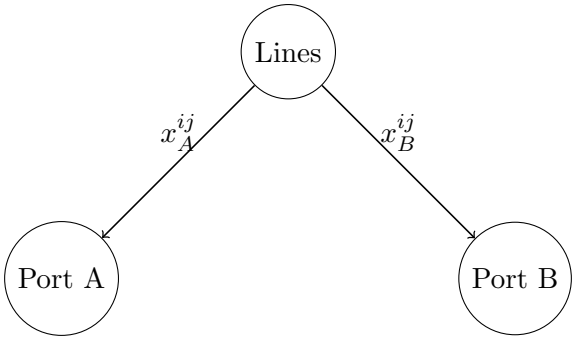

Figure 43: An illustration of decision variable x_k^{ij}, which could be considered as freight-flow allocation through k competing ports ($k = 2$ in this example).

- f_k^{ij} is free capacity of shipping line i allocated to commodity (i, j) through port k
- q^{ij} is the number of containers of the commodity (i, j)'s unfilled demand.
- y_k is total container traffic at port k.

As the coalition's objective is to minimize total operating costs for all shipping lines in a cooperative setting, we have the following.

$$\begin{aligned} \text{handling cost} &= \sum_k \sum_i \sum_j c_k^i x_k^{ij} \\ \text{transshipment loss} &= \sum_{(i,j)} TL^{ij} q^{ij} \\ \text{waiting cost} &= \sum_k < CW_k \cdot t_k \cdot y_k >, \end{aligned}$$

where t_k is the average waiting time at port k. In particular, t_k is a function of (i) arrival rate (r), measured in number of containers per time unit, (ii) processing time (p), measured in time unit per container, and (iii) number of berths or operating cranes (m).

Mathematically, t_k is defined as,

$$t_k(G/G/m) = \left(\frac{c_a^2 + c_e^2}{2}\right)\left(\frac{\rho_k^{\sqrt{2(m_k+1)}-1}}{m_k(1-\rho_k)}\right)p_k, \tag{94}$$

where c_a and c_e are the coefficients of variation in container arrival time and container processing time, and ρ_k is the average utilization of port k, i.e. $\rho_k = \frac{r_k p_k}{m_k}$.

By modeling the waiting cost as a piecewise linear function [33], we simply replace the waiting-cost term $\sum_k < CW_k \cdot t_k \cdot y_k >$ with,

$$\sum_k \sum_{n_k} s_{k,n_k} y_{k,n_k},$$

where r_k is the number of linear segments representing the average waiting cost at port k and s_{k,n_k} is the slope of the n_k^{th} segment. With this linearization technique, the total cost has become,

$$\text{Total Cost} \quad = \quad \sum_k \sum_i \sum_j c_k^i x_k^{ij} + \sum_{(i,j)} TL^{ij} q^{ij} + \sum_k \sum_{n_k} s_{k,n_k} y_{k,n_k}. \tag{95}$$

Based on Equation (95), this modeling approach clearly assigns different cost rates to the container flow as previously described. We may fix this problem by replacing the waiting cost function with Equation (96).

$$W_k(y_k) = \begin{cases} s_{k,1} y_k + b_{k,1} & \text{, if } y_k \in [0, u_{k,1}] \\ s_{k,2} y_k + b_{k,2} & \text{, if } y_k \in [u_{k,1}, u_{k,2}] \\ \quad . \quad . & \\ \quad . \quad . & \\ s_{k,r_k} y_k + b_{k,r_k} & \text{, if } y_k \in [u_{k,n_{r_{k-1}}}, u_{k,r_k}], \end{cases} \tag{96}$$

where $W_k(y_k)$ is the congestion cost at port k with y_k container traffic. Since Equation (96) is not in a proper form for the modeling purpose, we therefore introduce binary variable δ_{k,n_k} and decision variable z_{k,n_k} to help transform such an equation into one single linear equation.

More precisely, for each k, we have,

$$\bar{z}_k = z_{k,1} + z_{k,2} + \ldots + z_{k,r_{k-1}}, \tag{97}$$

where

$$z_{k,1} = \begin{cases} s_{k,2}y_k + b_{k,2} & \text{, if } \delta_{k,1} = 1 \\ s_{k,1}y_k + b_{k,1} & \text{, otherwise} \end{cases}$$

$$z_{k,2} = \begin{cases} (s_{k,3} - s_{k,2})y_k + (b_{k,3} - b_{k,2}) & \text{, if } \delta_{k,2} = 1 \\ 0 & \text{, otherwise} \end{cases}$$

$$z_{k,r_k-1} = \begin{cases} (s_{k,r_k} - s_{k,r_{k-1}})y_k + (b_{k,r_k} - b_{k,r_{k-1}}) & \text{, if } \delta_{k,r_{k-1}} = 1 \\ 0 & \text{, otherwise.} \end{cases}$$

With logical variable δ_{k,n_k}, it is obvious that $\bar{z}_k$ is the same as $W_k(y_k)$ in Expression (96).

In sum, the modified shipping line's operating costs, modeled as a piecewise-affine cost function, could be expressed as Equation (98).

$$\text{Total Cost} \quad = \quad \sum_k \sum_i \sum_j c_k^i x_{kk}^{ij} + \sum_{(i,j)} TL^{ij} q^{ij} + \sum_k \bar{z}_k, \tag{98}$$

where $\bar{z}_k$ is defined as Equation (97).

While these two cost functions differ slightly, the second modeling approach requires significantly more variables and sets of constraints to completely describe the problem — particularly, the waiting cost.

8.1.3 The Constraint Sets of Piecewise-Linear Cost Model

For simplicity, we will focus on a simple model, where transshipment traffic and capacity are key restrictions.

1. Proportion of transshipped containers at each port k.

$$\sum_k x_k^{ij} + q^{ij} \quad = \quad F^{ij} \ , \forall (i,j) \tag{99}$$

2. Boundary constraint for the capacity of each shipping line.

$$\sum_k \sum_j x_k^{ij} + \sum_k \sum_j f_k^{ij} \leq LCap^i \ , \forall i \tag{100}$$

3. Transshipment traffic could not exceed the capacity of each shipping line at ports.

$$\sum_j x_k^{ji} \leq \sum_j x_k^{ij} + \sum_j f_k^{ij}, \forall i, k \tag{101}$$

4. Waiting cost is a function of container traffic at a port.

$$\sum_{n_k} y_{k,n_k} = \sum_{(i,j)} x_k^{ij}, \forall k \tag{102}$$

Additionally, for each of y_{k,n_k}, let d_{k,n_k} and d_{k,n_k-1} be the breakpoints of the n_k^{th} segment of the waiting cost function at port k, where $d_{k,0}$ is 0, we need,

$$0 \leq y_{k,n_k} \leq d_{k,n_k} - d_{k,n_k-1},\ n_k = 1, 2, \ldots r_k, \forall k. \tag{103}$$

5. Additional constraints, i.e. capacity constraints at ports.

$$\sum_{n_k} y_{k,n_k} \leq PCap^k\ , \forall k \tag{104}$$

6. Non-negativity constraint.

8.1.4 The Constraint Sets of Piecewise-Affine Cost Model

In this modeling approach, the first three constraint sets are the same as those of the previous model, but the rest concerning the description of waiting cost are completely different.

1. Proportion of transshipped containers at each port k.

2. Boundary constraint for the capacity of each shipping line.

3. Transshipment traffic could not exceed the capacity of each shipping line at ports.

4. Container traffic at each port.

$$y_k = \sum_{(i,j)} x_k^{ij}, \forall k \tag{105}$$

5. As previously described, δ_{k,n_k} is used to capture the container traffic at port k. To control such a variable set, we need 2 logical constraints for each δ_{k,n_k} as follows.

$$D_{k,n_k}\delta_{k,n_k} \leq -(u_{k,n_k} - y_k) + D_{k,n_k}, \forall n_k = 1, \ldots, r_k - 1 \tag{106}$$

$$(d_{k,n_k} - \epsilon)\delta_{k,n_k} \leq (u_{k,n_k} - y_k) - \epsilon, \forall n_k = 1, \ldots, r_k - 1, \tag{107}$$

where D_{k,n_k} and d_{k,n_k} is the maximum and the minimum of $(u_{k,n_k} - y_k)$ defined by Equations (108) and (109), given that $y_k \in [0, u_{k,n_k}]$, and ϵ is a small value.

$$D_{k,n_k} = \max_{n_k}(u_{k,n_k} - y_k) = \max_{n_k}(u_{k,n_k}) - \min_{n_k}(y_k) = u_{k,n_k} \tag{108}$$

$$d_{k,n_k} = \min_{n_k}(u_{k,n_k} - y_k) = \min_{n_k}(u_{k,n_k}) - \max_{n_k}(y_k) = u_{k,1} - u_{k,n_k} \tag{109}$$

For example, let us consider the constraints that control $\delta_{k,1}$ as follows.

$$D_{k,1}\delta_{k,1} \leq -(u_{k,1} - y_k) + D_{k,1} \tag{110}$$

$$(d_{k,1} - \epsilon)\delta_{k,1} \leq (u_{k,1} - y_k) - \epsilon, \tag{111}$$

If $\delta_{k,1} = 1$ and $\delta_{k,2} = 0$, or equivalently $y_k \in [u_{k,1}, u_{k,2}]$, we have $d_{k,1} \leq (u_{k,1} - y_k) \leq 0$ and $\epsilon \leq (u_{k,2} - y_k) \leq D_{k,2}$, which properly describes the container traffic at port k.

Lastly, for $i > j$, we cannot have $\delta_{k,i} = 1$ while $\delta_{k,j} = 0$. Therefore, we need,

$$\delta_{k,n_k} \leq \delta_{k,n_k-1}, n_k = 2, \ldots, r_k. \tag{112}$$

6. Decision variable z_{k,n_k} must be controlled as described by Equation (97). In doing so, let M_{k,n_k} and m_{k,n_k} be the maximum and the minimum values of $s_{k,1}y_k + b_{k,1}$ for $n_k = 1$, $s_{k,2}y_k + b_{k,2}$ for $n_k = 2$, and z_{k,n_k} for $n_k \geq 3$, given that $y_k \in [0, u_{k,r_k}]$[1].

   To control the value of $z_{k,1}$, we need,

$$(M_{k,2} - m_{k,1})\delta_{k,1} - z_{k,1} \leq -[s_{k,2}y_k + b_{k,2}] + (M_{k,2} - m_{k,1}) \tag{113}$$

$$(M_{k,1} - m_{k,2})\delta_{k,1} + z_{k,1} \leq [s_{k,2}y_k + b_{k,2}] + (M_{k,1} - m_{k,2}) \tag{114}$$

$$(m_{k,2} - M_{k,1})\delta_{k,1} - z_{k,1} \leq -[s_{k,1}y_k + b_{k,1}] \tag{115}$$

$$(m_{k,1} - M_{k,2})\delta_{k,1} + z_{k,1} \leq s_{k,1}y_k + b_{k,1}. \tag{116}$$

   Based on Inequalities (113) and (114), if $\delta_{k,1} = 1$, we have $z_{k,1} \leq s_{k,2}y_k + b_{k,2}$ and $z_{k,1} \geq s_{k,2}y_k + b_{k,2}$, which implies $z_{k,1} = s_{k,2}y_k + b_{k,2}$. At the same time, from Inequalities (115) and (116), we have $z_{k,1} \geq s_{k,1} + b_{k,1} + (m_{k,2} - M_{k,1})$ and $z_{k,1} \leq$

[1]For example, $M_{k,3}$ and $m_{k,3}$ are the maximum and the minimum values of $(s_{k,3} - s_{k,2})y_k + (b_{k,3} - b_{k,2})$.

$s_{k,1}+b_{k,1}-(m_{k,1}-M_{k,2})$. Since M_{k,n_k} and m_{k,n_k} are defined as the maximum and the minimum of z_{k,n_k}, last two inequalities then provide us range that covers the resulting equation implied by the first two inequalities. On the contrary, if $\delta_{k,1}=0$, the last two inequalities would imply $z_{k,1}=s_{k,1}y_k+b_{k,1}$, which is covered by the range of the first two inequalities.

In sum, we have 4 additional constraints for each decision variable z_{k,n_k}; Expressions (117) - (120) for $n_k=3,\ldots,r_k$, together with Expressions (113) - (116), for all k.

$$\begin{aligned} M_{k,n_k}\delta_{k,n_k-1}-z_{k,n_k-1} &\leq -[(s_{k,n_k}-s_{k,n_k-1})y_k+(b_{k,n_k}-b_{k,n_{k-1}})] \\ &\quad +M_{k,n_k} \qquad (117) \\ -m_{k,n_k}\delta_{k,n_k-1}+z_{k,n_k-1} &\leq [(s_{k,n_k}-s_{k,n_k-1})y_k+(b_{k,n_k}-b_{k,n_{k-1}})] \\ &\quad -m_{k,n_k} \qquad (118) \\ m_{k,n_k}\delta_{k,n_k-1}-z_{k,n_k-1} &\leq 0 \qquad (119) \\ -M_{k,n_k}\delta_{k,n_k-1}+z_{k,n_k-1} &\leq 0 \qquad (120) \end{aligned}$$

Lastly, we need equation (97) to complete this set of constraints.

7. Additional constraints, i.e. capacity at ports.

$$y_k \leq PCap^k \ , \forall k \qquad (121)$$

8. Non-negativity constraints.

8.1.5 Piecewise-Linear Cost and Piecewise-Affine Cost Models

Model 1 — Piecewise-Linear Cost Model

$$\min C = \sum_k \sum_i \sum_j c_k^i x_k^{ij} + \sum_{(i,j)} TL^{ij} q^{ij} + \sum_k \sum_{n_k} s_{k,n_k} y_{k,n_k}$$

Subject To

$$\begin{aligned}
\sum_k x_k^{ij} + q^{ij} &= F^{ij} \ , \forall (i,j) \\
\sum_k \sum_j x_k^{ij} + \sum_k \sum_j f_k^{ij} &\leq LCap^i \ , \forall i \\
\sum_j x_k^{ji} &\leq \sum_j x_k^{ij} + \sum_j f_k^{ij} \ , \forall i,k \\
\sum_{n_k} y_{k,n_k} &= \sum_{(i,j)} x_k^{ij} \ , \forall k \\
y_{k,n_k} &\leq d_{k,n_k} - d_{k,n_k-1}, \ n_k = 1,2,\ldots r_k, \forall k \\
\sum_{n_k} y_{k,n_k} &\leq PCap^k \ , \forall k \\
&\text{All variables are positive}
\end{aligned}$$

Model 2 — Piecewise-Affine Cost Model

$$\min C = \sum_k \sum_i \sum_j c_k^i x_k^{ij} + \sum_{(i,j)} TL^{ij} q^{ij} + \sum_k \bar{z}_k$$

Subject To

$$\begin{aligned}
\sum_k x_k^{ij} + q^{ij} &= F^{ij} \ , \forall (i,j) \\
\sum_k \sum_j x_k^{ij} + \sum_k \sum_j f_k^{ij} &\leq LCap^i \ , \forall i \\
\sum_j x_k^{ji} &\leq \sum_j x_k^{ij} + \sum_j f_k^{ij} \ , \forall i,k \\
y_k &= \sum_{(i,j)} x_k^{ij} \ , \forall k \\
D_k \delta_{k,n_k} &\leq -(u_{k,n_k} - y_k) + D_k, \forall k, n_k = 1,\ldots,r_k - 1 \\
(d_k - \epsilon)\delta_{k,n_k} &\leq (u_{k,n_k} - y_k) - \epsilon, \forall k, n_k = 1,\ldots,r_k - 1 \\
\delta_{k,n_k} &\leq \delta_{k,n_k-1}, \forall k, n_k = 2,\ldots,r_k
\end{aligned}$$

$$
\begin{aligned}
(M_k - m_k)\delta_{k,1} - z_{k1} &\leq -[s_{k,2}y_k + b_{k,2}] + (M_k - m_k), \forall k \\
(M_k - m_k)\delta_{k,1} + z_{k1} &\leq [s_{k,2}y_k + b_{k,2}] + (M_k - m_k), \forall k \\
(m_k - M_k)\delta_{k,1} - z_{k1} &\leq -[s_{k,1}y_k + b_{k,1}], \forall k \\
(m_k - M_k)\delta_{k,1} + z_{k1} &\leq s_{k,1}y_k + b_{k,1}, \forall k \\
M_k\delta_{k,n_k-1} - z_{k,n_k-1} &\leq -[(s_{k,n_k} - s_{k,n_k-1})y_k + (b_{k,n_k} - b_{k,n_{k-1}})] + M_k, \forall k, n_k = 3, \ldots, r_k \\
-m_k\delta_{k,n_k-1} + z_{k,n_k-1} &\leq [(s_{k,n_k} - s_{k,n_k-1})y_k + (b_{k,n_k} - b_{k,n_{k-1}})] - m_k, \forall k, n_k = 3, \ldots, r_k \\
m_k\delta_{k,n_k-1} - z_{k,n_k-1} &\leq 0, \forall k, n_k = 3, \ldots, r_k \\
-M_k\delta_{k,n_k-1} + z_{k,n_k-1} &\leq 0, \forall k, n_k = 3, \ldots, r_k \\
\bar{z}_k &= z_{k1} + z_{k2} + \ldots + z_{k,r_k-1}\ , \forall k \\
y_k &\leq PCap^k\ , \forall k \\
& \text{All variables are positive and } \delta_{k,n_k} \text{ are binary variables}
\end{aligned}
$$

In this model, we replace D_{k,n_k} and d_{k,n_k} with D_k and d_k, where $D_k = u_{k,r_k}$ and $d_k = u_{k,1} - u_{k,r_k}$. Similarly, we replace M_{k,n_k} and m_{k,n_k} with M_k and m_k, where $M_k = \max_{n_k} M_{k,n_k}$ and $m_k = \min_{n_k} m_{k,n_k}$.

8.1.6 An Example of the Liner Shipping Cooperative Model

Consider a competition between two ports, A and B, with four container-shipping lines, where the infrastructure of both ports is given in Table 41 (Section 8.4.1) . In addition, the handling costs per container for all lines at ports A and B are 400 and 300, respectively.

Assume further that total capacities of these four shipping lines are 150, 120, 80, and 60 kTEUs, where the information about transshipment among lines and loss of unfilled demand is provided in Tables 42 and 43. Lastly, the operating cost per day per container is 80 for all shipping lines.

Table 42: Transshipment traffic among shipping lines (kTEUs).

Lines	1	2	3	4
1	100	20	10	5
2	20	75	10	10
3	15	5	55	5
4	15	0	0	35

Table 43: Loss per unfilled container.

Lines	1	2	3	4
1	1,200	1,000	800	800
2	1,000	1,200	800	700
3	1,000	900	1,200	900
4	1,000	1,100	1,000	1,200

Based on the aforementioned information, we found that total operating costs from the piecewise-linear cost model are much less than that of the piecewise-affine cost model (140.387M versus 178.661M), where the difference is mainly from the underestimated waiting cost (785.66K versus 20,613K) and loss from unfilled demand (0 versus 30,735k)[2]. Evidently, by using an improper estimate of waiting cost, the shipping lines will instead pay 253.29M, or 80% more than what they expected. This clearly stresses how important congestion is for the shipping lines.

With better waiting cost estimation, trade patterns also change, mainly at port B, where the waiting cost is much higher compared to that of port A (Figures 44 and 45).

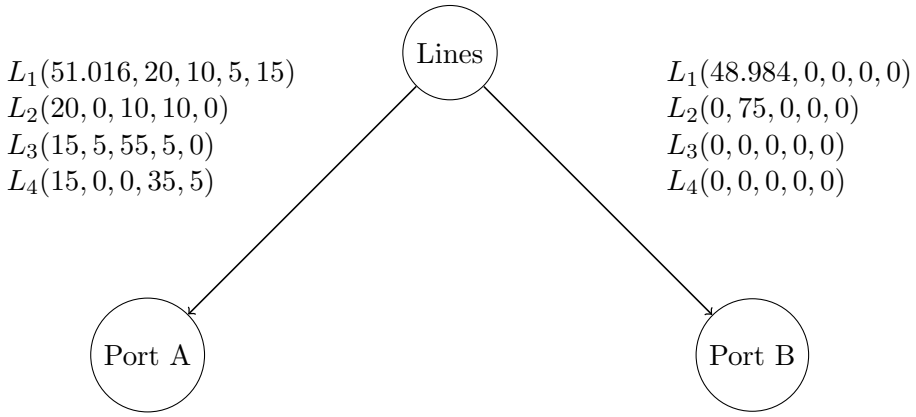

Figure 44: Solution to the piecewise-linear cost model, where $L_i(x^{i1}, x^{i2}, x^{i3}, x^{i4}, f)$ denotes the operational plan of shipping line i in kTEUs.

[2]Interestingly, while shipping lines have enough capacity to handle all transshipment traffic, it may be wiser for them to reject some shipment as it does not justify costly waiting time at ports.

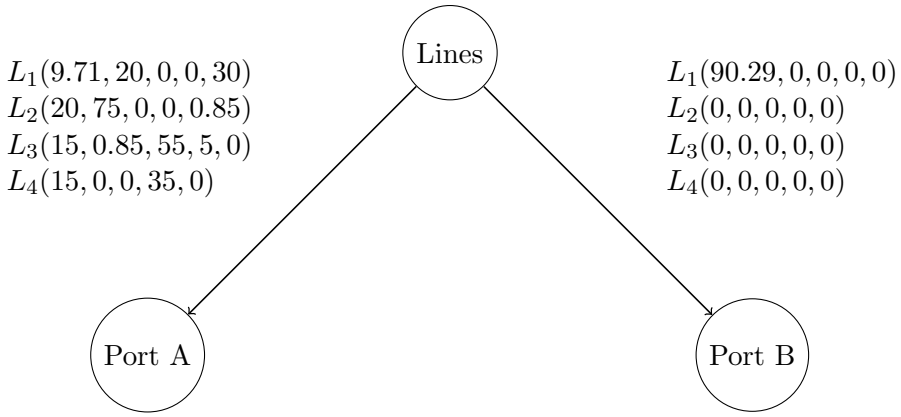

Figure 45: Solution to the affine-linear cost model, where $L_i(x^{i1}, x^{i2}, x^{i3}, x^{i4}, f)$ denotes the operational plan of shipping line i in kTEUs.

8.2 The Evaluation of Market Stability of a Logistics Hub

Conceptually, given infrastructure of ports in a competition and a set of actions to be executed by competitors, we can use the liner shipping cooperative model to predict the resulting container traffic at all ports. In doing so, we implicitly assume that all shipping lines deliberately cooperate and simultaneously decide on their operational plans re-routing their freight flow through ports in such a way that total operating costs are minimized — which resembles the formation of the grand coalition in the context of cooperative game theory.

In practice, it is less likely that all shipping lines could take action simultaneously, but rather through a series of formations from a singleton to the grand coalition. As total operating costs are less when the coalition grows larger, the grand coalition, or equivalently the solution to the liner shipping cooperative model, is therefore the most desirable state for all shipping lines defining stable community of liners at all ports.

If we consider the formation of the grand coalition as a sequential process, we could observe a progression of reductions in total operating costs, from one to another state until equilibrium. More specifically, let s_1 and s_2 be coalition sets such that $s_1 \subset s_2 \subset N$. In addition, let C_{s_1} and C_{s_2} be the associated cost vectors of s_1 and s_2. Namely, $C_{s_i} = TC(s_i)$, where $TC(S_i)$ is the total cost accrued by shipping lines in coalition s_i. Since we expect $C_{s_1} \geq C_{s_2}$, and $C_{s_i} \geq C_N$, $\forall s_i \subset N$, by solving a series of liner shipping cooperative

models, we can observe the effects of competitors' actions, both cost and coalition changes, as system gradually moves toward new equilibrium. With this piece of information, a hub can comprehend how a stable community of liners might be formed. This, in turn, allows the port authority to devise and evaluate counter strategies protecting its business from competing ports — by repeating the formation process once again using the previous equilibrium as the new initial state.

In summary, we can evaluate market stability of a logistics hub by the following steps.

1. Given infrastructure of ports in a competition and a set of actions to be executed, solve a series of liner shipping cooperative models in a coalition formation setting.

2. Evaluate shipping line's value of cooperation using the Shapley value, which may be regarded as incentive each shipping line expects from the cooperation.

3. Utilize the information from Steps 1 and 2 to devise and evaluate counter strategies protecting its business from competing ports by repeating these three steps.

In the context of cooperative game theory, we may regard the first two steps as the problem of finding the Shapley value in a coalition formation game, where the characteristic function of such a game is defined as total cost reduction caused by the coalition formed.

8.2.1 The Coalition Formation Game

In this setting, a set of shipping lines is divided in two groups, that is, a group of shipping lines with cooperation s and those outside s, denoted as $\bar{s}$. Given signals from competitors, we solve a series of liner shipping cooperative models from a singleton, i.e. $|s| = 1$, reflecting the decision of each shipping line in a non-cooperative setting, to the grand coalition, i.e. $|s| = N$, where all shipping lines cooperate, as shown in Figure 46.

Given a coalition s, the coalition formation game is defined as vector $v \in R^s$, where $v(s)$ denotes total cost reduction from coalition s. More specifically, $v(s) = C_{s_0} - C_s$, where C_{s_0} denotes total cost at base situation and C_s denotes total cost of coalition s obtained from the model.

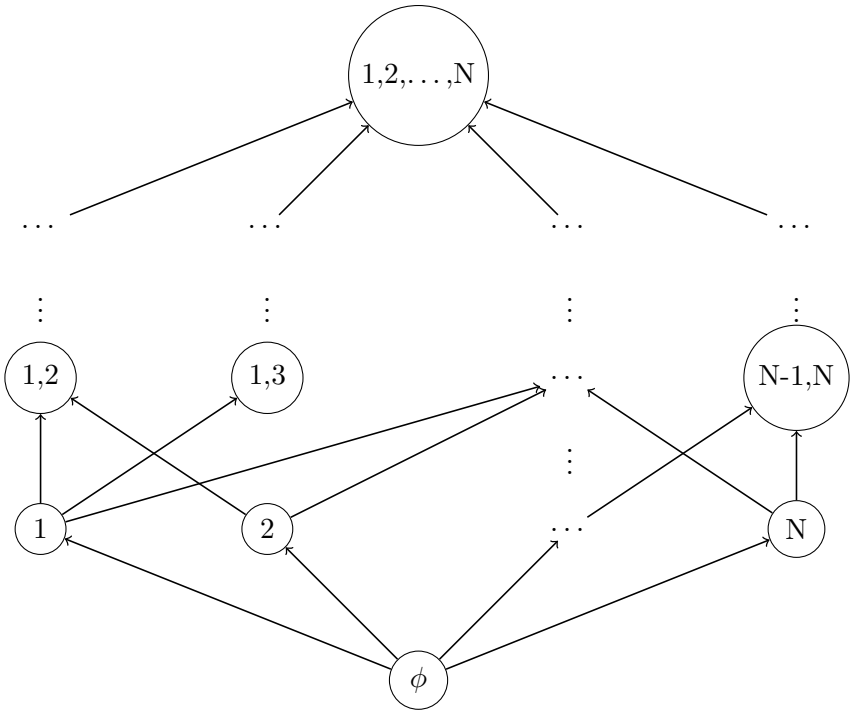

Figure 46: An illustration of the coalition formation game, where the numbers inside the circle indicate cooperative group s.

It is worth noting that, in the computation of C_s, we assume that the decisions of all shipping lines outside s, or $\bar{s}$, remain the same. In other words, we update only the re-routing of container traffic within coalition s, while treating all decision variables associated with shipping lines in $\bar{s}$ as parameters.

8.2.2 Experimental Results

Let us reconsider the example of liner shipping cooperative model previously discussed in Section 8.1.6, where the solution to the piecewise-linear cost model is assumed to be base situation s_0. By implementing better approximation technique for the calculation of waiting cost, trade flow is expected to gradually change and eventually reach new equilibrium, that is, the solution to the piecewise-affine cost model — assuming that the grand coalition is eventually formed. Figure 47 shows how trade flow at each port changes at each step of the formation, together with the coalition and the systemwide cost reductions.

By using the Shapley value as the allocation rule for the total cost reduction of 73.68M, shipping lines 1, 2, 3 and 4 anticipate to receive 26.71M, 36.03M, 6.16M, and 4.78M as

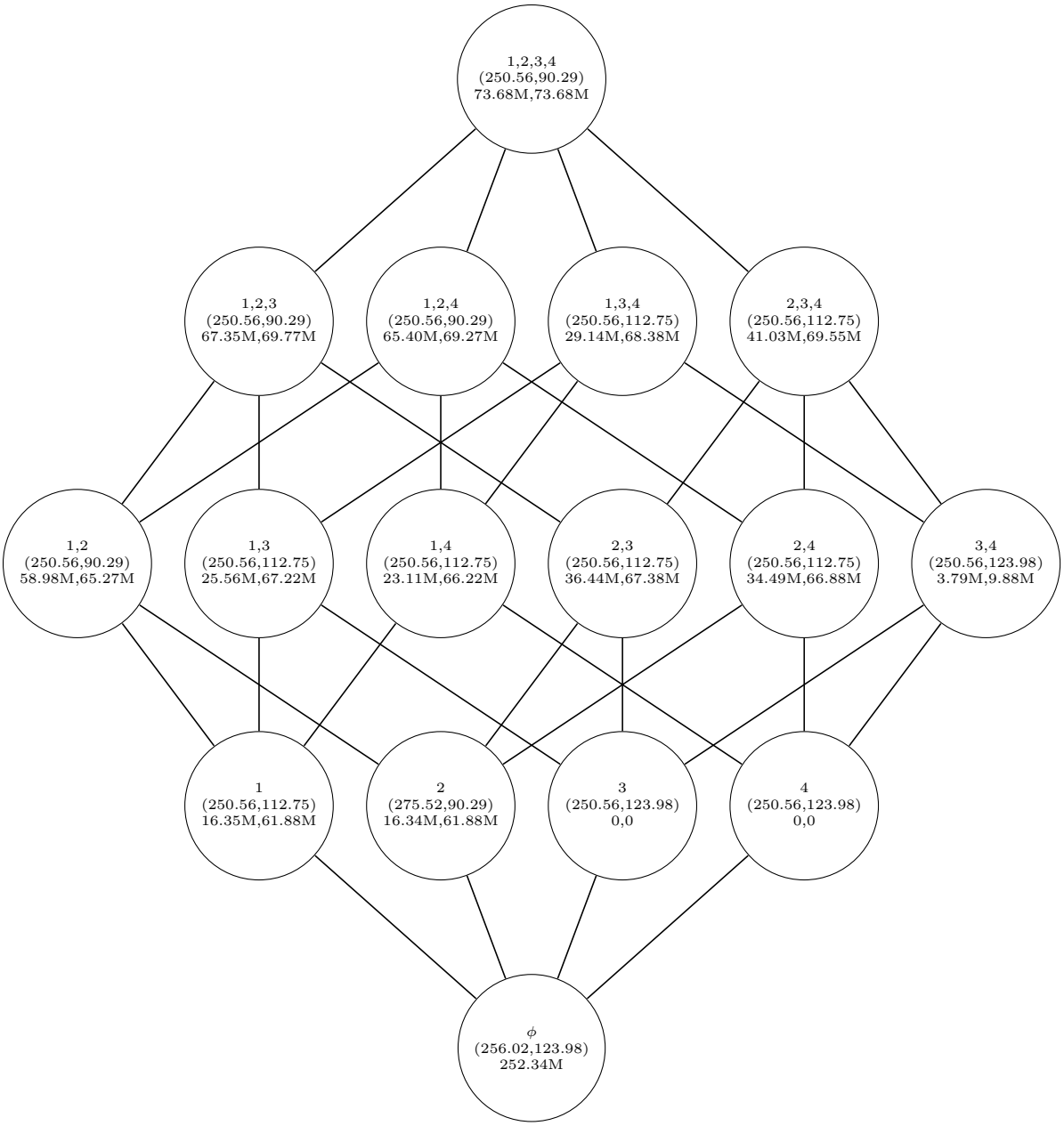

Figure 47: The result of a four-shipping-line coalition formation game with two ports in a competition. The numbers inside each circle indicate member(s) of cooperative group s, total flow at ports A and B measured in kTEUs, and total cost reduction from the coalition s followed by the systemwide cost reduction, except that of state ϕ, where total cost is shown.

expected incentives for joining the grand coalition. While this allocation is stable[3], it might seem surprising that shipping line 1 has to pay 8.57M more compared to the solution to

[3]By substituting this solution into the definition of the core solution.

the grand model. But this is because such a value is an expectation from all coalitions, not just the stability state alone.

Regarding flow diversion, interestingly, we have found that trade-flow difference between s_0 and s_N at port A is much less than that at port B (2.13% versus 27.18%), which could be explained by the costly waiting time at port 2. This implies that port infrastructure, or, equivalently, port efficiency, is the most influential factor for shipping lines in the selection of their transshipment hubs, not port fees, which is consistent with the empirical studies of [84] and [88].

8.3 Interesting Implications of the Liner Shipping Cooperative Model

8.3.1 The Order of Shipping Line Defection

In addition to the prediction of trade-flow diversion, we can also predict the order of shipping line's defections by defining the most likely coalition formation path based on the result of the coalition formation game. In particular, such a path is constructed based on the removal of all coalitions that are less likely to be formed, assuming that shipping lines could join the coalition one at a time.

These coalitions are usually the ones whose member's benefits are less than those of the base solution — in some coalitions, some shipping lines might be worse off as they sacrifice their own benefits for better coalition-wise results. For example, shipping line 4 in coalition {1,2,4} in our example has to pay 2.91M more for achieving the coalition-wise cost reduction of 69.27M. Unless there exists a fair allocation rule for this surplus, shipping line 4 would be reluctant to join such a coalition making it seem implausible.

From Figure 47, since there is no cost improvement from the singleton coalitions {3} and {4}, therefore, the most likely coalitions with one member are {1} and {2}. As we assume that shipping lines could join the coalition one at a time and the coalitions whose member's benefits are worse off are unlikely to be formed, so the most likely coalition formation path predicting the defection of shipping lines in order could be shown by Figure 48.

Based on Figures 47 and 48, it might be inferred that bigger shipping lines, such as line 1 or 2 in our example, are expected to be the first mover, inducing the smaller ones to

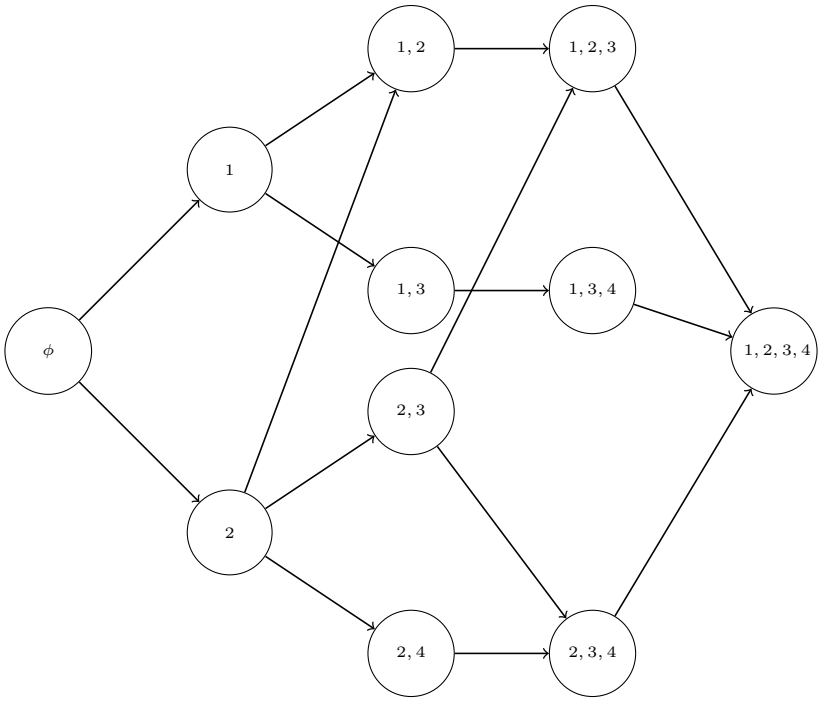

Figure 48: An illustration of the most likely coalition formation path.

new equilibrium. In addition, small lines, such as line 3 or 4, are more dependent on the decision made by bigger lines as they could not achieve any improvement, or may even be worse off[4], without joining a coalition.

While our model is only preliminary and not yet populated with actual data, nevertheless it seems consistent with the observation of shipping line's relocation at the port of Singapore, previously discussed in Chapter 6, where Maersk, the biggest operating line, was the first to move to the port of Tanjung Pelapas followed subsequently by Evergreen, the largest by the remaining lines at the port of Singapore.

8.3.2 Regaining Market Share

Another implication of the liner shipping cooperative model is the evaluation of counter strategies for a logistics hub to regain its market share from competitors. Based on our example, it is evident that both ports suffer from high level of congestion which does not make good economic sense for shipping lines to operate, especially at port B. With this piece

[4]For example, in the singleton coalition {2}, lines 3 and 4 outside the coalition are worse off as they have to pay 1.38M and 8.64M more as a result of line 2's decision. By realizing this threat, it might be better for them to seek cooperation with other shipping lines to help reduce their operating costs.

of information, it might be urgent for port B to improve its infrastructure to accommodate more freight flow, rather than to focus on lowering port fees, or handling charges. In such a case, depending on which players are interested, the liner shipping cooperative model, as well as the coalition formation game, could be used to predict the consequences of the strategies executed by ports, or shipping lines, in a *what-if-analysis fashion.*

8.4 Conclusions

The container-shipping industry is a dynamic system involving multiple players, of which ports and shipping lines might be considered the most crucial. We have established a model called the *liner shipping cooperative model* to evaluate market stability of a logistic hub in a competitive environment. Unlike other models, the liner shipping cooperative model takes decisions from both shipping lines and ports as input for evaluating the resulting freight-flow diversion at all ports. As we assume that shipping lines decide based solely on their operating costs and the grand coalition defines the stable community of liners at a hub, we can use this model to study the behavior of shipping lines with regard to the changes of policy or strategies made by ports. Consequently, expected trade-flow loss, as well as the order of shipping line's defections, could be predicted and avoided.

While the preliminary results from our model conform with the observation of shipping line's relocation at the port of Singapore, where the bigger lines are expected to be the first movers inducing the smaller ones to new equilibrium, there are several observations worth to be mentioned.

- Regarding the estimation of the average waiting cost, we have not specified the distribution of either the interarrival or the processing time of container flow, as information at this level is not generally accessible. However, by using a general distribution, our estimation of the average waiting cost might be overestimated since the variations in both interarrival and processing times, i.e. c_a and c_e, might not be that high in modern hubs with exceptional port planning and management.

- By using the Shapley value as an allocation rule for the computation of shipping line's value of cooperation, we implicitly assume that all coalitions are plausible and

equiprobable. Yet, if we pose some restrictions on the coalition formation process, like the one we propose for the finding of the most likely coalition formation path, coalitions {1,4} and {1,2,4} might not exist. In addition, we intentionally ignore the effects of externality, as well as those of the order of the formations, on the value of the game[5].

If any of the aforementioned matters, the Shapley value might not be a proper allocation rule since it is no longer fair for the coalition members in some critical dimensions. Rather, we might need to modify such an allocation rule, or use the existing variants of the Shapley value[6], that accounts for these kinds of special structures.

- While we use the Shapley value as guidelines for identifying the most likely coalition formation path, it might be interesting for both ports and shipping lines to know how the surplus would be allocated to the coalition members based on these specific sequences rather than the randomization scheme assumed by the original Shapley value.

According to the above observations, our model can be refined and improved, which would be useful for answering some interesting upcoming issues in the container-shipping industry — in particular, the effects of the *Panama Canal Expansion* on the patterns of freight-flow diversion. By the completion of its expansion, the Panama canal would be able to handle the so-called *Post-Panamax* ocean vessels whose capacity is more than double that of its current capacity, or up to 13,000 TEUs. Clearly, this would significantly decrease handling cost per container for the shipping lines deploying larger ocean vessels, but, without justified infrastructure, this could also be an operational trap as congestion might outweigh the reduction on operating costs. We also expect that the extension of our proposed framework would be beneficial for the players concerned as it supports what-if analysis in such a way that none of the existing models could.

[5]For example, if we consider coalition {1,2} in an arbitrary four-player game, such a routine will assume that the structure outside the coalition has no effect on the coalition value $v(12)$, or equivalently $v(\{12\}|\{12,3,4\}) = v(\{12\}|\{12,34\})$. In addition, $v(12) = v(21)$.

[6]See Chapter 7 for a detailed discussion of the Shapley value and its variants.

CHAPTER IX

CONCLUDING REMARKS AND FUTURE RESEARCH DIRECTIONS

In this dissertation, we establish a new measure, called the *Container Port Connectivity Index* (CPCI), to more accurately reflect the relative importance of container ports within the *Global Container-Shipping Network* (GCSN). Unlike any of the existing measures, the CPCI is based on both economics and network topology, where it expresses more than local connectivity to immediate neighbors but also neighbors-of-neighbors, and so on. In particular, as measured by the CPCI, the most important ports are not necessarily those with the most links, or those handling the most TEUs, but the ones with good connections with other well-connected ports. This is a reflection of fact that the CPCI does not depend only on the number of links but also on link quality and the connectivity of the ports to which they connect.

The CPCI also allows us to better understand the critical roles of some major ports, as well as the patterns of trade flow within the network of container shipping. For example, as measured by the CPCI, Los Angeles and Long Beach are ranked relatively high in terms of inbound which reflects the fact that these two ports are main entry ports for the products manufactured in East Asia. Once calling at these two ports, services that have to traverse the Pacific Ocean typically call at Oakland before returning to the large ports of Asia, making Oakland relatively important in terms of outbound.

We also show that the CPCI is so flexible that it could take alternative input other than the *Liner Shipping Connectivity Index* (LSCI) as link weights. We also show that, with proper modification, the CPCI could be decomposed into components. This helps us understand why a particular port has become important — and by which factors.

While the CPCI has many useful properties, it also has some weaknesses. Particularly, in the computation of the CPCI, link weights are represented by the LSCI reflecting

shipping capacity and not the actual number of TEUs transported or transshipped — as information at this level is generally unavailable. Nevertheless, as the LSCI has been vetted by economists as capturing intensities of trade, our index inherits that descriptive power and exercises it at a more granular level.

We expect the CPCI to be useful in some of the same ways as those used by the economists. This may include explaining how the container-shipping network changes over time or using the link weights and port scores as explanatory variables for economic phenomena. We believe these finer-grained statistics will be easier to understand and to explain because they directly reflect immediate decisions of primary actors such as shipping companies.

While powerful, the CPCI is only a descriptive index summarizing how well-connected a port is within the global structure of container-shipping network. It could not provide us insights into the behavior of shipping lines or ports with respect to major changes within the container-shipping industry. To better explain the dynamic between those key players, we establish an analytical framework for evaluating market stability of a logistics hub in a competitive environment. In particular, we build a model, called the *Liner Shipping Cooperative Model*, to help predict how the stable community of liners at a hub might be formed as the result of actions by competitors.

Although the liner shipping cooperative model is initially developed to explain the behavior of shipping line's defections at the port of Singapore in 2000 [10], nevertheless, it has been found to be useful for the behavioral study of both shipping lines and ports with respect to the environmental changes within the container-shipping industry. In particular, it allows us to alter critical parameters and evaluate the effects of such changes on the system from one to another stage until new equilibrium has been reached.

While our preliminary results conform with the empirical studies of [84] and [88], where efficiency is the most influential factor for shipping lines in the selection of their transshipment hubs, and the observation of shipping line's relocation at the port of Singapore, there are several observations about our model and framework to be mentioned.

- We assume that (i) shipping lines decide based solely on their operating costs and

(ii) the grand coalition which defines market stability of a logistics hub is eventually formed. While the first assumption is generally true, shipping lines rarely share information about their business, even with their partners in the same alliance. In addition, it is less likely that all shipping lines could cooperatively work as one single entity, but rather as a collective of alliances. Yet our model is still applicable by treating each alliance as if it were a single line.

- We consider only the allocation of freight flow through ports in a competition without considering other constraints, such as minimum contractual volume at ports or route restriction. Nevertheless, these could be integrated into the model without affecting our broad framework.

- While we use the Shapley value as guidelines for identifying the most likely coalition formation path, which indicates the order of shipping line's defections, it might be interesting for both ports and shipping lines to know how the surplus would be allocated to the coalition members based on these specific sequences rather than the randomization scheme assumed by the original Shapley value.

According to the above observations, our model can be refined and improved, which would be useful for answering some interesting upcoming issues in the container-shipping industry — in particular, the effects of the *Panama Canal Expansion* and the construction of a canal on *Kra Isthmus*, the narrowest part of the *Malay Peninsula* separating the *Gulf of Thailand* from the *Indian Ocean* with the distance of only 50 Km, on the patterns of freight-flow diversion. We expect that the extension of our proposed framework and model would be beneficial for the players concerned as it supports what-if analysis in such a way that none of the existing models could.

REFERENCES

[1] Abraham, M., Kotter, R., Krumnack, A., and Wanke, E., "A connectivity rating for vertices in networks," in *International Federation For Information Processing*, vol. 29, pp. 283–298, 2006.

[2] Agarwal, R. and Ergun, O., "Ship scheduling and network design for cargo routing in liner shipping," *Transportation Science*, vol. 42, no. 2, pp. 175–196, 2008.

[3] Anderson, C., Park, Y., Chang, Y., Yang, C., Lee, T., and Luo, M., "A game-theoretic analysis of competition among container port hubs: The case of Busan and Shanghai," *Maritime Policy and Management*, vol. 35, no. 1, pp. 5–26, 2008.

[4] Arenas, A., Dutch, J., Fernandez, A., and Gomez, S., "Size reduction of complex networks preserving modularity," *New Journal of Physics*, vol. 9, no. 176, 2007.

[5] Argawal, R. and Ergun, O., "Network design and allocation mechanisms for carrier alliances in liner shipping," *Operations Research*, vol. 58, no. 6, pp. 1726–1742, 2010.

[6] Arvis, J.-F., Mustra, M., Panzer, J., Ojala, L., and Naula, T., "Connecting to compete: Trade logistics in the global economy," tech. rep., The World Bank, 2007.

[7] Asgari, N., Farahani, Z., and Goh, M., "Network design approach for hub ports-shipping companies competition and cooperation," *Transportation Research Part A*, vol. 48, pp. 1–18, 2013.

[8] Audy, J.-F., D'Amours, S., and Ronnqvist, M., "An empirical study on coalition formation and cost/savings allocation," *International Journal of Production Economics*, vol. 136, pp. 13–27, 2012.

[9] Barigozzi, M., Fagiolo, G., and Mangioni, G., "Identifying the community structure of the international-trade multi-network," *Physica A*, vol. 390, pp. 2051–2066, 2011.

[10] Bichou, K. and Bell, M., "Internationalisation and consolidation of the container port industry: Assessment of channel structure and relationships," *Maritime Economics & Logisitcs*, vol. 9, pp. 35–51, 2007.

[11] Bonacich, P., "Some unique properties of eigenvector centrality," *Social Networks*, vol. 29, pp. 555–564, 2007.

[12] Bonacich, P., Holdren, A., and Johnson, M., "Hyper-edges and multidimensional centrality," *Social Networks*, vol. 26, pp. 189–203, 2004.

[13] Bonacich, P. and Lloyd, P., "Eigenvector-like measures of centrality for asymmetric relations," *Social Networks*, vol. 23, pp. 191–201, 2001.

[14] Bonacich, P. and Lloyd, P., "Calculating status with negative relations," *Social Networks*, vol. 26, pp. 331–338, 2004.

[15] Borgatti, S., "Centrality and network flow," *Social Networks*, vol. 27, pp. 55–71, 2005.

[16] Borgatti, S., "Identifying sets of key players in a social network," *Computational and Mathematical Organization Theory*, vol. 12, pp. 21–34, 2006.

[17] Borgatti, S. and Everett, M., "A graph-theoretic perspective on centrality," *Social Networks*, vol. 28, pp. 466–484, 2006.

[18] Brandes, U., Delling, D., Gaertler, M., Gorke, R., Hoefer, M., Nikoloski, Z., and Wagner, D., "On modularity clustering," *IEEE Transactions on Knowledge and Data Engineering*, vol. 20, no. 2, pp. 172–188, 2008.

[19] Bryan, K. and Leise, T., "The $ 25,000,000,000 eigenvector: The linear algebra behind Google," *Society for Industrial and Applied Mathematics*, vol. 48, no. 3, pp. 569–581, 2006.

[20] Council, W. S., "Top 50 world container ports," 2010. `http://www.worldshipping.org/about-the-industry/global-trade/top-50-world-container-ports`.

[21] del Pozo, M., Manuel, C., Gonzalez-Aranguena, E., and Owen, G., "Centrality in directed social networks. A game theoretic approach," *Social Networks*, vol. 33, pp. 191–200, 2011.

[22] Estrada, E., Higham, D., and Hatano, N., "Communicability betweenness in complex networks," *Physica A*, vol. 388, pp. 764–774, 2009.

[23] Estrada, E. and Rodriguez-Valazquez, J., "Subgraph centrality in complex networks," *Physical Review E*, vol. 056103, 2005.

[24] Estrada, E. and Rodriguez-Valazquez, J., "Subgraph centrality and clustering in complex hyper-networks," *Physica A*, vol. 364, pp. 581–594, 2006.

[25] Fan, L., Wilson, W., and Dahl, B., "Optimal network flows for containerized imports to the United States," *Transportation Research Part E*, vol. 46, pp. 735–749, 2010.

[26] Fan, L., Wilson, W., and Dahl, B., "Congestion, port expansion and spatial competition for US container imports," *Transportation Research Part E*, vol. 48, pp. 1121–1136, 2012.

[27] Fan, L., Wilson, W., and Tolliver, D., "Logistical rivalries and port competition for container flows to US markets: Impacts of changes in Canada's logistics system and expansion of the Panama Canal," *Maritime Economics & Logistics*, vol. 11, no. 4, pp. 327–357, 2009.

[28] Fan, Y., Li, M., Zhang, P., Wu, J., and Di, Z., "Accuracy and precision of methods for community identification in weighted networks," *Physica A*, vol. 377, pp. 363–372, 2007.

[29] Fan, Y., Li, M., Zhang, P., Wu, J., and Di, Z., "The effect of weight on community structure of networks," *Physica A*, vol. 378, pp. 583–590, 2007.

[30] Fiestras-Janeiro, M., Garcia-Jurado, I., and Mosquera, M., "Cooperative games and cost allocation problems," *An Official Journal of the Spanish Society of Statistics and Operations Research*, vol. 19, pp. 1–22, 2011.

[31] Fortunato, S., "Community dectection in graphs," *Physics Reports*, vol. 486, pp. 75–174, 2010.

[32] Fortunato, S. and Barthelemy, M., "Resolution limit in community detection," in *Proceedings of The National Academy of Sciences of The United States of America*, vol. 104, pp. 36–41, 2007.

[33] Fourer, R., Gay, D., and Kernighan, B., *AMPL: A Modeling Language for Mathematical Programming*. Thompson Brookes/Coles, 2003.

[34] Freeman, L., "Centrality in social networks: Conceptual clarification," *Social Networks*, vol. 1, pp. 215–239, 1978.

[35] Friedkin, N., "Theoretical foundations of centrality measures," *The American Journal of Sociology*, vol. 96, no. 6, pp. 1478–1504, 1991.

[36] Frisk, B., Gothe-Lundgren, M., and Ronnqvist, M., "Cost allocation in collaborative forest transportation," *European Journal of Operations Research*, vol. 205, pp. 448–458, 2010.

[37] Girvan, M. and Newman, M., "Community structure in social and biological networks," in *Proceedings of The National Academy of Sciences of The United States of America*, vol. 99, pp. 7821–7826, 2002.

[38] Gomez, D., Gonzalez-Aranguena, E., Manuel, C., Owen, G., Pozo, M., and Tejada, J., "Centrality and power in social networks : A game theoretical approach," *Mathematical Social Sciences*, vol. 46, pp. 27–54, 2003.

[39] Grofman, B. and Owen, G., "A game theoretical approach to measuring degree of centrality in social networks," *Social Network*, vol. 4, pp. 213–224, 1982.

[40] Guan, C. and Liu, R., "Modeling gate congestion of marine container terminal, truck waiting cost, and optimization," *Transportation Research Record: Journal of the Transportation Research Board*, no. 2100, pp. 55–67, 2009.

[41] Hopp, W. and Spearman, M., *Factory Physics*. McGraw-Hill, 2001.

[42] Jula, P. and Leachman, R., "Long- and short-run supply-chain optimization models for the allocation and congestion management of containerized imports from Asia to the United States," *Transportation Research Part E*, vol. 47, pp. 593–608, 2011.

[43] Jula, P. and Leachman, R., "A supply-chain optimization model of the allocation of containerized imports from Asia to the United States," *Transportation Research Part E*, vol. 47, pp. 609–622, 2011.

[44] Kaluza, P., Kolzsch, A., Gastner, M., and Blasius, B., "The complex network of global cargo ship movements," *Journal of The Royal Society Interface*, vol. 7, pp. 1093–1103, 2010.

[45] Kiss, C. and Bichler, M., "Idenification of influencers — measuring influence in customer networks," *Decision Support Systems*, vol. 46, pp. 233–253, 2008.

[46] Kleinberg, J., "Authoritative sources in a hyperlinked environment," *Journal of the Association for Computing Machinery*, vol. 460, no. 5, pp. 604–632, 1999.

[47] Kolaczyk, E., Chua, D., and Barthelemy, M., "Group betweenness and co-betweenness: Inter-related notions of coalition centrality," *Social Networks*, vol. 31, pp. 190–203, 2009.

[48] Lam, J. and Yap, W., "Competition for transshipment containers by major ports in Southeast Asia: Slot capacity analysis," *Maritime Policy and Management*, vol. 35, no. 1, pp. 89–101, 2008.

[49] Langville, A. and Meyer, C., "Deeper inside PageRank," *Internet Mathematics*, vol. 1, no. 3, pp. 335–400, 2004.

[50] Langville, A. and Meyer, C., *Google's PageRank and Beyond: The Science of Search Engine Rankings*. Princeton University Press, 2006.

[51] Latora, V. and Marchiori, M., "A measure of centrality based on network efficiency," *New Journal of Physics*, vol. 9, 2007.

[52] Leachman, R. and Jula, P., "Estimating flow times for conntainerized imports from Asia to the United States through the western rail road," *Transportation Research Part E*, vol. 48, pp. 296–309, 2012.

[53] Liu, J. and Lui, T., "Detecting community structure in complex networks using simulated annealing with k-means algorithms," *Physica A*, vol. 389, pp. 2300–2309, 2010.

[54] Low, J., Lam, S., and Tang, L., "Assessment of hub status among Asian ports from a network perspective," *Transportation Research Part A*, vol. 43, pp. 593–606, 2009.

[55] Lu, Z. and Huang, W., "Iterated tabu search for identifying community structure in complex networks," *Physical Review E*, vol. 80, 2009.

[56] Luo, M., Liu, L., and Gao, F., "Betrand competition with capacity expansion: Case study of container port competition between Hong Kong and Shenzhen, China," *Transportation Research Record: Journal of the Transportation Research Board*, vol. 2166, pp. 74–81, 2010.

[57] Minju, B., Chew, E., Lee, L., and Zhang, A., "Container transshipment and port competition," *Working Paper*, 2011.

[58] Moretti, S., Fragnelli, V., Fioravante, P., and Bonassi, S., "Using coalition games on biological networks to measure centrality and power of genes," *Bioinformatics*, vol. 26, no. 21, pp. 2721–2730, 2010.

[59] Myerson, R., "Graphs and cooperation in games," *Mathematical Operations Research*, vol. 2, pp. 225–229, 1977.

[60] Myerson, R., "Values of games in partition function form," *International Journal of Game Theory*, vol. 6, no. 1, pp. 23–31, 1977.

[61] Myerson, R., *Game Theory: Analysis of Conflict*. Harvard University Press, 1991.

[62] Nascimento, M. and de Carvalho, A., "Spectral methods for graph clustering — a survey," *European Journal of Operational Research*, vol. 211, pp. 221–231, 2011.

[63] Newman, M., "Analysis of weighted networks," *Physical Review E*, vol. 70, no. 056131, 2004.

[64] Newman, M., "A measure of betweenness centrality based on random walks," *Social Networks*, vol. 27, pp. 39–54, 2005.

[65] Newman, M., "Finding community structure in the networks using the eigenvectors of matrices," *Physical Review E*, vol. 74, no. 036104, 2006.

[66] Newman, M., "Modularity and community structure in networks," in *Proceedings of The National Academy of Sciences of The United States of America*, vol. 103, pp. 8577–8582, 2006.

[67] Newman, M. and Leicht, E., "Community structure in directed networks," *Physical Review Letters*, vol. 100, no. 118703, 2008.

[68] Nicosia, V., Mangioni, G., Carchiolo, V., and Malgeri, M., "Extended the definition of modularity to directed graphs with overlapping communities," *Journal of Statistical Mechanics: Theory and Experiment*, 2009.

[69] Nir, A., Lin, K., and Liang, G., "Port choice behaviour — from the perspective of the shipper," *Maritime Policy and Management*, vol. 30, no. 2, pp. 165–173, 2003.

[70] Nowak, A. and Radzik, T., "The shapley value for n-person games in generalized cahracteristic function form," *Games and Economic Behavior*, vol. 6, pp. 150–161, 1994.

[71] Ojala, L. and Hoffman, J., "A comparison of the LPI and the LSCI," 2010. `http://www.unctad.org/en/docs/webdtltlb20103_en.pdf`.

[72] Opsahl, T., Agneessens, F., and Skvoretz, J., "Node centralities in weighted networks: Generalizing degree and shortest paths," *Social Networks*, vol. 32, pp. 245–251, 2010.

[73] Palla, G., Farkas, J., Pollner, P., Derenyi, I., and Vicsek, T., "Directed network modules," *New Journal of Physics*, vol. 9, no. 186, 2007.

[74] Park, J. and Newman, M., "A network-based ranking systems for US college football," *Journal of Statistical Mechanics: Theory and Experiment*, 2005.

[75] Perra, N. and Fortunato, S., "Spectral centrality measures in complex networks," *Physical Review E*, vol. 78, 2008.

[76] Reyes, P., "Logistics networks: A game theory application for solving the transshipment problem," *Applied Mathematics and Computation*, vol. 168, pp. 1419–1431, 2005.

[77] Saeed, N. and Larsen, O., "An application of cooperative game among container terminals of one port," *European Journal of Operations Research*, vol. 203, pp. 393–403, 2010.

[78] Saeed, N. and Larsen, O., "Container terminal concessions: A game theory application to the case of ports of Pakistan," *Maritime Economics and Logistics*, vol. 12, no. 3, pp. 237–262, 2010.

[79] Saeed, W., Han, Z., Debbah, M., Hjorungnes, A., and Basar, T., "Coalitional game theory for communication networks," *IEEE Signal Processing Magazine*, vol. 77, 2009.

[80] Sanchez, E. and Bergantinos, G., "On values for generalized cahracteristic functions," *OR Spektrum*, vol. 19, pp. 229–234, 1997.

[81] Shavitt, Y. and Singer, Y., "Beyond centrality — clasifying topological significance using backup efficiency and alternative path," *New Journal of Physics*, vol. 9, 2007.

[82] Shen, H., Cheng, X., and Guo, J., "Quantifying and identification the overlapping community structure in networks," *Journal of Statistical Mechanics: Theory and Experiment*, 2009.

[83] Stanoev, A., Smilkov, D., and Kocarev, L., "Identifying communities by influence dynamics in social networks," *Physical Review E*, vol. 84, no. 064102, 2010.

[84] Steven, A. and Crosi, T., "Choosing a port: An analysis of containerized imports into the US," *Transportation Research Part E*, vol. 48, pp. 881–895, 2012.

[85] Tang, L.C. Joyce, M. and Lam, S., "Understanding port choice behavior — a network perspective," *Networks and Spatial Economics*, 2008.

[86] Thrall, R. and Lucas, W., "N-person games in partition function form," *Naval Research Logistics Quarterly*, vol. 10, no. 1, pp. 281–298, 1963.

[87] Tongzon, J., "Port choice and freight forwarders," *Transportation Research Part E*, vol. 45, pp. 186–195, 2009.

[88] Tongzon, J. and Sawant, L., "Port choice in a competitive environment: From the shipping lines' perspective," *Applied Economics*, vol. 39, no. 4, pp. 477–492, 2007.

[89] Trecate, G., Letizia, P., and Spedicato, M., "Optimization with piecewise-affine cost functions," tech. rep., Swiss Federal Institute of Technology, June 2001.

[90] Tutzauer, F., "Entropy as a measure of centrality in networks characterized by path-transfer flow," *Social Networks*, vol. 29, pp. 249–265, 2007.

[91] Tzekina, I., Danthi, K., and Rockmore, D., "Evolution of community structure in the world trade web," *The European Physical Journal B*, vol. 63, pp. 541–545, 2008.

[92] Wang, G., Shen, Y., and Luan, E., "A measure of centrality based on modularity matrix," *Progress in Natural Science*, vol. 18, pp. 1043–1047, 2008.

[93] Wang, S. and Meng, Q., "Schedule design and container routing in liner shipping," *Transportation Research Record: Journal of the Transportation Research Board*, no. 2222, pp. 25–33, 2011.

[94] Wang, S. and Meng, Q., "Liner ship fleet deployment with container transshipment operations," *Transportation Research Part E*, vol. 48, pp. 470–484, 2012.

[95] Wang, S., Meng, Q., and Sun, Z., "Container routing in liner shipping," *Transportation Research Part E*, vol. 49, pp. 1–7, 2013.

[96] Wang, X., Jiao, L., and Wu, J., "Adjusting from disjoint to overlapping community detection of complex networks," *Physica A*, vol. 388, pp. 5045–5056, 2009.

[97] Weise, H., "Applying cooperative game theory to power relations," *Qual Quant*, vol. 43, pp. 519–533, 2009.

[98] Wills, R., "Google's PageRank: The math behind the search engine," *The Mathematical Inteligencer*, vol. 28, no. 4, pp. 6–11, 2006.

[99] Wu, Z., Lin, Y., Wan, H., Tian, S., and Hu, K., "Efficient overlapping community detection in huge real-world networks," *Physica A*, vol. 391, pp. 2475–2490, 2012.

[100] Xu, G., Tsoka, S., and Papageorgio, L., "Finding community structures in complex networks using mixed interger optimisation," *The European Physical Journal B*, vol. 60, pp. 231–239, 2007.

[101] Yang, S. and Knoke, D., "Optimal connections : Strength and distance in valued graphs," *Social Networks*, vol. 23, pp. 285–295, 2001.

[102] Zhang, P., Li, M., Wu, J., Di, Z., and Fan, Y., "The analysis and dissimilarity comparison of community structure," *Physica A*, vol. 367, pp. 577–585, 2006.

VITA

Pisit Jarumaneeroj was born in Bangkok, Thailand, on August 6, 1982. Pisit received his Bachelor of Engineering in Industrial Engineering from Chulalongkorn University, Bangkok, Thailand, in 2004. After graduation, he spent two and a half years at the Regional Centre for Manufacturing Systems Engineering, Chulalongkorn University, as a research scientist. In 2007, he was awarded a scholarship from the Royal Thai Government to study in the area of logistics and supply chain management, after which he was admitted to the doctoral program at the School of Industrial and Systems Engineering, Georgia Institute of Technology. His research interests include applied mathematics in logistics and supply chain management, large-scale optimization, and complex network analysis. Upon his Ph.D. graduation, he will join the Faculty of Engineering at Chulalongkorn University, Thailand.